AFWAL-TR-86-2125

THE ROLE OF BULK ADDITIONS IN SOLID LUBRICANT COMPACTS

PHILLIP W. CENTERS
Lubrication Branch
Fuels and Lubrication Division

APRIL 1987

Final Report for Period November 1983 to November 1986

AERO PROPULSION LABORATORY
AIR FORCE WRIGHT AERONAUTICAL LABORATORIES
AIR FORCE SYSTEMS COMMAND
WRIGHT-PATTERSON AIR FORCE BASE, OHIO 45433-6563

UNCLASSIFIED
SECURITY CLASSIFICATION OF THIS PAGE

REPORT DOCUMENTATION PAGE

Form Approved OMB No. 0704-0188

A182 735

1a. REPORT SECURITY CLASSIFICATION: Unclassified	1b. RESTRICTIVE MARKINGS
2a. SECURITY CLASSIFICATION AUTHORITY	3. DISTRIBUTION/AVAILABILITY OF REPORT: Approved for public release; distribution unlimited.
2b. DECLASSIFICATION/DOWNGRADING SCHEDULE	
4. PERFORMING ORGANIZATION REPORT NUMBER(S): AFWAL-TR-86-2125	5. MONITORING ORGANIZATION REPORT NUMBER(S)
6a. NAME OF PERFORMING ORGANIZATION: Aero Propulsion Laboratory; 6b. OFFICE SYMBOL (If applicable): AFWAL/POSL	7a. NAME OF MONITORING ORGANIZATION
6c. ADDRESS (City, State, and ZIP Code): Air Force Wright Aeronautical Labs (AFSC) Wright-Patterson Air Force Base, Ohio 45433-6563	7b. ADDRESS (City, State, and ZIP Code): Wright-Patterson Air Force Base, Ohio 45433-6563
8a. NAME OF FUNDING/SPONSORING ORGANIZATION; 8b. OFFICE SYMBOL (If applicable)	9. PROCUREMENT INSTRUMENT IDENTIFICATION NUMBER
8c. ADDRESS (City, State, and ZIP Code)	10. SOURCE OF FUNDING NUMBERS

PROGRAM ELEMENT NO.	PROJECT NO.	TASK NO.	WORK UNIT ACCESSION NO.
62203F	3048	06	26

11. TITLE (Include Security Classification): The Role of Bulk Additions in Solid Lubricant Compacts

12. PERSONAL AUTHOR(S)

13a. TYPE OF REPORT	13b. TIME COVERED	14. DATE OF REPORT (Year, Month, Day)	15. PAGE COUNT
Final	FROM Nov 83 TO Nov 86	April 1987	241

16. SUPPLEMENTARY NOTATION

17. COSATI CODES			18. SUBJECT TERMS (Continue on reverse if necessary and identify by block number)
FIELD	GROUP	SUB-GROUP	
11	08		Solid Lubricant Additives
14	02		

19. ABSTRACT (Continue on reverse if necessary and identify by block number)

Oxide and sulfide additions to molybdenum disulfide and graphite solid lubricants were evaluated experimentally. Results indicate that the tribologically beneficial effect of bulk additions to solid lubricants originates in the ability of the additive to deform under asperity contact conditions to permit the solid lubricant to attain and retain preferred tribological orientation for overall improvement in tribological condition. Such improvement is evident in scanning electron microscopic examination of worn compact surfaces. Thermal mechanical analyses of solid lubricant compacts and calculated asperity flash temperatures indicate that the mechanism proposed is plausible.

Studies of antimony trioxide as an additive to molybdenum disulfide support the hypothesis. Previous hypothesis offered to explain the beneficial effect of Sb_2O_3 additions to MoS_2 including sacrificial oxidation of Sb_2O_3, retardation of MoS_2 oxidation by

over

20. DISTRIBUTION/AVAILABILITY OF ABSTRACT	21. ABSTRACT SECURITY CLASSIFICATION
☒ UNCLASSIFIED/UNLIMITED ☐ SAME AS RPT. ☐ DTIC USERS	UNCLASSIFIED
22a. NAME OF RESPONSIBLE INDIVIDUAL: PHILLIP W. CENTERS	22b. TELEPHONE (Include Area Code): 513/255-6608 — 22c. OFFICE SYMBOL: AFWAL/POSL

DD Form 1473, JUN 86 — Previous editions are obsolete.

19. ABSTRACT (Continued)

Sb_2O_3, or formation of a eutectic of antimony and molybdenum oxides to improve transfer film formation are refuted.

Evaluation of oxides and sulfides a bulk additions in MoS_2 indicate that the role of antimony trioxide is not unique; e.g., MoO_3 is superior to Sb_2O_3 at test temperature of 316°C. Confirmation is also provided by the finding that lower test temperatures are required for antimony oxide additions to graphite to improve performance of graphite, evidently resulting from higher asperity contact temperatures generated in the graphite compact.

A strong correlation of solid lubricant compact wear volume and weak correlation of friction coefficient with shear strength of additives are found. Therefore, the improvement in tribological performance is a bulk, rather than interfacial phenomenon.

In summary, lubricant compact properties and selection of bulk additions for improved tribological performance are hypothesized to be determined by the test or application conditions, the shear strength at asperity contact temperature of the additive and properties of the solid lubricant.

(Keywords:)

PREFACE

This technical report was prepared for the Lubrication Branch, Fuels and Lubrication Division, Aero Propulsion Laboratory (APL), Air Force Wright Aeronautical Laboratories (AFWAL), Air Force Systems Command, Wright-Patterson Air Force Base, Ohio. The work herein was accomplished under Project 3048, Task 304806, Work Unit 30480626, "Turbine Engine Lubricant Research" for the period November 1983 to November 1986, with Mr Phillip W. Centers, AFWAL/POSL, as project engineer. Special acknowledgement is given to Captain F. Dean Price, Chris Klenke, Robert Wright, Gayle Byrd and Corliss Goldsmith without whose assistance, this project could not have been completed.

ACKNOWLEDGEMENTS

Appreciation is expressed to the author's advisors, Dr Lawrence T. Drzal and Dr James A. Snide, for their advice, discussion and encouragement throughout the course of this research.

Special thanks are extended to the author's co-workers in the Aero Propulsion Laboratory at Wright-Patterson Air Force Base, Ohio for their valuable assistance in this effort.

The author also wishes to express very special thanks to his mother, brother Bob, and his wife Connie for their love, patience and understanding.

TABLE OF CONTENTS

CHAPTER I..... 1
INTRODUCTION..... 1

CHAPTER II..... 6
SCOPE OF THIS STUDY..... 6

CHAPTER III..... 8
LITERATURE SURVEY..... 8
FRICTION..... 8
WEAR..... 10
LUBRICATION..... 12
SOLID LUBRICANTS..... 13
PROPERTIES OF AN OXIDATION OF MOLYBDENUM DISULFIDE..... 18
ANTIMONY OXIDES..... 22
PROTECTIVE INTERACTION OF Sb_2O_3 ADDITION TO MoS_2..... 33

CHAPTER IV..... 43
ROLE OF OXIDATION OF ANTIMONY OXIDE..... 43
ISOTHERMAL OXIDATION OF Sb_2O_3..... 46
ISOTHERMAL OXIDATION OF Sb_2O_3(o)..... 51
ISOTHERMAL OXIDATION OF Sb_2O_3(c)..... 58
ISOTHERMAL OXIDATION OF MIXTURES OF Sb_2O_3(o)-Sb_2O_3(c)..... 61
EVALUATION OF ISOTHERMAL OXIDATION DATA..... 65
DIFFERENTIAL THERMAL ANALYSIS (DTA)..... 84
SUMMARY OF Sb_2O_3 OXIDATION STUDIES..... 92

CHAPTER V..... 96
PROPERTIES OF MoS_2-Sb_2O_3 SOLID LUBRICANT COMPACTS 96
COMPACTION..... 96
WEAR OF MoS_2-Sb_2O_3 COMPACTS..... 107
EUTECTIC FORMATION OF MoS_2-Sb_2O_3..... 129

TABLE OF CONTENTS (cont'd)

CHAPTER VI..... 140
DEVELOPMENT OF HYPOTHESIS FOR MoS_2-Sb_2O_3 SOLID LUBRICANT COMPACTS..... 140
ASPERITY CONTACT TEMPERATURE OF MoS_2-Sb_2O_3 COMPACTS..... 146

CHAPTER VII..... 156
OTHER OXIDES AN DISULFIDES AS BULK ADDITIONS TO MoS_2..... 156
WEAR STUDIES..... 156
MoO_3 and MoO_3-Sb_2O_3 AS BULK ADDITIONS..... 169

CHAPTER VIII..... 181
GRAPHITE Sb_2O_3 LUBRICANT COMPACT SYSTEM..... 181
ASPERITY CONTACT TEMPERATURE..... 181
WEAR STUDIES..... 187

CHAPTER IX..... 194
DISCUSSION..... 194

CHAPTER X..... 201
CONCLUSIONS..... 214

REFERENCES..... 205

APPENDIX
A 214
B 216
C 220
D 222

LIST OF ILLUSTRATIONS

Figure		Page
1.	Computation of Harmer and Pantano's Thermal Analysis Data.[8]	45
2.	Isothermal Oxidation Apparatus	47
3.	SEM Photograph of Sb_2O_3(c)	49
4.	SEM Photograph of Sb_2O_3(o)	50
5.	Isothermal Oxidation of Sb_2O_3(o)	53
6.	Repeatability of Sb_2O_3(o) Oxidation	54
7.	Parabolic Law Isothermic Oxidation of Sb_2O_3(o)	56
8.	Isothermal Oxidation of Sb_2O_3(c)	59
9.	Parabolic Law Isothermal Oxidation of Sb_2O_3(c)	60
10.	Oxidation of Sb_2O_3(o) in New and Used Reaction Tubes	62
11.	Oxidation of Mixed Dimorphic Sb_2O_3	63
12.	Parabolic Law Isothermal Oxidation of Mixed Dimorphic Sb_2O_3	64
13.	Arrhenius Plot for Sb_2O_3 Oxidation at 10% Theoretical Reaction Completion	66
14.	Arrhenius Plot for Sb_2O_3 Oxidation at 30% Theoretical Reaction Completion	67

LIST OF ILLUSTRATIONS (CONT'D)

Figure		Page
15.	Arrhenius Plot for Sb_2O_3 Oxidation at 50% Theoretical Reaction Completion.....	68
16.	Oxidation Rate of Sb_2O_3(o) as a Function of Equilibrium Sublimation Pressure.....	75
17.	Oxidation Rate of Sb_2O_3(c) as a Function of Equilibrium Sublimation Pressure.....	76
18.	Oxidation Rate of Mixed Dimorphic Sb_2O_3 as a Function of Equilibrium Sublimation Pressure.....	79
19.	Effect of Grinding on Oxidation of Sb_2O_3(o).....	86
20.	DTA of Sb_2O_3(o) Under Argon.....	87
21.	Effect of Sb_2O_4 Addition on Oxidation of Sb_2O_3(o).....	89
22.	Effect of Sb_2O_4 and Al_2O_3 Additions on Oxidation of Sb_2O_3(c).....	89
23.	DTA of Sb_2O_3(c), Sb_2O_3(o) and Mixed Dimorphic Sb_2O_3.....	90
24.	DTA of MoS_2.....	91
25.	DTA of Compacts of MoS_2-Sb_2O_3 and Sb_2O_3.....	95
26.	Theoretical Density Fraction as a Function of Forming Pressure from Harmer and Pantano.[8].....	100
27.	Density Ratio as Function of Volume Percent Additive.....	103
28.	TMA of MoS_2-Sb_2O_3 Compact.....	108
29.	Tripellet Wear Test Machine.....	113

LIST OF ILLUSTRATIONS (CONT'D)

Figure		Page
30.	Wear Cone and Pellet Mount Configuration.....	114
31.	MRI Mark-VB Single Pellet Wear Test Machine.....	119
32.	SEM Micrograph of MoS_2 Worn Surface Compact...	131
33.	SEM Micrograph of MoS_2-Sb_2O_3 Worn Compact Surface.....	132
34.	DTA of MoO_3-Sb_2O_3 Eutectic Composition.....	135
35.	Differential X-ray Diffraction Pattern for Worn and Non-Worn compact Surface.....	138
36.	Wear Volume as a Function of Mohs Hardness....	161
37.	Melt Temperature of Oxides as Function of Mohs Hardness.....	163
38.	Friction Coefficient of MoS_2-Oxide Compacts as a Function of Mohs Hardness of Oxides.....	164
39.	Wear Volume as Function of Additive Shear Strength.....	167
40.	Wear Volume and Friction Coefficient for MoS_2-MoO_3 Compacts.....	169
41.	Wear Volume for MoO_3-MoS_2 and Sb_2O_3-MoS_2 Compacts.....	170
42.	Wear Volume for MoS_2-MoO_3-Sb_2O_3 Compacts.....	171
43.	Ratio of Graphite-Sb_2O_3 to Graphite Friction Coefficients as Function of Test Temperature.	180
44.	Ratios of Graphite-Sb_2O_3 to Graphite Compact Wear Volumes as a Function of Test Temperature.....	181

LIST OF TABLES

Table		Page
1.	PROPERTIES OF ANTIMONY AND ANTIMONY OXIDES....	23
2.	ACTIVATION ENERGIES (E_a) AND PRE-EXPONENTIAL FACTORS (A) FOR THE ISOTHERMAL OXIDATION OF Sb_2O_3(o) AND Sb_2O_3(c).....	69
3.	REACTION RATES AND SUBLIMATION PRESSURES FOR Sb_2O_3(o).....	73
4.	REACTION RATES AND SUBLIMATION PRESSURES FOR Sb_2O_3(c).....	73
5.	MIXED Sb_2O_3 OXIDATION RATES AND SUBLIMATION PRESSURE.....	78
6.	FREE ENERGIES FOR OXIDATION REACTIONS.....	81
7.	FREE ENERGIES OF OXIDATION OF SUBLIMED Sb_4O_6.....	82
8.	FREE ENERGIES FOR OXIDATION OF Sb_2O_3(c) AND Sb_2O_3(o).....	83
9.	PRESSED PELLET COMPOSITION AND FORMING PRESSURE.....	97
10.	THEORETICAL COMPACT DENSITY FRACTION FOR DIFERENT FORMULATION AND FORMING PRESSURES.....	98
11.	COMPACTION OF MoS_2 AND MoS WITH Sb_2O_3 or MoO_3 AT AMBIENT.....	102
12.	DESCRIPTION OF MoS_2 FOR COMPACTS.....	108

LIST OF TABLES (CONT'D)

Table		Page
13.	SINGLE PELLET WEAR VOLUMES.....	117
14.	SINGLE PELLET WEAR DATA AT 160°C.....	120
15.	WEAR EVALUATIONS AT 232°C ON 440 C WEAR DISKS.....	121
16.	INITIAL WEAR STUDIES AT 316°C.....	124
17.	INITIAL MoS_2 ANTIMONY OXIDE WEAR TESTS ON 0.05 mm SS SHIM IN DRY AIR (100 g LOAD) AT 316°C.....	125
18.	EFFECT OF LOAD ON WEAR VOLUME FOR TESTS AT 316°C FOR 1000 SECONDS.....	127
19.	X-RAY DIFFRACTIONS MORE PROMINENET IN THE NON-WORN AREAS.....	138
20.	PELLET WEAR IN DRY AIR AT 316°C.....	158
21.	ADDITIVE DATA FOR EVALUATION OF SHEAR STRENGTH AT TEMPERATURE.....	165
22.	EFFECT OF TEST TIME ON WEAR VOLUME OF MoS_2-Sb_2O_4 COMPACTS.....	170
23.	WEAR VOLUME OF MoS_2 WITH Sb_2O_3, OR MoS_2 WITH MoO_3 AND Sb_2O_3 (DRY AIR, 316°C; 100 g LOAD).....	173
24.	WEAR VOLUME OF MoS_2 WITH Sb_2O_3, OR MoS_2 WITH MoO_3 AND Sb_2O_3 (DRY AIR, 316°C; 100 g LOAD).....	174
25.	WEAR VOLUMES AND FRICTION COEFFICIENT FOR MoS_2, MoS_2 and MoO_3 WITH MoO_3-Sb_2O_3 AND COMPOSITIONS (DRY AIR AT 589 k, 100 g LOAD, 16.7 mm).....	175

LIST OF TABLES (CONT'D)

Table		Page
26.	EFFECT OF VARYING MoO_3-Sb_2O_3 ADDITIVE CONCENTRATION ON PELLET WEAR VOLUME (316°C, 1000 SEC., DRY AIR, 100 g LOAD).....	176
27.	EFFECT OF VARYING MoO_3-Sb_2O_3 ADDITIVE CONCENTRATION ON COEFFICIENT OF FRICTION (316°C, DRY AIR, 100 g LOAD).....	177
28.	GRAPHITE AND GRAPHITE/Sb_2O_3(o) WEAR DATA.....	178

CHAPTER I

INTRODUCTION

An effort to develop high temperature solid lubricants for 315-540°C usage has recently been reported.[1] One potential application for such materials is to lubricate roller bearings in small turbine engines.[2] Typically, such an engine weighs about 65 kg, produces 3.3 kN thrust and has a shaft speed of up to 63,500 rpm. By use of solid rather than liquid lubrication, it may be possible to reduce engine weight and complexity while permitting an increase in thermodynamic efficiency due to higher operating temperature limits.

Of lubricant candidates evaluated for the proposed application, a compact of molybdenum disulfide and antimony trioxide first described by Murphy,[3] and pursued by others,[4-6] appears to be most promising. Several investigators found that such compacts, whether evaluated with or without resinous binder, are superior to molybdenum disulfide when evaluated at temperatures up to 232°C, i.e., Lavik, Hubbell and McConnell[7] noted that pellets of MoS_2-Sb_2O_3 as well as bonded film formulations containing MoS_2-Sb_2O_3 evaluated in a standard pin in V-block configuration and in a dual rub-shoe test, were all

superior to MoS_2 without the additions. Those authors offered an explanation of the beneficial interaction by attributing the superior performance of MoS_2-Sb_2O_3 compacts to a hypothesized eutectic formed of MoO_3 and Sb_2O_3. It was proposed that the low melting eutectic reduces both friction and wear volume by enhancement of effective transfer film formation in both vacuum and air and reduces the detrimental effects of wear debris generated on sliding MoS_2 in air.

Subsequently, Harmer and Pantano[8] studied MoS_2-Sb_2O_3 compacts. In that effort, chemical and mechanical properties were examined. They concluded that (i) Sb_2O_3 influenced the oxidation of MoS_2, (ii) Sb_2O_3 or Sb_2O_4 reacted with MoO_3 to produce a dense product, (iii) the morphology of wear surfaces are different if compacts contain Sb_2O_3 as compared with non-additive MoS_2 pellets, and (iv) Sb_2O_3 evidently modified the chemistry of burnished surfaces. The authors proposed that several areas were worthy of additional investigation but did not provide a conclusive explanation for the beneficial effects of Sb_2O_3 additions to MoS_2.

Nosov[9] then evaluated MoS_2, MoS_2-Sb_2O_3, and MoS_2-Sb_2S_3 solid lubricants in a dual roller test arrangement. Additions of Sb_2O_3 were found to increase MoS_2 lubricant life under both rolling and sliding conditions. If a roller coated with MoS_2-Sb_2O_3 were

pretreated by holding it at 350°C for three hours and then evaluated under ambient conditions, its life was typically increased significantly compared with MoS_2 identically pretreated. However, non-pretreated MoS_2-Sb_2O_3 formulations routinely only had 0-50% of the life of non-pretreated formulations. Nosov concluded that Sb_2O_3 and Sb_2S_3 improved the lubricating properties of MoS_2. Nosov speculated that the formation of a low melting eutectic proposed earlier [7] was not probable under the test conditions; however, it was stated that Sb_2O_3 increased the oxidation resistance of MoS_2. Nosov did not offer supporting experimental evidence for either speculation.

Later, Gardos and McConnell[1] in their study on high-temperature, high-load lubricating composites evaluated at 316°C (600°F) found that the MoS_2-Sb_2O_3 formulation was comparable with, if not superior to, other candidate solid lubricants. Those authors speculated that Sb_2O_3 might act sacrificially in oxidizing to Sb_2O_4 or higher oxides, thus retarding MoS_2 oxidation, and providing improved high temperature compact properties.

In a recent study[10] of anti-galling agents for threaded parts, it was found that formulations containing MoS_2, Sb_2O_3, and a resinous binder were superior in rider-plate and bolt-nut tests. Those authors assumed that one role of Sb_2O_3 was to prevent MoS_2 oxidation. However,

those workers did not provide experimental data to support that explanation.

Thus, in summary, since a patent in 1967[3] concerning the use of Sb_2O_3 in MoS_2 solid lubricant formulations, studies of friction and wear of MoS_2-Sb_2O_3 compacts containing up to 45 weight percent Sb_2O_3 have demonstrated that such solid lubricants are superior to MoS_2 under a variety of test conditions. During that same period, no experimental study has been conducted to confirm or disprove any of a number of hypotheses advanced to explain the beneficial effect of Sb_2O_3 additions to MoS_2.

Although the emphasis of most efforts hypothesize that the beneficial interaction of Sb_2O_3 and MoS_2 involves reduction of MoS_2 oxidation, many authors[7-10] describe the lubricating films formed when Sb_2O_3 is present as being more dense and sintered in appearance. None of the authors attribute the improved performance to the generation of a superior tribological surface by addition of Sb_2O_3.

Thus, several studies have concluded that formulations of MoS_2-Sb_2O_3 are superior to MoS_2 as solid lubricants. Alternative hypotheses have been made to rationalize the beneficial effects of Sb_2O_3 additions to MoS_2; however, a comprehensive study has not been undertaken to critically examine the validity of the hypotheses advanced and to elucidate the beneficial effects of bulk additions of Sb_2O_3

to MoS_2 or to determine if the beneficial mechanism is unique for solid lubricant compacts.

CHAPTER II

SCOPE OF THIS STUDY

Based upon a review of previous work regarding improved tribological properties of MoS_2-Sb_2O_3 formulations compared with MoS_2 solid lubricants, this effort was undertaken to critically examine the beneficial role played by Sb_2O_3 in MoS_2 solid lubricant compacts. That effort was organized as follows:

(i) Study the kinetics of oxidation of Sb_2O_3 to determine if Sb_2O_3 plays an antioxidant role in MoS_2 lubricant compacts.

(ii) Examine the possibility of Sb_2O_3-MoO_3 or Sb_2O_4-MoO_3 eutectic formation and possible beneficial role for those eutectics.

(iii) Mapping of the tribological characteristics of Sb_2O_3-MoS_2 under various conditions to elucidate the performance of the system.

(iv) Develop an understanding of the beneficial role of Sb_2O_3 and other additives in MoS_2 and determine if that role is unique for Sb_2O_3 as an additive and for MoS_2 as a solid lubricant.

(v) Develop a hypothesis for the behavior of bulk additions in solid lubricants to provide a basis for improvement of such systems.

CHAPTER III

LITERATURE SEARCH

Important in the study of beneficial bulk additions to solid lubricants is an understanding of friction and wear, lubrication, and protective mechanisms for solid compact systems containing a proven beneficial additive, Sb_2O_3.

FRICTION

The laws of friction as summarized by Clauss[11] are:

(i) Frictional resistance is proportional to the normal load on sliding surfaces:

$$F = \mu N$$

where F = frictional resistance

μ = coefficient of friction

N = normal force

μ may be additionally specified as μ_s, the static coefficient of friction experienced at sliding initiation, and μ_k, the kinetic coefficient obtained during constant sliding velocity.

(ii) Frictional resistance is proportional to the true area of contact, but not to the apparent area of contact between two bodies.

(iii) Frictional resistance is not proportional to velocity. There is an effect; but over a wide range of

sliding velocities, the coefficient tends to be rather stable unless frictional heating is involved.

(iv) The materials in contact do strongly affect frictional resistance, i.e., frictional coefficients may range from less than 0.02 to more than 1.0 depending upon the materials selected.

Additional considerations are that all surfaces are rough when examined in close detail. Early theorists thought that frictional work results from raising asperities over opposite asperities, and friction itself involves interlocking of opposing asperities. Thus, lubricants performed the simple task of filling voids between asperities and finally providing a smooth surface. However, modern theory claims that friction originates from two causes: shearing of welded junctions formed at asperity contact and ploughing that occurs as a harder material comes into contact with a softer one.

Clauss also states that important considerations regarding friction are:

(i) The true area of contact is very small compared with the projected area of contact. The amount of true contact may be roughly estimated by dividing the load by the yield strength of the material. That is, if the yield strength is 3.45 GPa and the load is 0.345 GPa, then a rough estimate of the fraction of real contact area compared to projected area is 0.10.

(ii) High temperatures, e.g., 1250 K,[12] in the contact area may be generated under sliding even at ambient temperature.

(iii) Finally, sliding is a "stick-slip" process. Under reasonable conditions, the process proceeds without detection by the casual observer.

WEAR

Wear, defined as the removal of material from solid surface, has been conveniently categorized by Rabinowicz[13] as adhesive, abrasive, corrosive, surface fracture, erosive and fretting.

Adhesive wear is thought to be most common and originates in the attractive atomic forces as two surfaces are brought together. The adhesion may result in material removal from either surface dependent upon many material and environmental factors.

Quantitatively, it has been found that for adhesive wear:

(i) Wear is directly proportional to load

(ii) Wear is directly proportional to sliding distance

(iii) Wear is typically inversely proportional to the worn surface hardness.

An adhesive law of wear as developed by Archard[14] is as follows:

$$V = \frac{k\,L\,x}{3p} \qquad (3.1)$$

where V = wear volume

L = load

x = sliding distance

p = hardness of material being worn

k = material wear constant

Thus, it is possible to predict the effect of changing critical parameters in a typical wear experiment. The relationship does not consider the effects in changes in temperature or environment that occur in wear situations.

The other common form of wear is abrasive. This form of wear occurs when a hard surface slides across a softer one creating grooves with the loss of material. Abrasive wear can be differentiated as two- or three-body wear. Two-body wear occurs when a hard, rough surface interacts with another surface, while three-body wear occurs when hard, abrasive particles interact at the sliding interface of two other materials.

A simple abrasive wear equation proposed by Rabinowicz[13] which takes the same form as the equation for adhesive wear is as follows:

$$V = \frac{\overline{\tan\theta}\ Lx}{\pi\ p} \qquad (3.2)$$

where V, L and x are as defined in the adhesive equation and

p = hardness of softer surface

$\overline{\tan\theta}$ = weighted average of tan θ's for all abrasive cones where θ is the angle between the intersecting cone and the surface minus 180°. Rabinowicz' equation yields an abrasive wear constant, k_{abr}, as follows:

$$k_{abr} = 0.96\ \overline{\tan\theta} \qquad (3.3)$$

Thus, it is possible to generate similar, simplified relationships for adhesive and abrasive wear.

For other less common types of wear, which should not be significant in this effort, similar mathematical relationships have been derived which may be applied for engineering purposes.[13]

LUBRICATION

The most effective method of lubrication[15] is to provide a hydrodynamic film between two surfaces, in which a fluid film is drawn into the contact area separating two sliding surfaces. The coefficient of friction is very low, and with good design and maintenance, component lives can be exceedingly long. When the load becomes great, the lubrication regime is elastohydrodynamic. In that regime,

lubrication is influenced by the elastic properties of the substrates. Under very high load, surface asperities come into contact, and boundary lubrication begins. Boundary lubrication occurs frequently in high load sliding, e.g., automotive and truck differentials. That type of application requires an extreme pressure additive which provides a source of renewable surface boundary lubricant. The extreme pressure additive reacts at hot spots on the surface and forms a solid lubricating surface. For most lubrication applications, fluids are adequate and perform remarkably well especially when formulated with an additive package, e.g., anti-oxidants, dispersants, and/or viscosity improvers to enable their use over a wider temperature range. However, applications under extreme environmental conditions, such as very high temperatures or vacuum, preclude the use of fluid lubricants and extreme pressure additives. In these cases a solid lubricant may be singularly applied as a replacement for a liquid lubricant or combined with a solid organic resin to form a compact for high temperature applications.

SOLID LUBRICANTS

A solid lubricant has been defined as "any solid used between two surfaces to provide protection from damage during relative movements to reduce friction and wear".[16] Many references are available[16] in which such

materials are discussed at length. Some advantages cited for use of solid lubricants include good stability at extreme temperatures and in chemically active environments which permit greater flexibility in design. Solid lubricants can be used under extremely high loads, and they are lightweight compared with conventional liquid systems. Solid lubricants, however, have many disadvantages, including a higher coefficient of friction than that in hydrodynamic lubrication, unavoidable solid sliding contact wear, finite lifetime, and no cooling capability.

Solid lubricants may be classified into several categories: (i) soft metals, such as silver and gold; (ii) laminar solids, such as graphite, molybdenum disulfide, and tungsten disulfide; (iii) non-laminar solids, such as lead monoxide, silver iodide, and calcium fluoride; (iv) complex solid compacts, exemplified by tungsten diselenide/gallium/indium; (v) soaps, fats, and waxes, such as stearic acid; and (vi) polymers, such as polytetrafluoroethylene. Each of the above solid lubricants functions by a common mechanism within that category, but typically unlike those of different categories. Also, often it is the application that critically determines which class and even which specific solid lubricant may be used.

Properties of candidate solid lubricants related to friction and wear are shear strength, hardness, mating surface adhesion and ductility. Important propeties related to overall solid lubricant performance are thermal stability, chemical inertness, particle size, purity, surface mobility , corrosion prevention and electrical conductivity. These property relationships and interactions are often complex and lead to development of completely different capabilities even within categories. For example, graphite and molybdenum disulfide lubricate by shearing interlaminarly with small forces while carrying high normal loads. For graphite, it has been observed that adsorbed water and gases improve lubrication performance. However, adsorbed species are not required for molybdenum disulfide lubrication.[17] Therefore, oxidatively stable graphite loses adsorbed species and, thus, much of its lubricating ability at higher temperatures, whereas MoS_2 lubricates effectively to relatively high temperatures without adsorbed species, but oxidizes at lower temperatures than graphite. The comparison of graphite with MoS_2 demonstrates that within each category of solid lubricants there may be examples of dissimilar performance requiring knowledgeable assessment to match a solid lubricant with an application.

Not only do solid lubricants differ chemically, physically, and in mechanisms of lubrication, but also

frequently in the method of application. Typical application methods include dispersions in oils and greases, fine powders, organic monolayers and films established by transfer, burnishing, plating, sputtering, or resin-bonding. Although transfer and burnished films have been employed with limited success over a wide temperature range, resin-bonded systems are under intensive evaluation for high temperature appliations.(16)

High temperature properties of several solid lubricants have encouraged investigations of solid lubricant capabilities in aerospace applications. Of current interest is the possibility of using solid lubricants in selected turbine engine mainshaft bearings for limited lifetime applications.(1) The rationale for using solid lubricants in such engines is that weight savings will result from the elimination of the liquid lubrication system. Also, higher operating temperatures permissible with the use of a solid lubricant shall permit improved thermodynamic efficiency. Additionally, the short operational time requirement minimizes problems resulting from the limited life of solid lubricants.

The potential for solid lubrication of small turbine engines has generated considerable developmental effort in the area of high temperature solid lubricants.(4) Many of recent developmental efforts have focused on molybdenum disulfide or other dichalcogenides. The potential

lubricating dichalcogenides are formed from Group IVB, VB, and VIB metals with a chalcogen, i.e., sulfur, selenium and tellurium. There are approximately sixty dichalcogenides formed, with two-thirds of these being layered. Of the possibilities, Magie,[18] Jamison,[19] and Gardos[1] have found that structural considerations limit good solid lubricating properties to the molybdenum, tungsten, and some niobium dichalcogenides. MoS_2 is the well-known example of this class.

Jamison[20] has observed that from a Madhukar plot[21] of the ratio of cation/anion radii versus ionicity of the bond that good solid lubricants are to be found in one area of that plot. His data imply that there are basic structural and bonding parameters which are required for a dichalcogenide to be a useful solid lubricant. The data of Jamison and Cosgrove[22] was employed to correlate predicted and actual performance of the solid lubricants.

Also, it has been observed that good solid lubricants have a trigonal prism structure with a minimum c/a (unit cell dimension ratio) of 1.93, while poor lubricants have the trigonal antiprism structure with a c/a smaller than that of the good lubricants (e.g., 1.6 or near the hard-sphere full density model). In solid lubrication studies, "c" is standardized by dividing the true crystallographic "c" value by the number of X-M-X layers in a single unit cell, where "X" is the chalcogen and "M" is the metal.

Based upon these observations, several efforts have been made to prepare intercalates, i.e., materials with atoms inserted into the X-X layer. The intercalates have been predicted to have superior lubricating properties as compared with nonintercalates. The premise is that if atoms can be introduced between the chalcogenic layers, then shearing will require less force; thus, lubrication would be improved.[19]

Compacts consisting of WS_2/Ga/In have also been developed[23,24] and have excellent static thermal properties and good room temperature lubricant properties. When compared with MoS_2, however, the alternative solid lubricant may have one modestly superior property, but other properties, such as fatigue strength often fall short of that of MoS_2.[25] These materials also must be produced synthetically at considerable cost while the natural MoS_2 ore, molybdenite, can be processed for use as a solid lubricant with little effort at lower costs. Thus, the search for a good high temperature solid lubricant for many applications has not proven fruitful.

PROPERTIES OF AND OXIDATION OF MOLYBDENUM DISULFIDE

Historically, molybdenum disulfide[26] was confused with graphite because general appearance and lubricating characteristics were similar. That confusion ended when Scheele demonstrated in 1778 that MoS_2 contained sulfur and prepared molybdic acid ($MoO_3 \cdot 2H_2O$) from molybdenite.[27]

Molybdenum disulfide is a soft lead-grey compound. It has a metallic luster and contains 59.94 weight percent molybdenum and 40.06 weight percent sulfur. MoS_2 has a specific gravity of 4.8 and melts at 1185°C.[28] Other sulfides such as Mo_3S_4, Mo_2S_3, MoS_4 and MoS_3 are known.[28] Oxysulfides are known but are not stable.[29]

A comprehensive review[17] of molybdenum disulfide structures and lubricating properties has been prepared. The structure was first determined by Dickinson and Pauling.[30] Molybdenum is strongly bonded between layers of sulfur while adjacent sulfur layers are only weakly bonded by van der Waals forces. Sliding takes place interlaminarly between sulfur layers and, unlike graphite, no interlaminar adsorption of water or condensable gases is required for lubricating action; however, water vapor does have a beneficial effect up to about 65% relative humidity.

The review[17] also summarizes the effect of load, sliding speed, temperature, vacuum, radiation, substrate, particle size, impurities and crystallographic orientation on the behavior of MoS_2 as a lubricant. The substrate and orientation of MoS_2 films does affect frictional properties. Particle size effects are related to ease of oxidation and the formation of MoO_3.

Of the MoS_2 oxidation studies, Cardoen's[31] appears to be the most comprehensive. In that study, compacts of molybdenite were oxidized under various oxygen

concentrations. After test, weights of pellets and observation of the oxidation interface, if available, were used to assess oxidation behavior over the 450° to 700°C temperature range. In the studies, the formation of MoO_2 was considered and calculations were made which showed that MoO_2 is metastable at temperatures over 350°C and at oxygen pressures exceeding 10^{-21} atmosphere.

Cardoen[31] was also able to define five oxidation regions for molybdenite. It should be emphasized that those regions were established for the oxidation of molybdenite containing impurities, not pure MoS_2, and for compressed samples in which cracks and pathways for oxygen transport probably exist. Both objections were addressed by Cardoen, although his arguments are not completely satisfying.

In discussion, Cardoen notes that there are five steps in a gas-solid reaction. Those steps are:

(i) Diffusion of reactants to solid surface.

(ii) Adsorption of reactants on the surface.

(iii) Reaction on the surface.

(iv) Desorption of products of reaction.

(v) Diffusion of products away from surface.

If steps (i) or (v) are rate controlling, the rates are parabolic and usually involve a protective coating of reaction products.

The Pilling-Bedworth (PB) ratio[32] is used to assess the possibility of a protective layer being formed. Essentially, if the ratio of the volume of oxide formed is greater than the volume of the solid from which it is formed, then the oxide may protect (PB = 1 to 2). However, if the PB is less than one, then coverage of the substrate cannot be complete and the outer layer will not protect. Of course, if PB is large, then the layer can spall and provide reduced protection. The ratios are only approximate and the rule is only for guidance.

The PB for MoO_3/MoS_2 is 0.916. Therefore, Cardoen[31] concluded that the oxide is nonprotective. This conclusion was supported by his experimental data since linear kinetics were observed. His linear rate law conclusion is unlike the parabolic laws found by others.[33] Cardoen[31] cites the exothermic surface reaction as the origin of incorrect rate law interpretation problems of others.

Based upon his results, Cardoen proposed that the linear oxidation of molybdenite takes place as follows:

$$\text{¦}S + O_2 \rightleftarrows \text{¦}\ddagger\text{¦} + \text{¦}S \cdot O_2$$

$$\text{¦}S \cdot O_2 + MoO_2 + S_2$$

$$2MoO_2 + O_2 \rightleftarrows 2MoO_3$$

$$S_2 + 2O_2 \rightleftarrows 2SO_2$$

where ¦ represents the surface and ‡ an activated complex.

Modern surface analytical instrumentation has been employed to examine molybdenum sulfide and molybdenum oxide surfaces.[34-42]

ANTIMONY OXIDES

Antimony[43] forms several oxides which are listed along with handbook data[28] on those oxides in Table 1. In the listed oxides, antimony is either tri or penta valent. Sb_2O_4 ($Sb_2O_3 \cdot Sb_2O_5$) contains both tri and penta valent antimony. Additionally, evidence exists for Sb_6O_{13}.[44] Hydrated forms of Sb_2O_3 and Sb_2O_5 are known as antimonious and antimonic acids, respectively. Antimony and some antimony compounds are toxic and must be handled cautiously.

Remy[45] reported that the cubic structure of the dimorphic trioxide is composed of Sb_4O_6 groups (antimony sequioxide) occupying the points of a diamond lattice with a cube edge of 11.14Å. Adjacent molecular centers are 4.84Å apart. The Sb_4O_6 molecule consists of an octahedron of oxygen atoms, with Sb atoms forming an interpenetrating tetrahedron. The Sb-O distance is 2.22Å. The orthorhombic dimorph has infinite chains of Sb_2O_3 composition where weak Sb-O bonds hold the structure together.

Roberts and Fenwick[46] found that the trioxide in the low temperature cubic form is stable up to the transition temperature of 570 ± 10°C, while the orthorhombic dimorph

TABLE 1. PROPERTIES OF ANTIMONY AND ANTIMONY OXIDES

ELEMENT OR COMPOUND	FORMULA	FORMULA WEIGHT	CRYSTAL FORM	SP GRAV	MELT POINT (°C)	BOILING POINT (°C)
Antimony	Sb	121.75	Hex, Silver White Metal	6.69	630.5	1380
Senarmontite	Sb_2O_3(c)	291.5	Cubic, White	5.2	656	1550 (subl)
Valentinite	Sb_2O_3(o)	291.5	Rhomb. Colorless	5.67	656	1550
Cervantite	Sb_2O_4	307.5	White Powder	5.82	-0,930	--
Antimony Pentaoxide	Sb_2O_5	323.5	Yellow Powder	3.80	-0,380 $-O_2$,930	

is stable up to the melting point of about 650°C. $Sb_2O_3(o)$ exists at room temperature in a metastable state.

More recent data generated by White, et al.,[47] in a high pressure study of the transition temperature of Sb_2O_3 indicates a reversible transition temperature of 606°C with a heat of transition of about 1000 cal/mole. They employed the Clausius-Clapeyron relationship as follows:

$$\frac{dp}{dT} = \frac{\Delta H}{T\Delta V} \qquad (3.3)$$

where p = pressure

T = temperature

ΔH = enthalpy of transition

ΔV = volume change

and calculated molar volumes from x-ray data of 52.216 cm^3 for $Sb_2O_3(c)$ and 50.021 cm^3 for $Sb_2O_3(c)$ to determine the heat of transition.

The metastable $Sb_2O_3(c)$ to $Sb_2O_3(o)$ transition has been studied in the 490-530°C temperature range.[48] In that effort, infrared spectroscopy was employed to analyze mixtures after thermal treatment. The activation energy for the transformation was found to range from 46 to 50.8 kcal/mole. It was claimed that heterogeneous nucleation of the $Sb_2O_3(c)$ on the $Sb_2O_3(o)$ surface is followed by growth of the more stable $Sb_2O_3(o)$. The rate controlling step was stated to be sublimation of $Sb_2O_3(o)$. Additional

supporting evidence was offered in noting that the heat of sublimation of $Sb_2O_3(o)$ is about 43.6 kcal/mole. This concept supported by the sublimation pressure data of Hincke[49] and Jungermann and Plieth.[50] Hincke[49] measured the vapor sublimation pressure data of the solid Sb_2O_3 dimorphs over the temperature range of 470° to 650°C by weighing sublimate in an inert atmosphere. The vapor pressure of liquid Sb_2O_3 was determined from 656° to 800°C. The vapor pressure as function of temperature relationships are expressed as follows:

$$\log_{10}p = 12.195 - \frac{10357}{T} \text{ (cubic)} \qquad (3.4)$$

$$\log_{10}p = 11.318 - \frac{9625}{T} \text{ (orthorhombic)} \qquad (3.5)$$

$$\log_{10}p = 5.137 - \frac{3900}{T} \text{ (liquid)} \qquad (3.6)$$

where p = sublimation pressure (torr)
and T = absolute temperature (K).

The heats of sublimation found by Hincke are 47.32 kcal/mole (cubic), 44.08 kcal/mole (orthorhombic), and heat of vaporization is 17.83 kcal/mole (liquid). The heat of transition was found to be 3.24 kcal/mole at 557°C. Heat of fusion for the cubic form was found to be 29.49 kcal/mole and for the orthorhombic form, 26.25 kcal/mole.

Much more recently, Jungermann and Plieth[50] used a Knudsen cell and a sublimation weight apparatus to derive the following sublimation pressure equations:

$$\log_{10}p = 11.74 - \frac{9568}{T} \text{ (cubic)} \qquad (3.7)$$

$$\log_{10}p = 11.35 - \frac{9535}{T} \text{ (orthorhombic)} \qquad (3.8)$$

where p and T are defined above.

Jungermann and Plieth found the heat of sublimation for Sb_2O_3(c) is 43.8 ± 1.0 kcal/mole and 43.6 ± 1.8 kcal/mole for Sb_2O_3(o).

The heats of formation (298°K) for the antimony sesquioxide are as follows: $\Delta H^o_{f(c)}$ = -164,430 cal/mole (cubic) and $\Delta H^o_{f(o)}$ = -167,210 cal/mole (orthorhombic), and for free energies, ΔG^o_c = -149,690 cal/mole and ΔG^o_o = -147,900 cal/mole.[51]

The specific heat from 273-929°K for Sb_2O_3 is reported by Maier[51] as follows:

$$Cp_{Sb2O3} = 19.1 + 0.0171T \qquad T = K \qquad (3.9)$$

and for Sb_2O_4 over undefined temperature range,

$$Cp_{Sb2O4} = 22.6 + 0.0162T \qquad T = K \qquad (3.10)$$

It is assumed that C_p for cubic and orthorhombic forms of Sb_2O_3 are identical.

In a vibrational and thermal study of the antimony oxides, Cody, DiCarlo and Darlington[52] found that both $Sb_2O_3(c)$ and $Sb_2O_3(o)$ when heated to 1000°C under nitrogen lose weight by a two-stage process: sublimation of the solid followed by volatilization of the melt. Examination of the thermograms presented by those authors indicate that $Sb_2O_3(c)$ loses weight over a smaller temperature interval than $Sb_2O_3(o)$ and that volatilization of $Sb_2O_3(c)$ is complete at a lower temperature than $Sb_2O_3(o)$.

The oxidation studies of the trioxide dimorphs by Cody, et al.[52] addressed some controversy generated in earlier thermogravimetric analysis (TGA) and differential thermal analysis (DTA) studies by Agrawal, et al.[53] In that study, TGA and DTA data for cubic Sb_2O_3 in inert and oxidizing atmospheres was reported. They claimed a TGA weight gain under oxidizing conditions of 4.5% for $Sb_2O_3(c)$ which is slightly less than the 5.49% expected for the following reaction if no sublimation of the starting material occurs:

$$2Sb_2O_3 + O_2 \rightarrow 2Sb_2O_4 \qquad (3.11)$$

Agrawal, et al.,[53] data for cubic Sb_2O_3 is similar to that of Cody, et al., for orthorhombic Sb_2O_3 and may be

rationalized if dimorphic identification by Agrawal, et al., was incorrect.

The oxidation at 490°C of orthorhombic Sb_2O_3 to orthorhombic Sb_2O_4 ($Sb_2O_3 \cdot Sb_2O_5$) was found to be topotactic by Gopalakrishnan and Manohar[54] who used x-ray techniques to determine structure of the reaction product. In a topotactic reaction there is a three-dimensional orientational relationship between the original and final lattice. The same investigators calculated shifts in individual atom positions during oxidation is no more than 0.6Å. The oxidation was thought to be the result of oxygen moving along empty channels in the Sb_2O_3(o) structure to the reaction site. Then an oxygen atom bridges two antimony atoms of neighboring chains. Calculations based on unit cell dimensions indicated that there is a 7.4% volume contraction when Sb_2O_3(o) is oxidized to Sb_2O_4. Additional experiments indicated that the reduction of Sb_2O_4 to Sb_2O_3(o) under hydrogen (430°C, 1 atm., 4 hrs.) is also topotactic. Sb_2O_3(o) was formed, not Sb_2O_3(c), even though Sb_2O_3(c) is stable at the reaction temperature.

Those authors[55] also determined in poly and single crystal Sb_2O_3(o) oxidation studies that the rate law is parabolic suggesting an oxygen diffusion mechanism as the rate controlling step. Using a polarized light method for single crystals, they determined the activation energy for

two crystallographic directions. The activation energies were found to vary from 36 to 55.5 kcal/mole depending upon the crystallographic axis observed. The fastest reaction occurred through openings between chains of Sb_2O_3(o). The authors concluded that since the openings are not sufficiently large for simple free oxygen diffusion, the mechanism probably consisted of making, breaking and remaking bonds between oxygen and antimony atoms. A similar oxidative study of Sb_2O_3(c) has not been reported in the literature.

Harmer and Pantano[8], in a study of the synergistic interaction of Sb_2O_3 additions to the solid lubricant MoS_2, obtained TGA data for those materials. Those investigators noted a 21.7% weight loss for Sb_2O_3. They did not identify the dimorph evaluated nor the TGA heating rate. A proposed reaction to rationalize the weight loss was given as follows:

$$4Sb_2O_3 + \frac{5}{2}O_2 \rightarrow 3Sb_2O_4 + Sb_2O_5 \qquad (3.12)$$

followed by

$$Sb_2O_5 \rightarrow 2Sb\uparrow + \frac{5}{2}O_2\uparrow \qquad (3.13)$$

The hypothesis was justified by the handbook decomposition temperature[28] of Sb_2O_5 reported to be

400°C, near the 410°C inflection temperature observed in the thermogram, and the calculated weight loss is 20.9% in good agreement with the observed value. However, decomposition temperatures reported by Golunski, et al.,[56] in more recent experiments where Sb_2O_5 gradually loses O_2 at temperatures above 400°C and decomposes as follows at higher temperatures:

$$Sb_2O_5(c) \xrightarrow{650\text{-}700^0C} Sb_2O_4(o) \text{ (stable to 1000°C)} \qquad (3.14)$$

This decomposition reaction and temperature do not support the overall mechanism proposed by Harmer and Pantano.[8]

In the subsequent comprehensive study, Cody, et al.,[52] obtained additional oxidative thermograms. In those studies, it was found that when the temperature of either $Sb_2O_3(c)$ or $Sb_2O_3(o)$ is increased rapidly (20°C/min) in air, the product is orthorhombic Sb_2O_4. However, $Sb_2O_3(c)$ experiences a 21% weight loss while $Sb_2O_3(o)$ gains 0.8% weight. They claimed that the competing processes of sublimation and reaction of $Sb_2O_3(c)$ and $Sb_2O_3(o)$ are responsible for the weight loss and gain, respectively.

Thus, it is seen that if Harmer and Pantano[8] evaluated $Sb_2O_3(c)$ and if their TGA heating rate was sufficiently less than that of Cody, et al.,[52] then their data are in agreement with that of Cody, et al., but are in disagreement with that of Agrawal, et al.,[53]. Comparison

of thermograms suggests that Agrawal, et al., may have oxidized Sb_2O_3(o) rather than Sb_2O_3(c) as noted earlier. These contradictory data suggest that the Agrawal, et al., DTA on Sb_2O_3(c) is suspect.

Golunski, et al.,[56] resolved some of the issues generated in earlier studies in their comprehensive study of the thermal stability of the oxides of antimony. They found that Sb_2O_3(o) produced a large DTA endotherm under flowing nitrogen with onset at 628°C and peak at 643 ± 2°C. By TGA, weight loss was not significant until temperatures above 625°C under nitrogen were reached. Infrared and x-ray analysis of the cooled DTA product indicated no change. Therefore, it was concluded that in an inert atmosphere, orthorhombic Sb_2O_3 begins to melt at 628°C after which the liquid formed volatilizes.

In flowing air, DTA for Sb_2O_3(o) exhibited a large irreversible exotherm with a peak at 463°C with TGA indicating large changes in output depending upon experimental conditions. Infrared and x-ray analysis confirmed that Sb_2O_3(o) is converted to Sb_2O_4 in the temperature range of 500-700°C. Sb_2O_4 was found to be stable to a temperature of 1105°C.

In similar experiments with Sb_2O_3(c), Golunski, et al. found in DTA analysis that the dimorph in flowing nitrogen exhibited two peaks. The first, which was irreversible with onset at 629°C and peak at 639°C, was attributed to

the transformation to Sb_2O_3(o). This was confirmed by infrared analysis of the product. The second peak, reversible, with an onset at 643 ± 2°C and peaked at 651 ± 2°C was related to as the melting and immediate progressive vaporization of molten Sb_2O_3.

For DTA experiments, the heating rate was 10°C/min. For nitrogen or air, the flow rate was 500 cm^3/min. In TGA experiments, the heating rate was 15°C/min with a flow rate of either air or nitrogen of 200 cm^3/min.

The data of Golunski, et al.,[56] confirm the work of Cody, et al.,[52] regarding the inaccuracies in the data presented by Agrawal, et al.[53] DTA for the oxidation of Sb_2O_3(c). The data also offer an alternative to the mechanism proposed by Harmer and Pantano[8] for oxidation of Sb_2O_3 generated in their TGA study. That is, the Sb_2O_3 (unknown structure) thermally analyzed in air by Harmer and Pantano was, most probably, oxidized while a portion of the sample volatilized simultaneously thus explaining their results. DTA and TGA results are obviously dependent upon the dimorph used, particle size and distribution, heating rate and atmospheric conditions which offer an explanation for the varied results generated experimentally and the hypotheses proposed to rationalize the data.

It is noted that in addition to orthorhombic α-Sb_2O_4, formed in the above oxidation reactions, another polymorph,

β-Sb_2O_4 (monoclinic), exists as reported by Rogers and Skapski.[57] The structure was determined using x-ray methods. Since it is claimed that α-Sb_2O_4 forms in air or oxygen, Rogers and Skapski suggested the following mechanism for the transformation:

$$2\alpha\text{-}Sb_2O_4(s) + Sb_4O_6(vapor) + O_2 \rightarrow 2\ \beta\text{-}Sb_2O_4(s) \qquad (3.15)$$

In more recent studies by Cody, et al.,[52] it is suggested that the above mechanism may be erroneous, since β-Sb_2O_4 was not produced when α-Sb_2O_4 was exposed to flowing oxygen at 1130 - 1180°C. Evidently, β-Sb_2O_4 is a stable high pressure form of Sb_2O_4, since β-Sb_2O_4 was formed in a few minutes at 960°C in sealed capillaries (~5 atm) by the latter investigators. The mechanism of transformation is still uncertain. Temperature and pressure for the transformation are yet to be adequately defined.

Analytical methods employed in the above and other studies of antimony oxides which have proven useful include x-ray,[44,52] infrared,[48,52] Raman,[52] Mossbauer,[44] XPS,[58,59] and Auger[59,60] spectroscopy.

PROTECTIVE INTERACTION OF Sb_2O_3 ADDITION TO MoS_2

The first description of the use of Sb_2O_3 in a MoS_2 solid lubricant system was made in a 1966 patent by Murphy.[3] He claimed that solid film epoxy-phenolic-

bonded solid lubricants containing both Sb_2O_3 and MoS_2 with other inorganic or organic components exhibited Falex test machine wear lives of 500 minutes, and time to failure for coated 1020 steel panels under 20% salt spray of 120 hours. In his formulation, the weight percentage of Sb_2O_3 was 6.2% while MoS_2 was 17.4%.

Since the granting of Murphy's patent, there have been several studies directed toward developing an optimum Sb_2O_3-MoS_2 formulation with only minor effort devoted to examining mechanisms repsonsible for the protective role of Sb_2O_3 when added to MoS_2.

Following several exploratory efforts[4,5] to develop optimum resin-bonded film performance, the first study to offer an interaction rationale for the Sb_2O_3-MoS_2 system was given by Lavik, Hubbell and McConnell.[7] In 1975, they offered the hypothesis that an eutectic of Sb_2O_3 and MoO_3 forms on a lubricating compact of Sb_2O_3 and MoS_2. During sliding interfacial oxidation at hot asperity sites would provide materials for eutectic formation so that additional enhanced transfer films formation occurs. Those authors evaluated resin-bonded MoS_2/Sb_2O_3 lubricants, 'n a dual rub-shoe test, bonded films of MoS_2/Sb_2O_3 using the Falex method, and compacts of MoS_2/Sb_2O_3 in a pellet test. The addition of Sb_2O_3 improved the wear life of MoS_2 in the resin-bonded materials. Significantly, when the effects of the resin binder were eliminated in a pellet

study, wear life was again superior for MoS_2 compacts containing 45 volume percent Sb_2O_3 compared with MoS_2 compacts without Sb_2O_3.

The authors did not offer any evidence to support the mechanism proposed. That is, no evidence for the existence or formation of the proposed eutectic was given, rather only test data indicating superiority of the MoS_2/Sb_2O_3 lubricant as cited above was provided.

They also noted that improvement in coefficient of friction was found for the compounded lubricant compared with noncompounded MoS_2.

A subsequent study of the system was conducted by Harmer and Pantano[8] who reviewed the work of Hopkins and Campbell[61] noting that the study was inconclusive regarding the properties of the MoS_2-Sb_2O_3 solid lubricant system. Harmer and Pantano stated that the inconsistencies in data reported for the MoS_2-Sb_2O_3 system might be related to the use of polyimide as a resin binder as compared with MoS_2-Sb_2O_3 bonded with a phenolic-epoxy. Close examination of the data presented indicates that some test were run in dry atmosphere while others were conducted in relatively high humidity conditions. The effect of water on the polyimide available at that time is well-known;[62,63] thus, the data can be rationalized since the polyimide composite was far superior to the phenolic-epoxy and all others in a nitrogen pellet test, yet inferior to the

phenolic-epoxy when run in ambient air journal bearing tests. Therefore, it appears that the Hopkins and Campbell[61] data can be satisfactorily rationalized based solely on consideration of the deleterious effects of water on the properties of polyimides.

Harmer and Pantano[8] conducted a preliminary study directed towards the elucidation of the interaction of MoS_2 and Sb_2O_3 as referred to earlier. They employed thermogravimetric methods (TGA), x-ray diffraction, and Auger analyses of compacted and burnished materials to generate some basic data on the interaction. Among their conclusions were that: (i) distinct evidence of chemical interaction Sb_2O_3/MoS_2 was found in TGA (air) studies; (ii) MoS_2 was oxidized to MoO_3 and Sb_2O_3 to Sb_2O_4 as shown by x-ray studies; (iii) Sb_2O_3 or its oxidation product, Sb_2O_4, did promote sintering of MoO_3; (iv) MoO_3 showed little solubility in Sb_2O_4, and conversely, Sb_2O_4 showed little solubility in MoO_3; (v) Auger studies indicated that Sb_2O_3 containing treated pellet surfaces were significantly different from those of pure MoS_2; and (vi) Mo concentrations near pellet surfaces of MoS_2/Sb_2O_3 were anomalously low. Rationale for these results was not presented.

Harmer and Pantano indicated that additional efforts should be expended to determine if (i) the microstructures of the solid lubricant transfer film changes with Sb_2O_3

addition; (ii) segregation of Sb_2O_3 or Sb_2O_4 occurs at the sliding interface; (iii) there is a role for water vapor; and (iv) changes in the surface chemistry affect the lubricant properties of MoS_2/Sb_2O_3 films, especially the role of sulfur.

Although Harmer and Pantano[8] claimed to find evidence of interaction and thought that eutectic formation might play a role, no direct evidence of the formation of a eutectic was offered. Because of lack of funding, their effort was, unfortunately, discontinued.

A subsequent effort by Nosov[9] in 1978 reported upon the lubricating properties of molybdenum disulfide with additives of antimony oxide and antimony sulfide. Nosov conducted an empirical study of MoS_2 coatings containing various concentrations of Sb_2O_3 or Sb_2S_3. Those tests determined the time required to abrade coating in both sliding and rolling contact. Nosov concluded that the antimony compounds showed high tribochemical activity and improved the lubricating properties of MoS_2 base coatings. He further stated without evidence that the formation of an eutectic in the contact zone was not very likely under standard test conditions because of temperatures as proposed by Lavik, et al.[7] Nosov also claimed without direct evidence that antimony trioxide increases the oxidation resistance of MoS_2 coatings.

The most recent work in which MoS_2/Sb_2O_3 formulated solid lubricants were used is that of Gardos and McConnell.[1] In the study potential high-temperature solid lubricants were evaluated in resin-bonded dual rub-shoe test configuration. Sb_2O_3/MoS_2 lubricant was employed as the standard. The reference shoe composition was 40 weight percent MoS_2, 30 weight percent Sb_2O_3, and 30 weight percent polyimide.

They compared various other solid lubricants to the above reference formulation. The results indicated that only one of the studied formulations was marginally superior to the standard MoS_2-Sb_2O_3 formulation. Gardos and McConnell's concluding comment regarding the protective mechanism of Sb_2O_3 additions to MoS_2 was that, based upon all the evidence to date, Sb_2O_3 has an oxygen scavenging role, i.e., in mixtures of MoS_2 and Sb_2O_3, the Sb_2O_3 will be preferentially oxidized. No experimental evidence was offered to support their conclusion.

The above summarizes the significant work concerning the apparent synergism of Sb_2O_3 additions to MoS_2 which provide improved tribological performance.

In review of the hypotheses, it is plausible that an eutectic of Sb_2O_3 and MoO_3 might be formed at the sliding interface and in some manner improve tribological properties, since eutectics of Sb_2O_3-MoO_3 are known.[64] The second hypothesis, proposing sacrificial oxidation of

Sb_2O_3 to Sb_2O_4 or higher oxides thus preventing oxidation of MoS_2, lacks plausibility since earlier workers had found that Sb_2O_3 additions were beneficial even when evaluated in vacuum.[7] Thirdly, hypotheses involving an assumed role for Sb_2O_3 in retardation of MoS_2 oxidation have not been sufficiently defined to critically analyze without additional data. The eutectic and oxidation retardation hypotheses will be discussed in greater detail.

The eutectic hypothesis proposes that is might be possible for an eutectic of oxides to promote attachment of a MoS_2 transfer film to a sliding surface. Although consideration of the possible role of eutectic formation and/or oxygen scavenging by Sb_2O_3 was given by some investigators,[1] none of the workers sought or found the Sb_2O_3-MoO_3 phase diagram in the literature as reported by Parmentier, Courtois and Gleitzer in 1974.[64] Coincidentally, the empirically optimized formulations, found by Lavik, et al.,[7] and Gardos and McConnell,[1] are very close in composition to that of the highest melting point eutectic composition found by Parmentier, et al., which would be derived from a compact containing the largest fraction of MoS_2.

If the eutectic performs a role, then the selected formulations may be rationalized as resulting from the need to form the compact with as much MoS_2 as possible since it is obviously the primary lubricant along with the need to

form a low-temperature eutectic for improved tribological properties. Such a point is near the experimental formulations[1,7] which appear to offer the best combination of properties. The coincidence of a eutectic point with typical formulations does not provide direct evidence for the role of a eutectic, but it is obvious that the possibility exists from a study of the phase diagram.

However, if one considers that investigators[65] have estimated a typical MoS_2 film is 1-2 x 10^{-6}m, and since the distance between molybdenum layers in MoS_2 is 6.16 x 10^{-10}m,[66] then under typical sliding conditions more than 3,000 layers of MoS_2 might be between the substrate and sliding interface. The thickness of MoS_2 weighs against attachment of MoS_2 to a substrate by an oxide as being the critical mechanism involved in improvement of tribological properties when such bulk additions are required. Because there are nearly 3,000 layers of MoS_2 between the site of the proposed effect and the sliding zone, it would appear that an alternative mechanism involving the entire solid lubricant film structure would be more plausible.

One possible mechanism for Sb_2O_3 retarding MoS_2 oxidation could be similar to the mechanism in which it is employed as an antitoxidant in plastics and other solids.[67] However, it is known that the presence of a halogen is required for Sb_2O_3 to act effectively as an

antioxidant involving the formation of $SbCl_3$ where Cl is an example of a halogen as follows:

$$Sb_2O_3 + 2HCl \rightarrow 2SbOCl + H_2O \quad (3.16)$$

followed by

$$SbOCl + 2HCl \rightarrow SbCl_3 + H_2O \quad (3.17)$$

$SbCl_3$ acts as both a dehydrating agent and a free radical chain terminator. In the MoS_2-Sb_2O_3 formulations evaluated previously, none contained halogens. Alternatively, if the mechanism is assumed to be one where Sb_2O_3 acts to block diffusion of oxygen into the MoS_2 matrix, thereby retarding oxidation, then many other materials would be effective additives which previous investigators did not claim.

Similarly, MoO_3 has been used as a flame retardant,[68] although the mechanism is evidently not similar to Sb_2O_3. In polyvinyl chloride, MoO_3 acts to isomerize trans conjugated polyene structures produced on the loss of hydrogen chloride which is the first step in the pyrolysis of polyvinyl chloride.[69] The cis isomer produced in the presence of MoO_3 as a Lewis acid is more thermally stable. Therefore, the flame retardant mechanism of MoO_3 is totally dissimilar to that of Sb_2O_3 which is also used in polyvinyl chloride. The mechanisms by which

Sb_2O_3 and MoO_3 act as flame retardants for other materials do not appear to be possible in MoS_2-Sb_2O_3 compacts.

CHAPTER IV

ROLE OF OXIDATION OF ANTIMONY OXIDE

An understanding of Sb_2O_3 oxidation is required for elucidation of its beneficial role in MoS_2 compacts, since previous investigators have suggested that such Sb_2O_3 oxidation may be critical. For example, Gardos and McConnell[1] proposed, without experimental data to support the concept, that Sb_2O_3 is preferentially oxidized rather than MoS_2. Thus, the sacrificial oxidation of Sb_2O_3 would reduce the rate of oxidation of MoS_2 to MoO_3 and to molybdenum sulfate compounds, which would result in reduced wear while maintaining low friction. With respect to this hypothesis, Harmer and Pantano[8] in thermal gravimetric apparatus (TGA) studies found that MoS_2 started to oxidize at 300°C with oxidation to MoO_3 being completed by 490°C followed by loss of MoO_3 by sublimation. They also found that Sb_2O_3 initially lost weight at 410°C followed by more rapid weight loss until 545°C. Then the weight remained constant until 955°C. Harmer and Pantano interpreted these data as oxidation of Sb_2O_3 to Sb_2O_4 and rationalized the unexpected weight loss as resulting from a reaction involving the formation of Sb_2O_5, which then decomposed to Sb sublimate and O_2. They did not consider sublimation of

Sb_2O_3, which was found to occur simultaneously with oxidation in similar experiments by Cody, et al.[52] The net effect of oxidation and sublimation of Sb_2O_3(c) resulted in a 21 percent weight loss nearly identical with the Harmer and Pantano results.

Harmer and Pantano also obtained TGA data for mixed MoS_2 (75 weight percent) and Sb_2O_3 (25 weight percent). In dry air, they found a slight increase in weight at 348°C followed by weight loss until 468°C. Then the weight remained stable until a slight increase at 550°C followed by very dramatic weight loss from about 650° to 863°C. These data, based upon Cody, et al., conclusions can be rationalized as a combination of MoS_2 and Sb_2O_3 oxidation, Sb_2O_3 and MoO_3 sublimation, followed by eventual sublimation of Sb_2O_4, without proposing a mechanism wherein Sb_2O_3 retards oxidation of MoS_2. Especially significant in Harmer and Pantano's analysis was a conclusion that since the weight loss at 480°C was only 9.5 weight percent rather than nearly 14 weight percent predicted by theory, then some role for Sb_2O_3 in retarding MoS_2 oxidation must be assigned. Again, however, simultaneous oxidation and sublimation of Sb_2O_3 was not considered. Harmer and Pantano also analyzed a 45 weight percent Sb_2O_3 55 weight percent MoS_2 mixture. TGA results for that mixture of Harmer and Pantano[8] are redrawn in Figure 1 where those data are compared with oxidation of MoS_2 and Sb_2O_3. Weight

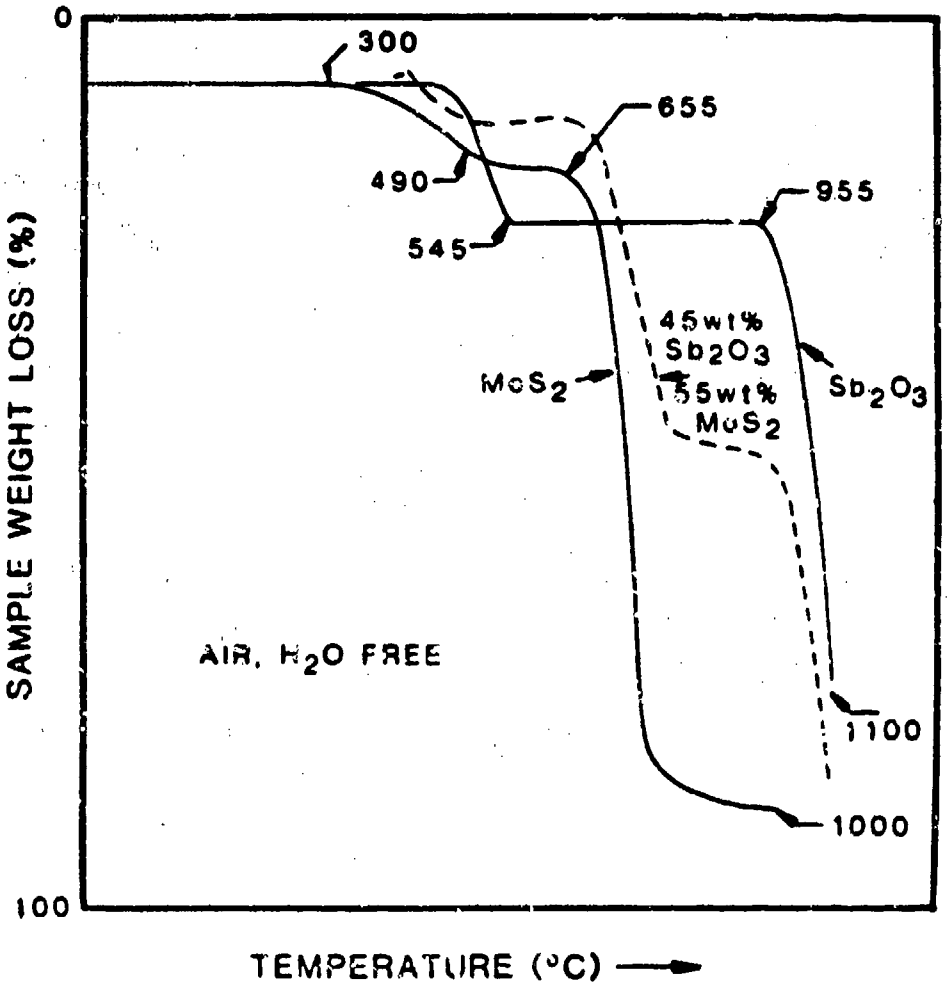

Figure 1. Compilation of Harmer and Pantano's Thermal Analysis Data.(8)

losses and temperatures of inflections were slightly different from those found for the 25 weight percent Sb_2O_3 -75 weight percent MoS_2 data, however, differences in the analyses may be rationalized if sublimation of Sb_2O_3 and its effect on reaction rates are considered.

Therefore, because of the evident need to examine the role of antimony oxide oxidation as a beneficial mechanism of Sb_2O_3 additions to MoS_2, and the fact that isothermal kinetic data for the oxidation of Sb_2O_3(c) have not been reported, which might be significant in such a protective role, a study of the oxidation of Sb_2O_3 and its possible influence on lubricant compact performance was undertaken.

ISOTHERMAL OXIDATION OF Sb_2O_3

Isothermal kinetic studies were undertaken using various particle sizes of the dimorphs of Sb_2O_3. Each dimorph and mixtures were oxidized. The method was to employ a closed glass reaction system that could be used to maintain oxygen at nearly constant pressure (140 torr) and that would permit measurement of the volume of O_2 consumed by means of an O_2-filled gas buret as given in Figure 2. A Stone differential thermal analysis (DTA) Model F-1DF furnace was used to maintain a constant reaction tube temperature, which was measured using a chromel-alumel thermocouple accurate to ±0.4%. This system is similar to the one used by Gopalakrishnan and Manohar in their

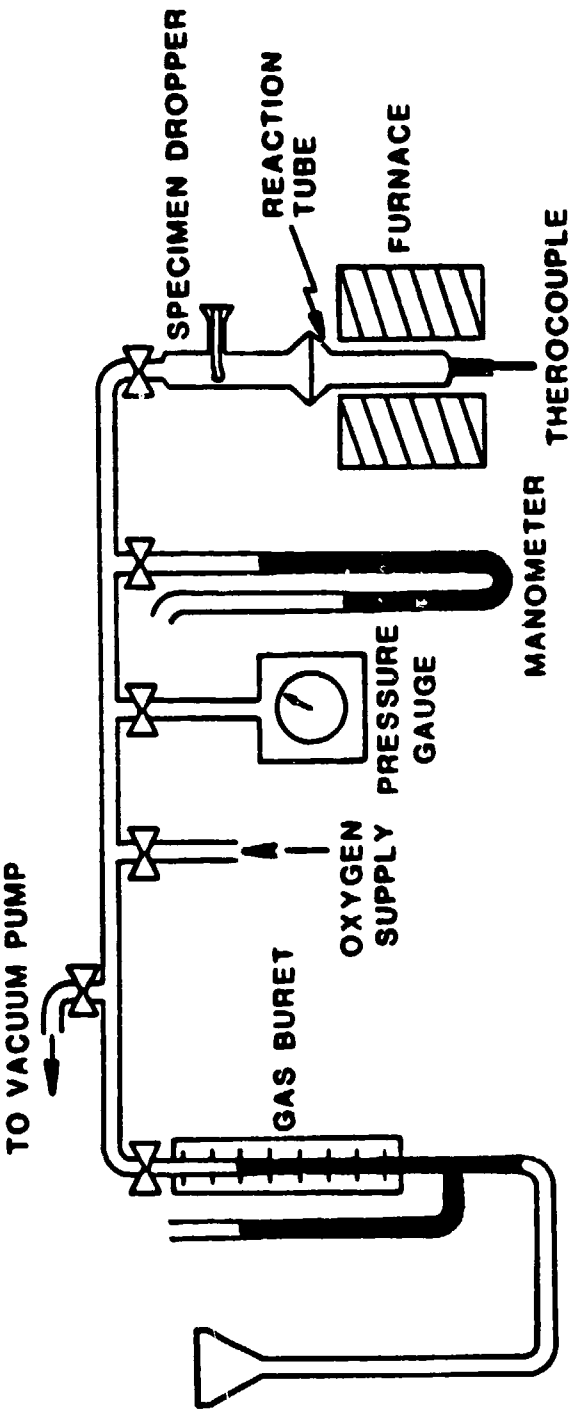

Figure 2. Isothermal Oxidation Apparatus.

oxidation studies of Sb_2O_3(o). The experimental procedure is given in Appendix A.

Sb_2O_3 for reaction studies was prepared from 99.999% pure (metals basis) Sb_2O_3 (Alfa, Danvers, MA). Materials were placed in a closed Pt cylinder which was then placed in a quartz tube. After evacuating the quartz tube three times to 10^{-6} atm and refilling with 99.9995 percent pure argon (Matheson, East Rutherford, NJ), the tube was filled to 0.2 atm with argon after which the tube was sealed. The quartz tube was then placed into a muffle furnace adjacent to an indicating thermocouple. Desired muffle furnace temperatures were obtained within an hour with set point temperatures at about 520-540°C for Sb_2O_3(c) and about 620-640°C for Sb_2O_3(o) production. Oven temperatures were proportionally controlled throughout the heat treatment. Photographs of typical Sb_2O_3 products obtained by scanning electron microscopy are presented in Figures 3 and 4.

The infrared spectrometric method used by Gopalakrishnan and Manohar[48] as developed by Borger and Krogh-Moe[70] was used initially to analyze both reactants and products. The accuracy[48] of the method based upon analysis of dimorph mixtures indicated that accuracy was limited to ±5%.

Another method used for analysis was Raman spectrometry as reported by Cody, et al.[52] The Raman spectra for Sb_2O_3(o), Sb_2O_3(c), and Sb_2O_4 consists of

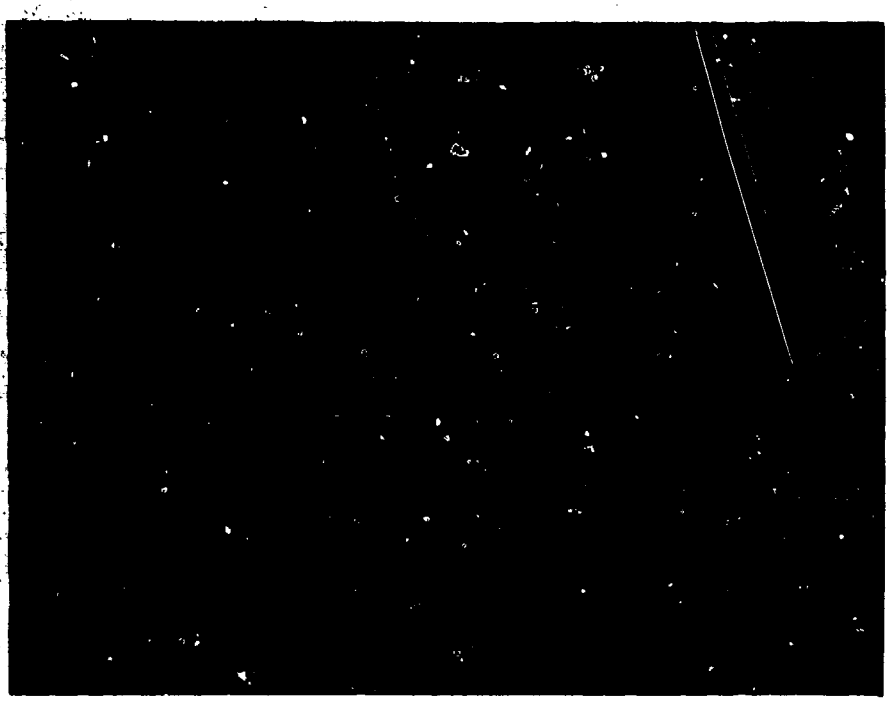

Figure 3. SEM Photograph of Sb_2O_3(c).

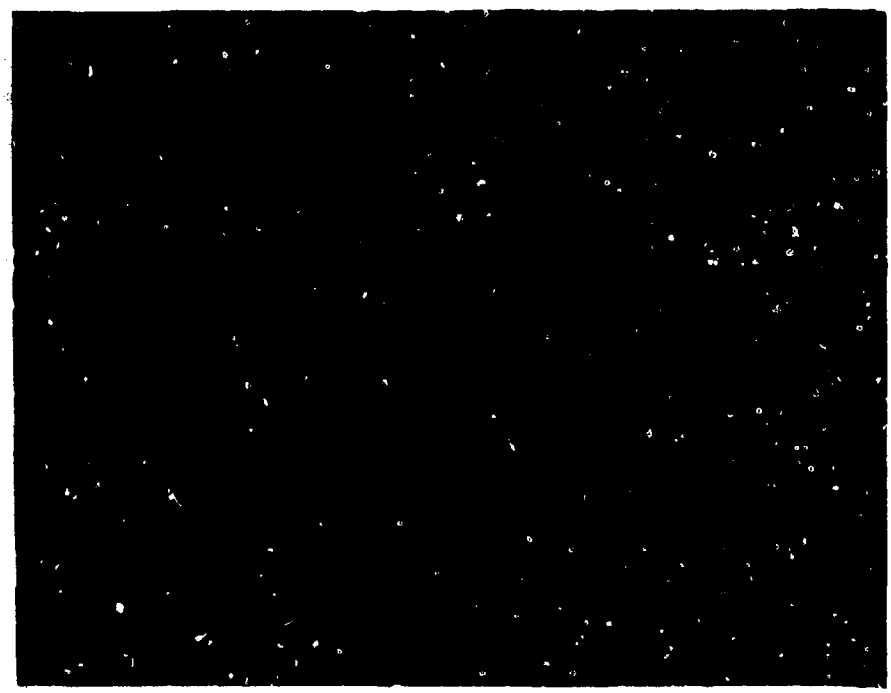

Figure 4. SEM Photograph of Sb_2O_3(o).

sharp, well-separated peaks useful for qualitative purposes. Analyses of known mixtures suggested that packing variations of powders in Raman tubes of different particle sizes adversely affected the accuracy of analyses. It was also observed that Raman intensities decreased markedly as Sb_2O_3(o) crystals were ground into fine powders. These results are in agreement with those of Ferraro, et al.[71] Therefore, analysis performed using either technique was employed on a semi-quantitative basis only.

ISOTHERMAL OXIDATION OF Sb_2O_3(o)

The isothermal oxidation of Sb_2O_3(o) was reported by Gopalakrishnan and Manohar[55] to take place at increasing rates of reaction from 470° to 520°C. Their reaction rates for very large crystal size Sb_2O_2(o) (2 x .1 x .02 mm) could not be reproduced for crystals of about that size. It was found that similar crystals did not oxidize at 470°C after 50 minutes. They report over 65 percent theoretical completion after 50 minutes at 470°C under oxygen at 140 torr. In this work it was found that such large crystals could only be oxidized to 60 percent theoretical completion if the reaction temperature was increased, e.g., a temperature of 533°C under oxygen at 163 torr for one hour.

It was then decided to grind Sb_2O_3(o) to a much smaller particle size to determine if the oxidation rate would be increased for samples with more surface area.

Therefore, a sample of $Sb_2O_3(o)$ was ground mechanically on a mechanical amalgamator (Wig-L-Bug, Cresent Dental, Chicago, IL) for 16 minutes. Samples were analyzed by both infrared and Raman spectrometric techniques which always indicated that Sb_2O_4 had not been formed during the grinding process.

The 16-minute ground $Sb_2O_3(o)$ was then oxidized isothermally in the kinetics rig at temperatures ranging from 453°C to 521°C. These data are presented in Appendix B and Figure 5. In these experiments it was found that the theoretical limit of oxygen consumption could only be approached at higher temperatures. At such reaction temperatures, a light coating on the interior of the reaction tube identified as Sb_2O_4 was found at increasing height above the reactant at higher reaction temperatures, but Sb_2O_4 was never found at more than about one cm above the top of the solid sample.

Repeat of isothermal oxidation of $Sb_2O_3(o)$ at 521°C indicated good repeatability for oxidation conducted in the glassware system as presented in Figure 6.

Examination of the reaction data indicates that after an initial induction time, which shortened as the reaction temperature increased, the oxidation of $Sb_2O_3(o)$ appears to be directly proportional to the reaction time. After some time, the reaction slows down and appears to become proportional to the square root of time, a parabolic rate,

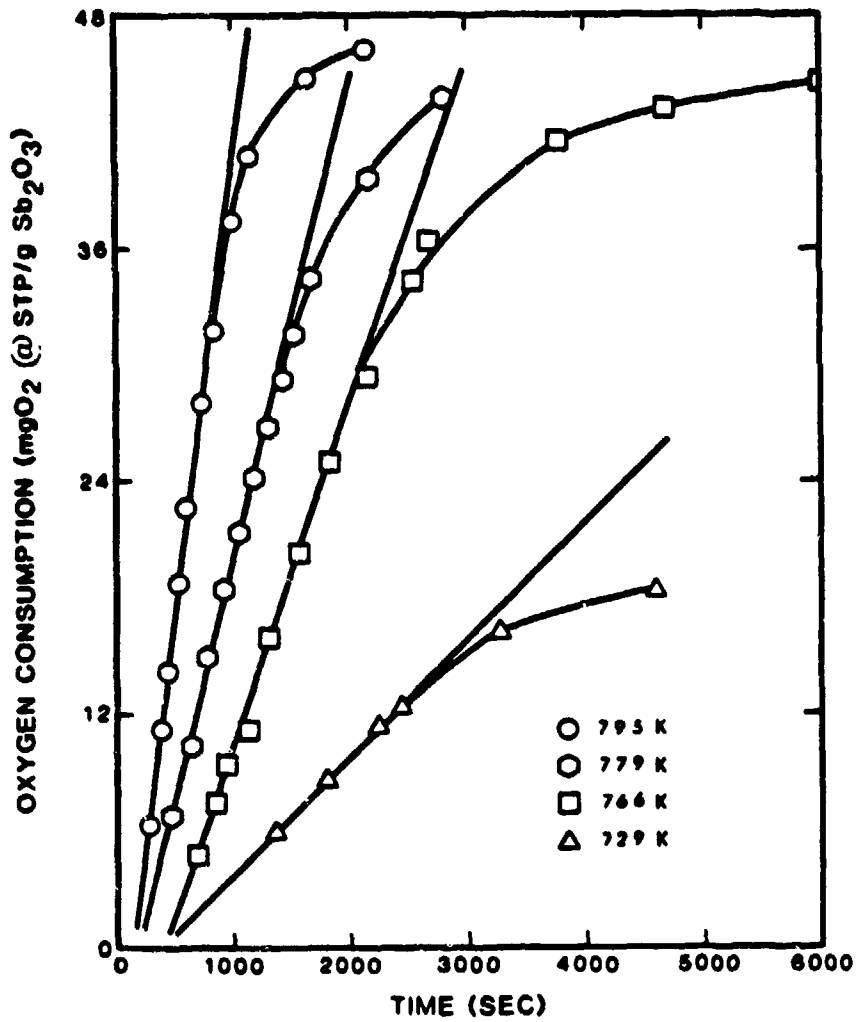

Figure 5. Isothermal Oxidation of Sb_2O_3(o).

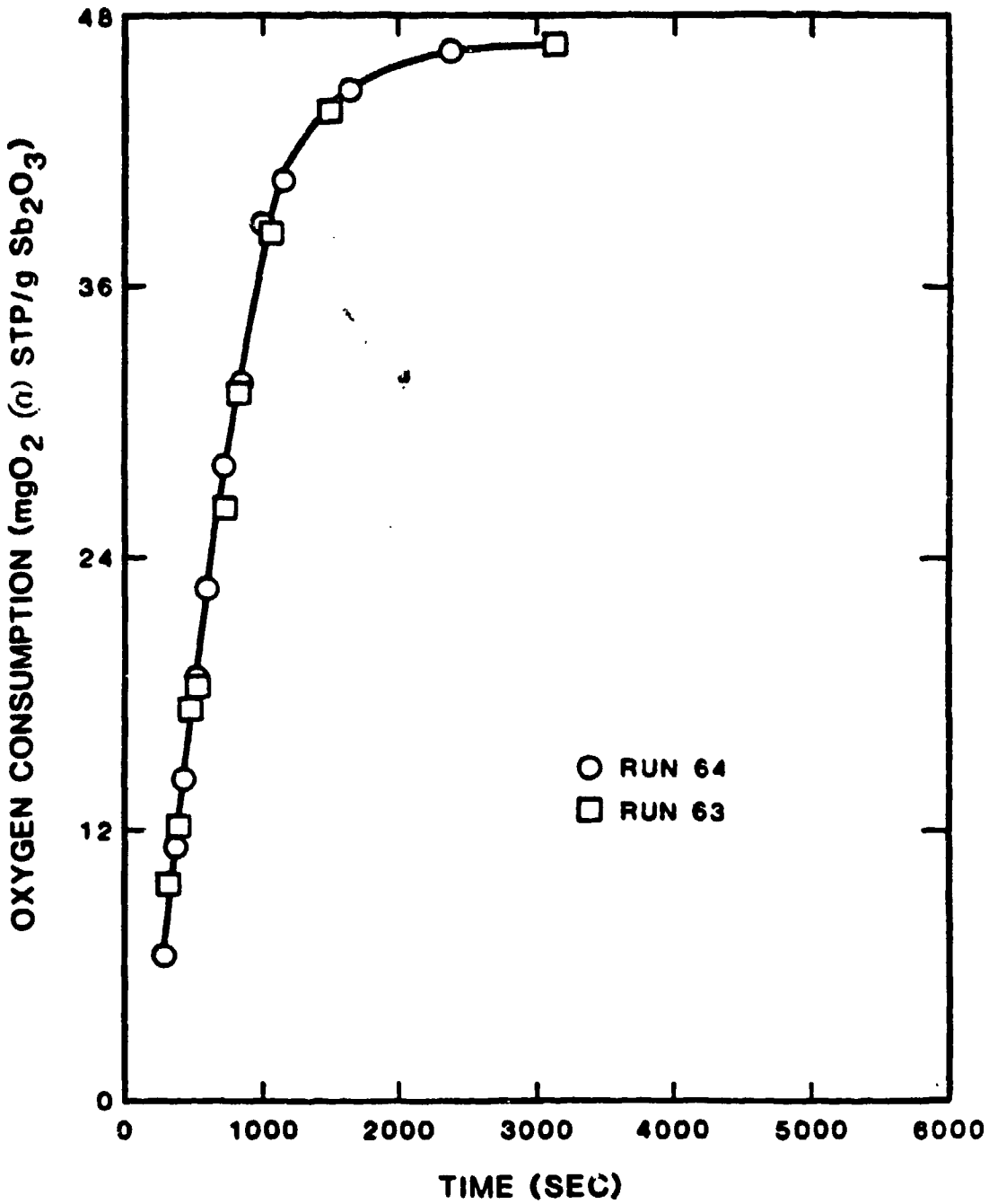

Figure 6. Repeatability of Sb_2O_3(o) Oxidation.

or even slower for later segments of the reaction. Oxygen consumption as a function of the square root of time is presented in Figure 7.

Trofimov and co-workers[72] have provided a basis for such a change of reaction rates during the reaction. They found in an x-ray heated cell experiment that fine powdered Sb_2O_3(o) oxidized at lower temperatures than did equivalent fine Sb_2O_3(c). However, when mixtures Sb_2O_3(o) and Sb_2O_3(c) were oxidized, Sb_2O_3(c) oxidized prior to Sb_2O_3(o). They rationalized those reactions by hypothesizing that oxidation is nucleated in a low energy process when orthorhombic Sb_2O_4 is formed coherently on orthorhombic Sb_2O_3(o) surface. Because Sb_2O_4 also provides such a surface, oxidation continued by sublimation of Sb_2O_3(c), which has a higher equilibrium sublimation pressure than Sb_2O_3(o), until the supply of Sb_2O_3(c) is exhausted. Oxidation of covered Sb_2O_3(o) may continue but the process is controlled by a slow bulk diffusion process compared with gaseous diffusion of sublimed Sb_4O_6.

Thus, for the isothermal oxidation of Sb_2O_3(o), the process may be initiated by sublimation of Sb_2O_3(o), or more correctly Sb_4O_6, which oxidizes on the Sb_2O_3(o) surface. Eventually, all readily sublimable Sb_2O_3(o) is oxidized with remaining Sb_2O_3(o) covered with Sb_2O_4. At this point, oxidation can only occur by bulk diffusion. Then, at some point, the process terminates when the Sb_2O_4

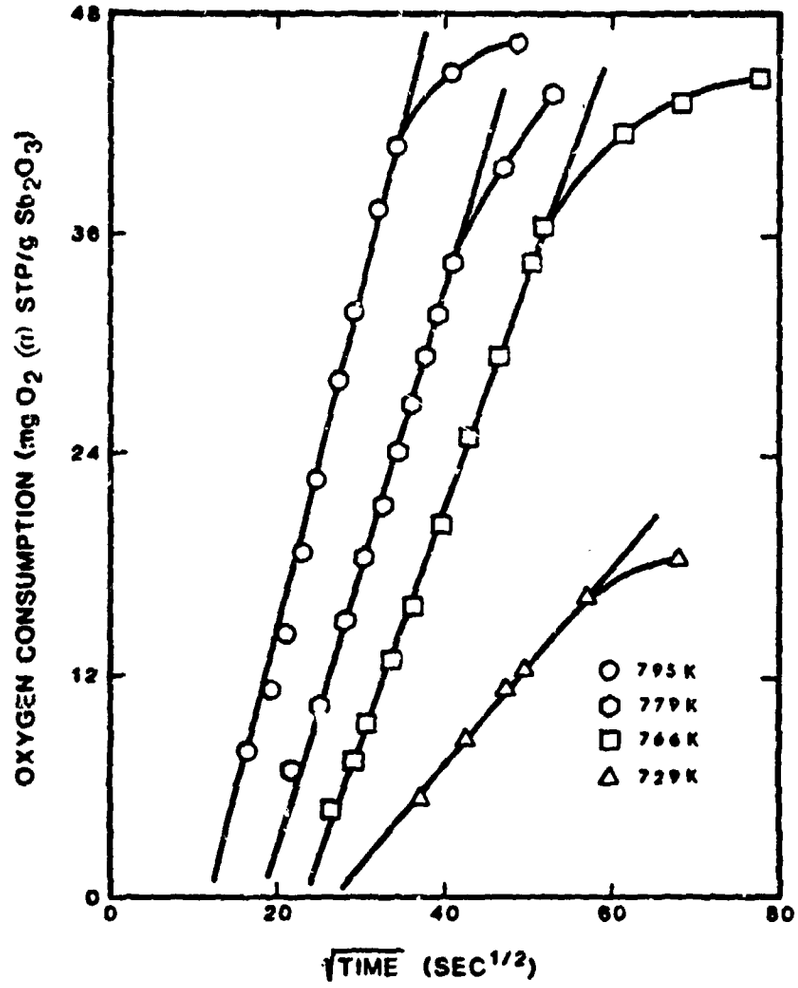

Figure 7. Parabolic Law Isothermic Oxidation of Sb_2O_3(o).

layer becomes too thick. In a plot of oxygen consumption as a function of reaction time, the initial section may be explained as sublimation of Sb_4O_6 through some distance to a low energy nucleation site which continues linearly until coverage nears completion, at which time, a much slower bulk diffusion process becomes predominant. The rate of the bulk process not only slows rapidly, but any traces of sublimable reactant are oxidized quickly. If coverage is uniformly coherent and thick, then residual Sb_2O_3 cannot be oxidized in a reasonable time and the reaction terminates.

In these experiments, if the temperature is very high, e.g., 521°C, then sublimation is dominant and the reaction proceeds to near theoretical limit. At lower temperatures, e.g., 456°C, the reaction forms Sb_2O_4 on Sb_2O_3(o) surfaces more effectively, reducing the rate of sublimation so that the reaction becomes bulk diffusion controlled which results in termination of oxidation.

In contrast, Gopalakrishnan and Manohar[55] claim that reaction is completely oxygen diffusion controlled for the entire temperature range. Differences in distribution and sizes of Sb_2O_3(o) crystals could provide the basis for the dissimilar hypotheses for the oxidation. However, the observations of Trofimov, et al., and the data presented here suggest that a sublimation controlled mechanism for oxidizing Sb_2O_3 to Sb_2O_4 is plausible, at least for a portion of the oxidation.

ISOTHERMAL OXIDATION OF Sb_2O_3(c)

Sb_2O_3(c) formed from Sb_2O_3 (Alfa) was produced during heat treating in smaller crystal sizes than Sb_2O_3(o). The Sb_2O_3(c), as found, was sieved through 20 micron onto 10 micron nickel mesh screens (0.336 m^2/g BET surface area Micromeritics, Norcross, GA).

Oxidation data are given in Figures 8 and 9. The reaction rates are, like Sb_2O_3(o), a function of temperature. Isothermal oxidation of Sb_2O_3(c) requires significantly higher temperatures than does Sb_2O_3(o). The reaction rate is very slow at first, and quickly increases until some later time in the reaction. Depending upon the reaction temperature, the rate slows from an apparently linear region, like Sb_2O_3(o), to a parabolic rate, becoming even slower at latter stages until termination of the reaction. These rates generate a reaction curve having an elongated sigmoidal appearance. A plausible explanation is that cubic Sb_2O_3 does not have the low energy reaction sites[72] for an orthorhombic product; but as orthorhombic Sb_2O_4 is formed, it may provide the low energy nucleation site and become similar to Sb_2O_3(o) in reaction characteristics.

Sb_2O_3(c) oxidized at 521°C in a used tube previously coated with the Sb_2O_4 product showed an increase in reaction rate up to about 50 percent of theoretical completion. This experiment suggests that the orthorhombic

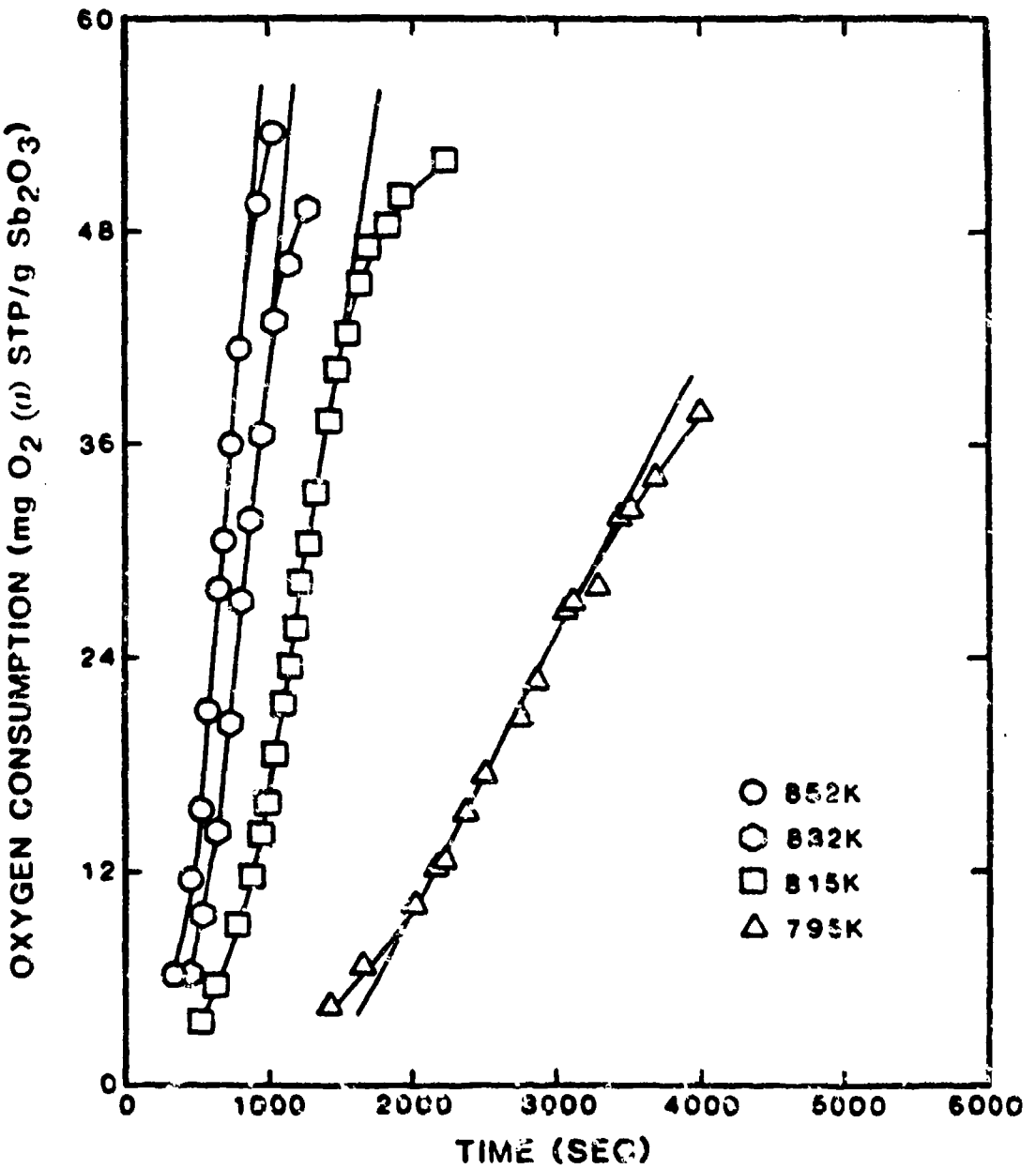

Figure 8. Isothermal Oxidation of Sb_2O_3(c).

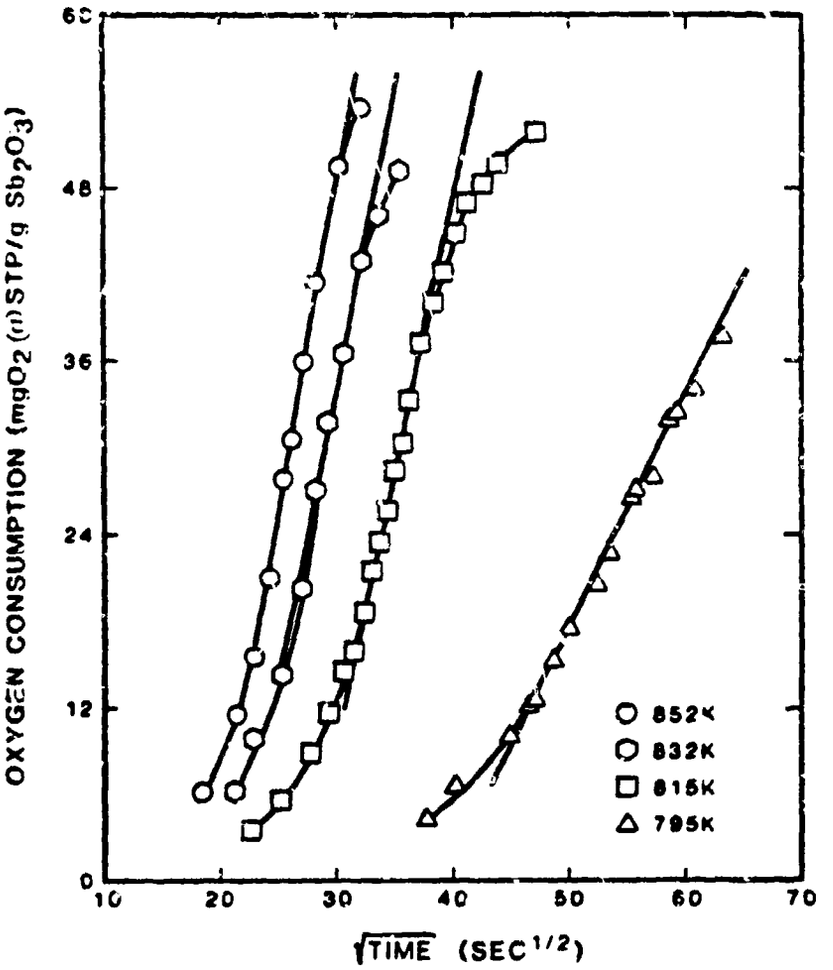

Figure 9. Parabolic Law Isothermal Oxidation of $Sb_2O_3(c)$.

surface of Sb_2O_4 may be a low-energy nucleation site as suggested by Trofimov, et al.[72] These data are presented in Figure 10.

ISOTHERMAL OXIDATION OF MIXTURES OF Sb_2O_3(o) AND Sb_2O_3(c)

50-50 weight percent mixtures of ground Sb_2O_3(o) and sieved, unground Sb_2O_3(c) were oxidized at temperatures from 492° to 530°C. The results are presented in Figures 11 and 12. The reaction rates for the mixtures are intermediate between the pure dimorphs and as of Sb_2O_3(o) and Sb_2O_3(c) appear to obey the same reaction mechanism. These data do not directly support the observation of Trofimov, et al.[72] that in mixtures of Sb_2O_3, the rate of oxidation is faster than would be predicted by summing of the rate for each dimorph. However, these oxidation rates employ larger Sb_2O_3(c) than that used in Sb_2O_3(c) oxidation rate determinations. These experiments were not repeated because after all other oxidation data was analyzed, an understanding of oxidation and its role in the beneficial mechanism of Sb_2O_3 in MoS_2 became clearer.

Use of sieved, unground Sb_2O_3(c) may also provide an explanation for mixed oxidation data at 803 K compared with data at 793 K. Crossover of oxygen consumption near the end of reaction may result from significant differences in surface area of Sb_2O_3(c) added to the mixture.

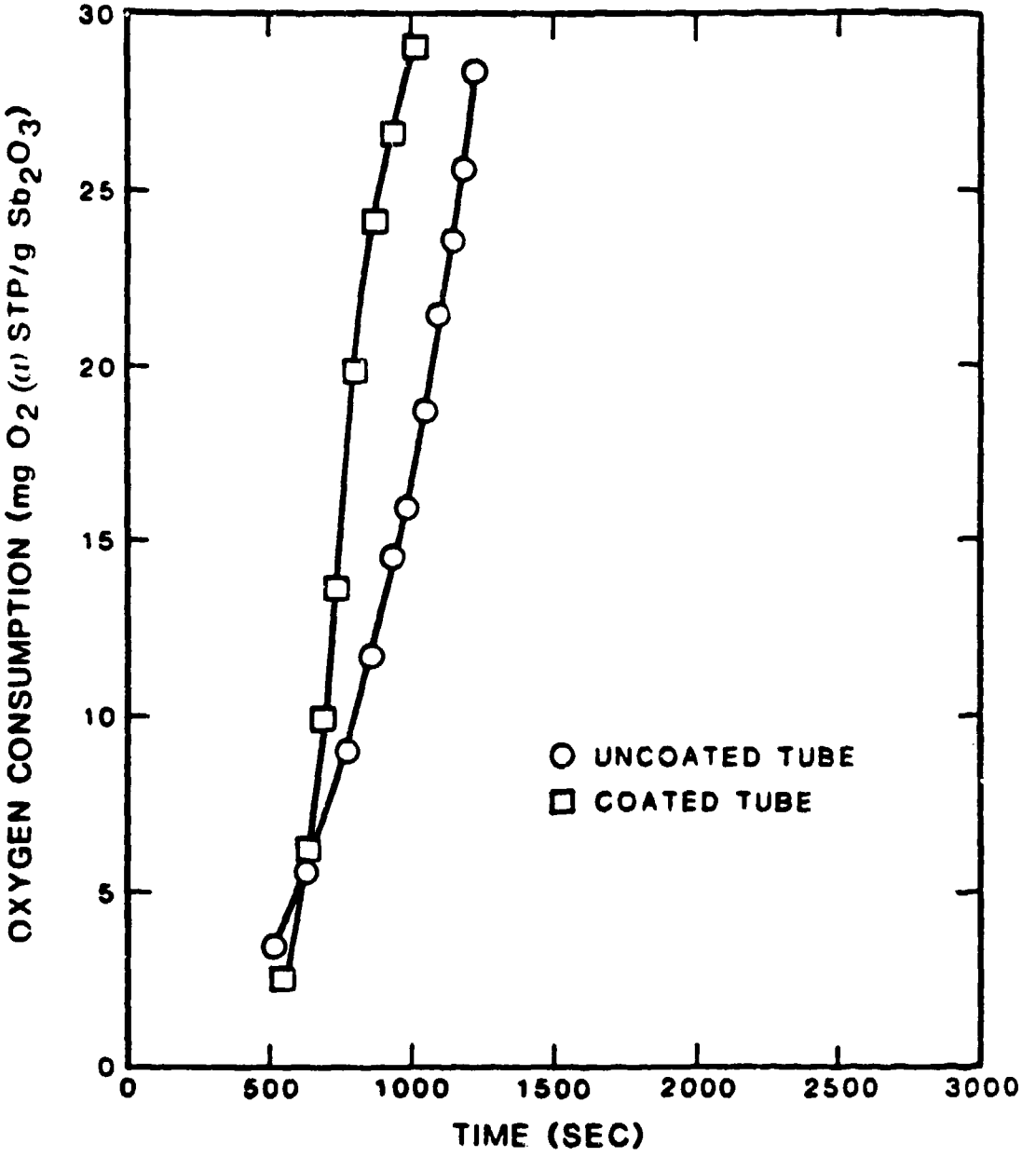

Figure 10. Oxidation of Sb_2O_3(o) in New and Used Reaction Tubes.

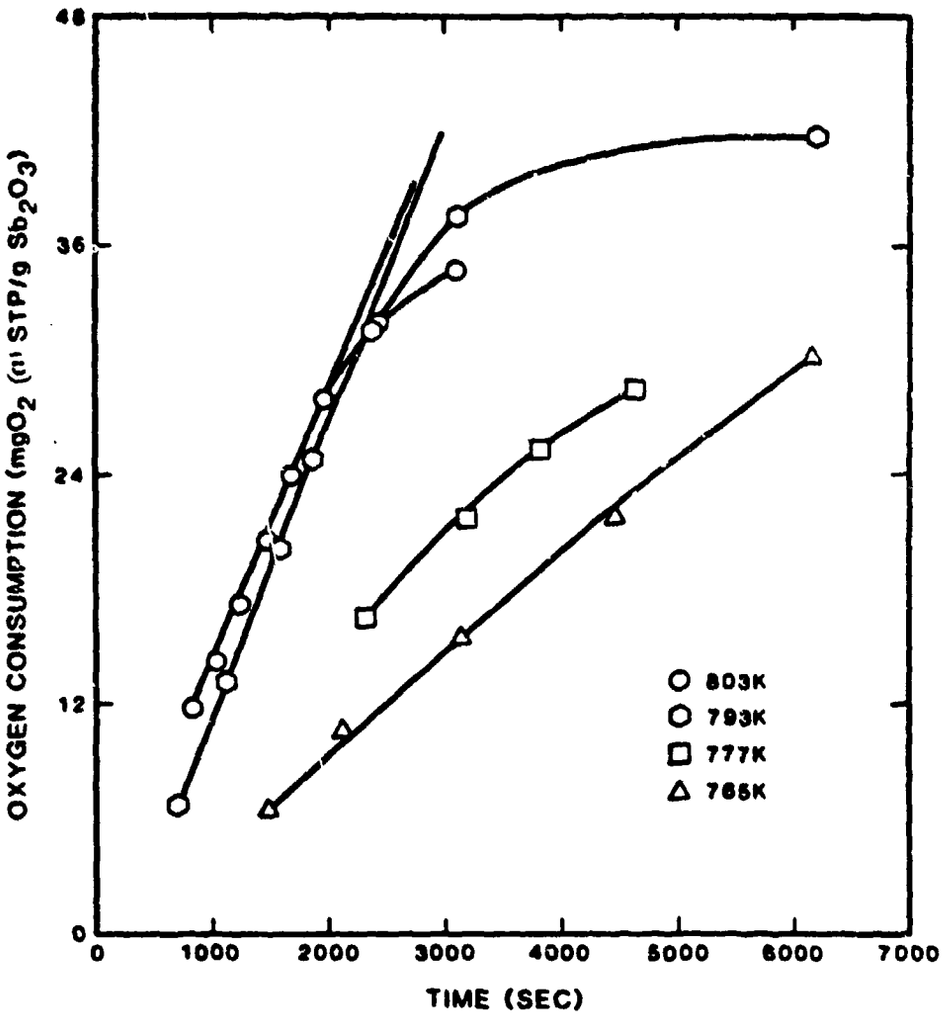

Figure 11. Oxidation of Mixed Dimorphic Sb_2O_3.

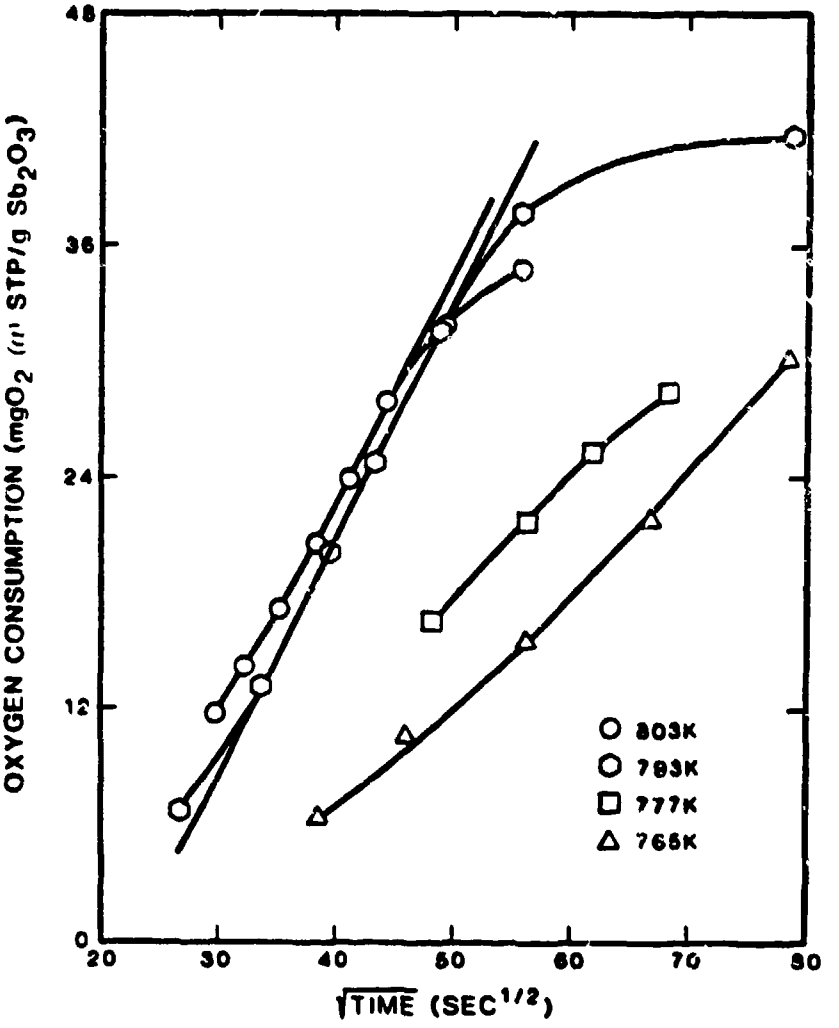

Figure 12. Parabolic Law Isothermal Oxidation of Mixed Dimorphic Sb_2O_3.

EVALUATION OF ISOTHERMAL OXIDATION DATA

To determine the apparent activation energy for oxidation of $Sb_2O_3(c)$, $Sb_2O_3(o)$ and mixed Sb_2O_3, the reaction rates were plotted as a function of the reciprocal of reaction temperature using the Arrhenius relationship as follows:

$$k = A\, e^{-E_a/RT} \tag{4.1}$$

where

k = rate constant

A = pre-exponential or frequency factor

E_a = apparent activation energy

R = gas constant

T = absolute temperature

By taking the logarithm of both sides,

$$\ln k = \ln A - \frac{E_a}{RT} \tag{4.2}$$

Then, when ln k is plotted as a function of $\frac{1}{T}$, the slope is equal to $\frac{E_a}{R}$, while the intercept is ln A. E_a is related to the energy required for the reaction to proceed. As calculated from data presented in Figures 13, 14 and 15, the mean E_a for $Sb_2O_3(c)$ is 48.0 ± 1.9 kcal/mole, 47.4 ± 10.0 kcal/mole for $Sb_2O_3(o)$, and 44.7 ± 0.8 kcal/mole for mixed Sb_2O_3 as given in Table 2. Least square lines were

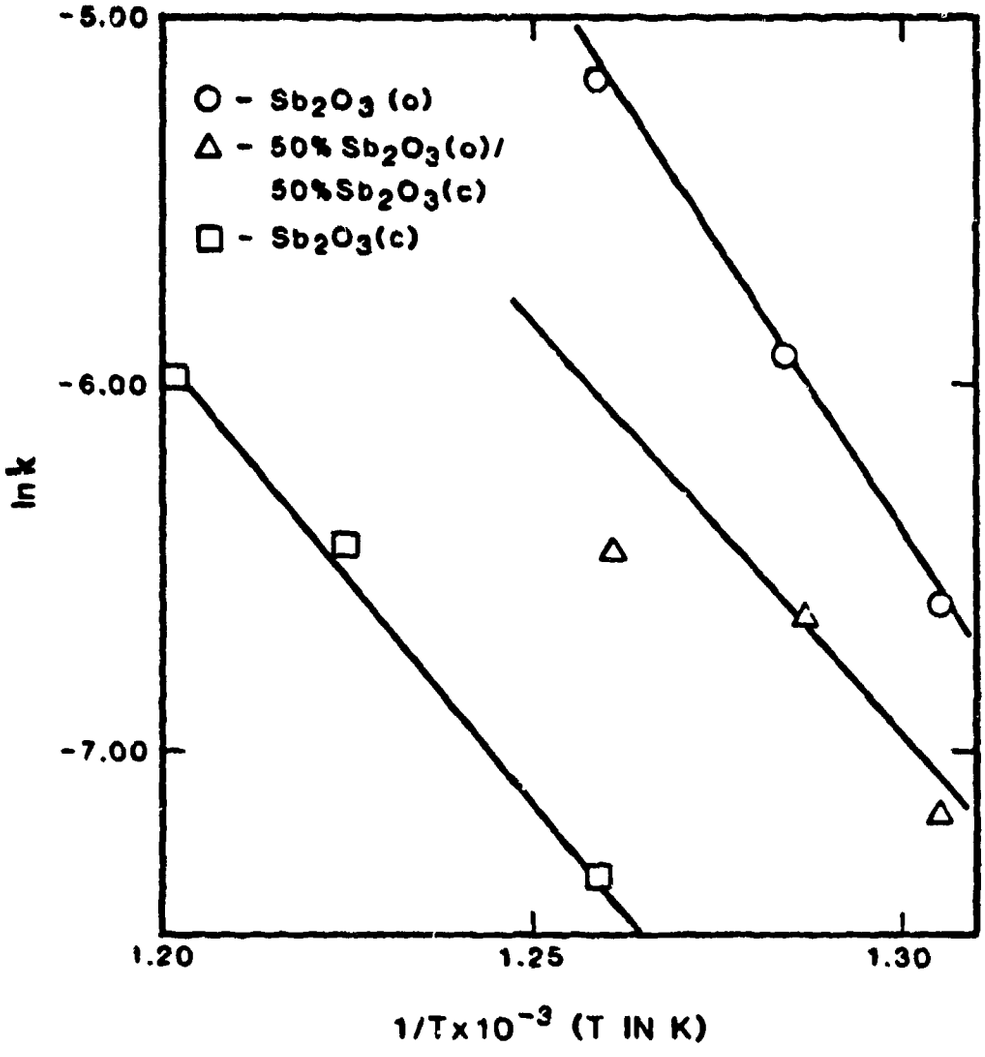

Figure 13. Arrhenius Plot for Sb_2O_3 Oxidation at 10% Theoretical Reaction Completion.

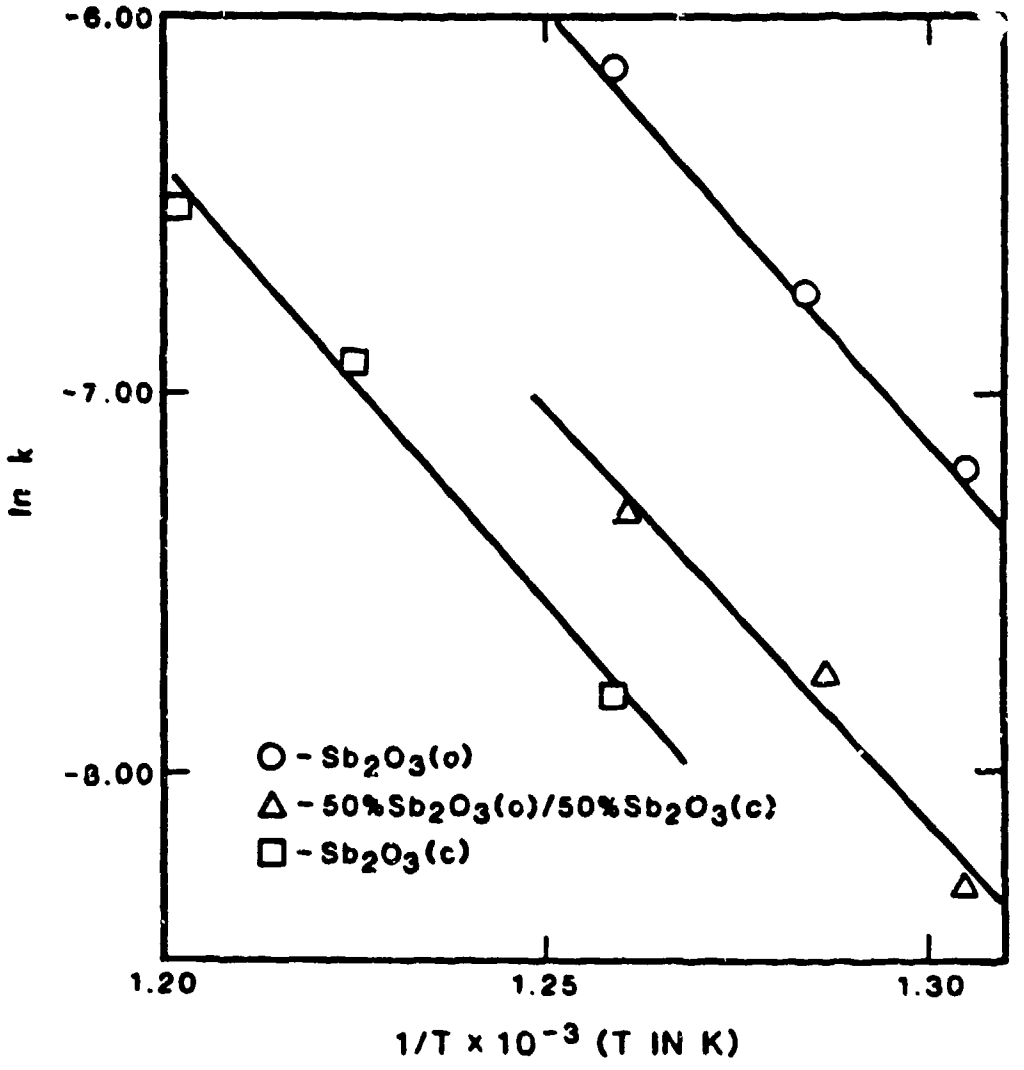

Figure 14. Arrhenius Plot for Sb_2O_3 Oxidation at 30% Theoretical Reaction Completion.

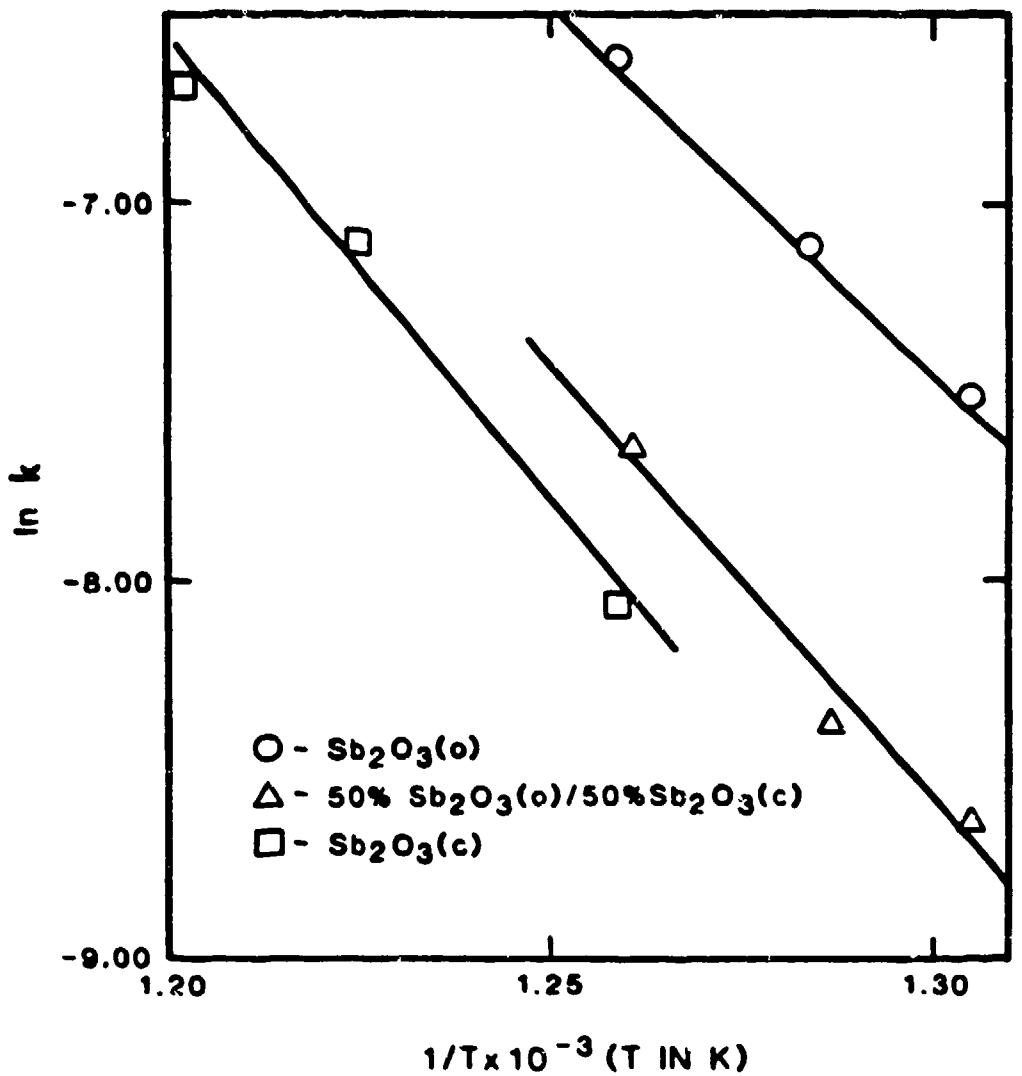

Figure 15. Arrhenius Plot for Sb_2O_3 Oxidation at 50% Theoretical Reaction Completion.

Table 2. ACTIVATION ENERGIES (E_a) AND PRE-EXPONENTIAL FACTORS (A) FOR THE ISOTHERMAL OXIDATION OF Sb_2O_3(o) and Sb_2O_3(c)

Reactant	Sb_2O_3(o)					Sb_2O_3(c)					Mixed Sb_2O_3(o) - Sb_2O_3(c)				
% Theoretical Completion	10	30	50	65	mean	10	30	50	65	mean	10	30	50	65	mean
E_a(kcal/mole)	61.7	45.8	38.7	43.5	47.4 ±10	47.8	45.7	48.3	50.3	48.0 ±1.9	44.8	43.9	45.5	--	44.7 ±0.8
A (s^{-1})	5.33 $\times 10^{14}$	8.74 $\times 10^{9}$	5.96 $\times 10^{7}$	9.7 $\times 10^{8}$	2.4 $\times 10^{10}$	9.48 $\times 10^{9}$	1.62 $\times 10^{9}$	6.52 $\times 10^{9}$	1.87 $\times 10^{10}$	6.53 $\times 10^{9}$	4.81 $\times 10^{9}$	8.65 $\times 10^{8}$	1.6 $\times 10^{9}$	--	1.9 $\times 10^{9}$

constructed for the data, except high temperature data for 10 percent oxidation of mixed Sb_2O_3 for which the oxidation appears to be unreasonable. The means are for apparent activation energies over the range of 10 to 50 or 65 percent reaction completion and standard deviations are for those data. Values of , the pre-exponential constant, are typically 10^9-10^{1} ^{1}.

The computed values of E_a are very close to those of Jungermann and Plieth[50] who found that the enthalpy of sublimation (ΔH_s) of Sb_2O_3(c) is 43.8 ± 1.0 kcal/mole and 43.6 ± 1.8 kcal/mole for Sb_2O_3(o). From the similarity of E_a and ΔH_s, and the observation of product on reaction tube walls, one may hypothesize that under these psuedo-isobaric conditions, sublimation is the rate controlling step for the oxidation of the antimony trioxides. However, the role of oxygen was not determined, and the adsorption of oxygen may indeed be critical. Because the interest here is in oxidation of Sb_2O_3 in air, the role of oxygen was not examined.

To determine if a correlation between the equilibrium sublimation pressure of the antimony oxides and oxidative reaction rate should exist, if sublimation is rate determining, Langmuir's equation for sublimation was considered.[73]

In Langmuir's technique to determine the equilibrium sublimation pressure, P_e, the weight loss during

evaporation is determined. The following relationship is then used to obtain the equilibrium sublimation pressure,

$$P_e = \dot{m} \frac{\left(\frac{2\pi RT}{M}\right)^{1/2}}{\alpha} \qquad (4.3)$$

Where

P_e = equilibrium (e) sublimation pressure

$\dot{m}$ = rate of loss of mass per cm^2 sample per second

R = gas constant (1.987 cal/mole K)

T = sample temperature (K)

M = molecular weight of subliming species (583.04g/mole for Sb_4O_6)

α = accommodation coefficient

It is assumed in Langmuir's treatment that the accommodation coefficient, α, is equal to α_c, the condensation coefficient or fraction of molecules condensing per collision, and equal to α_s or the sublimation coefficient which is the ratio of the observed ratio of sublimation to the maximum possible rate of sublimation pressure. For reasonable values of α, values of $\dot{m}$, close to experimentally determined values could be calculated.

Based upon Equation 4.3, the slope relating equilibrium sublimation pressure and mass loss is obtained as follows:

$$\alpha \left(\frac{P_e}{\dot{m}}\right) = \left(\frac{2\pi RT}{M}\right)^{1/2} \qquad (4.4)$$

Thus, the slope deviates from linearity by a product of reaction temperature divided by the molecular weight of the subliming species to the half power which on inspection will be small over the oxidation temperatures investigated here. Therefore, if one simply plots $\dot{m}$, the reaction rate for antimony trioxide oxidation, as a function of sublimation pressure, there should be an approximate linear correlation.

To determine if such a relationship exists for the oxidation of Sb_2O_3, reaction rate data gathered in the isothermal studies was analyzed.

Reaction rates (mg O_2/g Sb_2O_3/sec) were determined graphically from Figures 5 and 8. Sublimation pressures at those reaction temperatures were calculated using the appropriate relationships developed by Jungermann and Plieth.[50] Those data are presented in Tables 3 and 4 as follows:

Table 3. REACTION RATES AND SUBLIMATION PRESSURES FOR Sb_2O_3(o)

REACTION TEMP., K (°C)	REACTION RATE (mg O_2/g Sb_2O_3/sec)	SUBLIMATION PRESSURE (torr)
729 (456)	0.00584	0.0188
766 (493)	0.01756	0.0788
779 (506)	0.02449	0.1295
795 (522)	0.04729	0.2244

Table 4. REACTION RATE AND SUBLIMATION PRESSURES FOR Sb_2O_3(c)

REACTION TEMP. K (°C)	REACTION RATE (mg O_2/g Sb_2O_3 /sec)	SUBLIMATION PRESSURE (torr) Sb_2O_3(c)	SUBLIMATION PRESSURE (torr) Sb_2O_3(o)
794 (521)	0.01547	0.4894	--
816 (543)	0.04784	1.0340	--
832 (559)	0.06683	1.7378	0.7756
852 (579)	0.08449	3.2356	1.4411

Values of sublimation pressure for Sb_2O_3(o) at 832 and 852 K were also calculated because the reaction temperature of 832 K is just 3 K above the Sb_2O_3(c) to Sb_2O_3(o) transition temperature while 852 K is about 33 K above that transition.

Figure 16 is a plot of the $Sb_2O_3(o)$ sublimation pressure versus the reacton rate. As seen in Figure 17, there is an equivalent plot for $Sb_2O_3(c)$ oxidation. The sublimation pressure data plotted are for $Sb_2O_3(c)$ at the lower two temperatures and for $Sb_2O_3(o)$ at the highest temperature. For the reaction at 832 K, a mean (1.2567 torr) of the sublimation pressures for $Sb_2O_3(c)$ and $Sb_2O_3(o)$ is plotted. Again, it is evident that there is a linear dependence of the reaction rate upon the sublimation pressure.

Using least squares regression methodology, estimates of the appropriate regression coefficients were determined. For the reaction rate of $Sb_2O_3(o)$ over the temperature range investigated, the least squares equation is as follows:

$$(\text{mg } O^2/\text{g } Sb_2O_3(o)/\text{sec}) = 0.1995\ P_{eq} + 0.0013 \qquad (4.5)$$

(correlation coefficient = 0.995)

For $Sb_2O_3(c)$, the equation is as follows:

$$(\text{mg } O_2/\text{g } Sb_2O_3(c)/\text{sec}) = 0.0715\ P_{eq} - 0.0217 \qquad (4.6)$$

(correlation coefficient = 0.995)

where

P_{eq} = appropriate sublimation pressure in torr

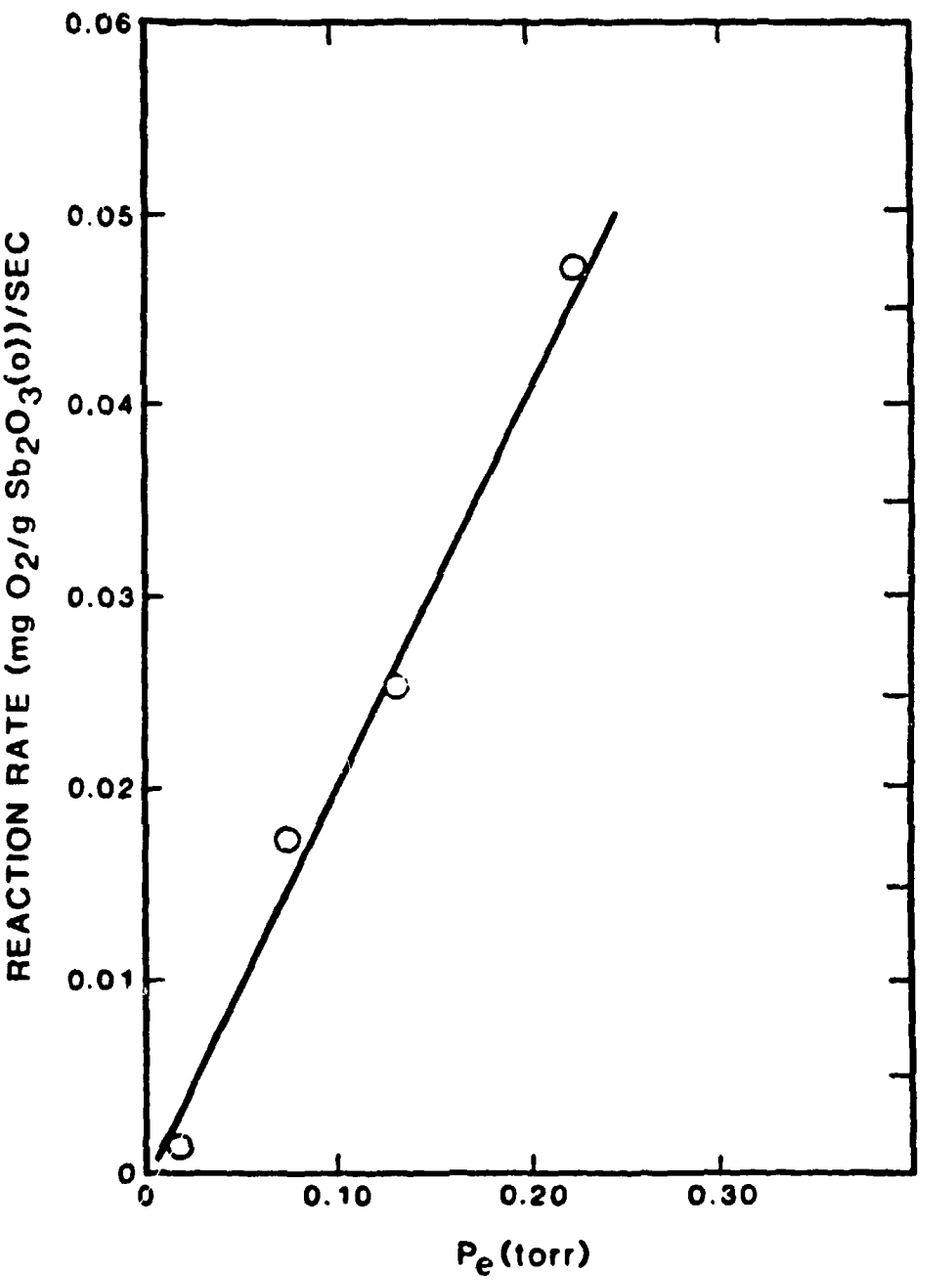

Figure 16. Oxidation Rate of Sb_2O_3(o) as a Function of Equilibrium Sublimation Pressure.

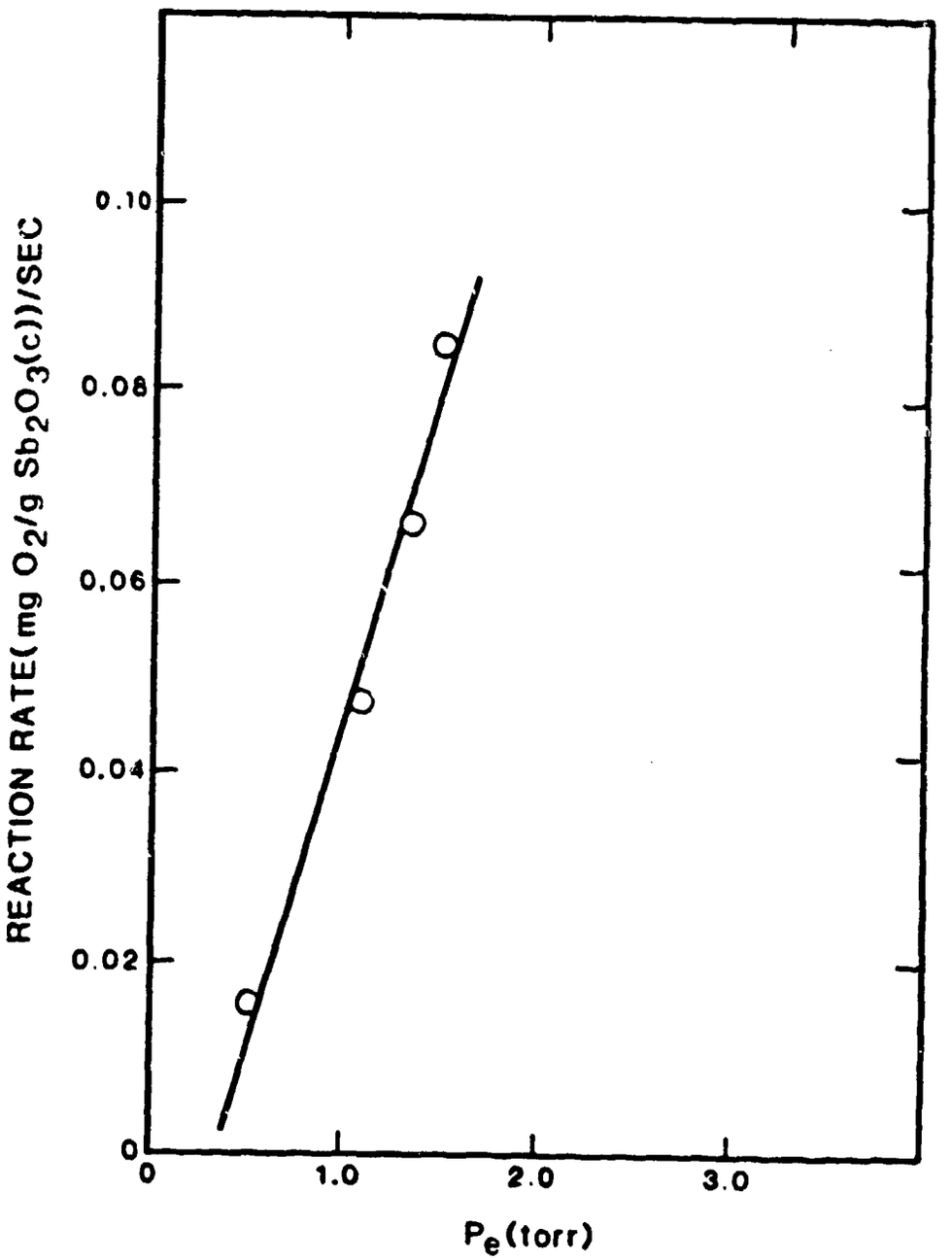

Figure 17. Oxidation Rate of Sb_2O_3(c) as a Function of Equilibrium Sublimation Pressure.

When the rate of oxidation of equimixed Sb_2O_3, which is intermediate between pure Sb_2O_3(o) and Sb_2O_3(c) as presented in Table 5, is plotted as a function of mean sublimation pressure calculated using the Jungermann and Plieth[50] relationships, the correlation is not linear as data generated for the Sb_2O_3(c) and Sb_2O_3(o) reactions as seen in Figure 18. Comparing the oxidation rate at 520°C (793 K) with that at 530°C (803 K), there still appears to be a significant correlation of reaction rate with sublimation pressure, which supports the hypothesis that sublimation of Sb_4O_6 is the rate controlling step in oxidation of either Sb_2O_3(o) or Sb_2O_3(c).

Additionally, to determine if the free energy of oxidation for Sb_2O_3 is favorable for reaction to involve sublimed species, the following analysis was performed.

For the oxidation of antimony trioxide, two reactions must be considered. Those are:

$$Sb_2O_3(s) + 1/2\ O_2 \rightarrow Sb_2O_4(s) \qquad (4.7)$$

$$Sb_4O_6(g) + O_2 \rightarrow Sb_4O_8(s) \qquad (4.8)$$

where Sb_4O_6 is the structure of the trioxide in the vapor state[74] and Sb_2O_4 is more correctly noted as $Sb_2O_3 \cdot Sb_2O_5$ or Sb_4O_8.[28]

Table 5. MIXED Sb_2O_3 OXIDATION RATES AND SUBLIMATION PRESSURE

REACTION TEMP., K(°C)	REACTION RATE [$(mgO_2/gSb_2O_3)/sec$]	SUBLIMATION PRESSURE (torr) $Sb_2O_3(c)$	$Sb_2O_3(o)$	MEAN
765 (492)	5.42×10^{-3}	0.171	0.077	0.124
777 (504)	6.02×10^{-3}	0.267	0.120	0.194
793 (520)	15.7×10^{-3}	0.473	0.219	0.346
803 (530)	15.0×10^{-3}	0.668	0.299	0.484

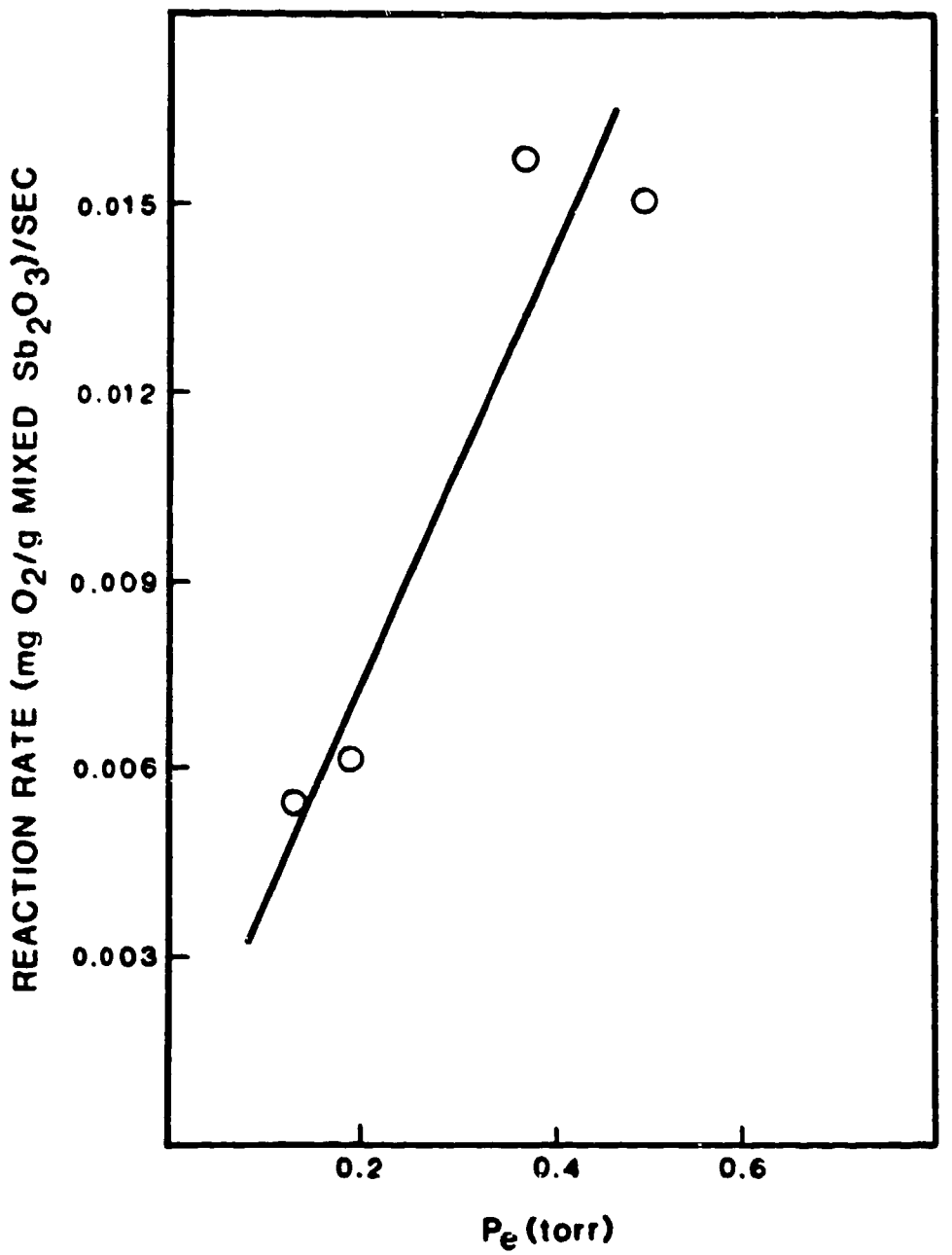

Figure 18. Oxidation Rate of Mixed Dimorphic Sb_2O_3 as a Function of Equilibrium Sublimation Pressure.

By application of the free energy relationship,

$$\Delta G^\circ = -RT \ln K_{eq} \qquad (4.9)$$

where ΔG° = standard Gibbs free energy change for reaction at T

R = Gas constant = 1.987 cal/deg-mole

T = Temperature (K)

K_{eq} = Equilibrium constant

It is possible to compare free energies of the reactions as follows:

For Equation 4.7,

$$K_{eq}(1) = \frac{[Sb_2O_4]}{[Sb_2O_3][p_{O_2}]^{1/2}} \qquad (4.10)$$

and for Equation 4.8,

$$K_{eq}(2) = \frac{[Sb_4O_8]}{[p_{Sb_4O_6}][p_{O_2}]} \qquad (4.11)$$

Standard states for $p_{O_2} = p_{Sb_4O_6}$ = 1 atm. For purposes of these calculations, the activities of $Sb_2O_3(s)$ and $Sb_4O_8(s)$ are assumed to be 1.

Values of ΔG° as a function of p_{O_2} for a reaction at 726°K with $Sb_2O_3(o)$ sublimation pressure of 0.01648 torr

calculated using the Jungermann and Plieth relationship[50] are presented in Table 6.

Table 6. FREE ENERGIES FOR OXIDATION REACTIONS

P(atm)	ΔG°(cal/mole)	
	Equation 4.7	Equation 4.8
1.0	0	-15,490
0.5	- 500	-16,490
0.25	-1000	-17,490
0.184 (140 torr)	-1220	-17,930
0.1	-1660	-18,810
0.01	-3320	-22,140
0.001	-4980	-25,460

The values of ΔG° indicate that there is a much stronger driving force for the oxidation of the sublimed species. This is consistent with a mechanism involving sublimation of Sb_4O_6 followed by reaction with O_2 to form Sb_4O_8.

To determine the effect of sublimation pressure of Sb_4O_6 on ΔG° for Equation 4.8, calculations of ΔG° as a

function of temperature for P_{O_2} of 0.184 atm (140 torr) were made. Those data are presented in Table 7.

Table 7. FREE ENERGIES OF OXIDATION OF SUBLIMED Sb_4O_6

T(K)	$P_{Sb_4O_6}$ equil (torr)	$P_{Sb_4O_6}$ (atm)	ln K_{eq}	$\Delta G°$ (cal/mole)
726	0.01648	21.68×10^{-6}	12.432	-17,930
766	0.07984	105×10^{-6}	10.854	-16,520
779	0.1288	169.5×10^{-6}	10.375	-16,060
794	0.2194	288.7×10^{-6}	9.843	-15,530

These data indicate that there is slightly less driving force for the reaction as the temperature is increased.

To compare the reaction tendency of $Sb_2O_3(c)$ with that of $Sb_2O_3(o)$, the sublimation pressure of $Sb_2O_3(c)$ is computed using the relationship developed by Jungermann and Plieth[50] and substituted into Equation 4.9. The results are given in Table 8.

Table 8. FREE ENERGIES FOR OXIDATION OF Sb_2O_3(c) and Sb_2O_3(o)

Dimorph	T(K)	(atm)	(torr)	760	$\ln k_{os}$	$\Delta G°$(cal/mole)
Sb_2O_3(c)	298	0.184	4.29×10^{-21}	5.65×10^{-24}	55.22	-32,700
	726	0.184	0.03639	4.79×10^{-5}	11.64	-16,790
	794	0.184	0.48935	6.44×10^{-4}	9.04	-14,260
Sb_2O_3(o)	298	0.184	2.26×10^{-21}	2.97×10^{-24}	55.87	-33,080
	726	0.184	0.01648	2.17×10^{-5}	12.43	-17,930
	794	0.184	0.2194	2.89×10^{-4}	9.84	-15,530

The data indicate slightly less driving force for the reaction of Sb_2O_3(c) in the 726-794 K interval compared with Sb_2O_3(o) because of the higher sublimation pressure of the cubic dimorph at identical temperatures.

Based upon these analyses, the correlation of oxidation reaction rate with equilibrium sublimation pressure, and the previous observation that the reaction apparent activation energy is equivalent to the enthalpy of sublimation of the oxides, it appears that sublimation of Sb_4O_6 is the rate controlling step for the oxidation of both Sb_2O_3(o) and Sb_2O_3(c). For Sb_2O_3(o), the proximity of a low energy reaction surface evidently increases the actual rate of reaction.

DIFFERENTIAL THERMAL ANALYSIS (DTA)

DTA was employed in additional thermal studies of antimony trioxides and MoS_2. The DTA instrument is a

Tracor-Stone Model 202 equipped with a Platinel thermocouple system to measure sample and reference temperatures with an accuracy of ± 0.4 percent. NBS-ITCA Standard References Materials (Set 758) were routinely employed to confirm calibration. Typical 3-5 mg samples were heated at 10°C per minute under air or argon. Sample and references pans were nickel. Al_2O_3 was the reference material for all determinations. The Stone Model F1DF DTA furnace was also used in the isothermal oxidation studies.

Several DTA of Sb_2O_3 and other lubricant compact materials were completed. Those data are summarized in Appendix C. For samples of Sb_2O_3(o) from one lot ground for various lengths of times, it was found that as grinding time and hence surface area increased, an endothermic peak at about 650°-656°C associated with melting of Sb_2O_3 decreased in size. For the same samples, an exothermic peak around 485°-515°C associated with oxidation of Sb_2O_3 tended to increase in size, implying more complete oxidation, and decrease in peak temperature as grinding time increased. Figure 19 represents DTA 102-107 for 15 seconds, one and two minutes of grinding. Similar results were observed when Sb_2O_3(c) was ground, i.e., the temperature of peak oxidation decreased as grinding time increased. These data may be rationalized as oxidation of smaller particle size Sb_2O_3(o) followed by melting and,

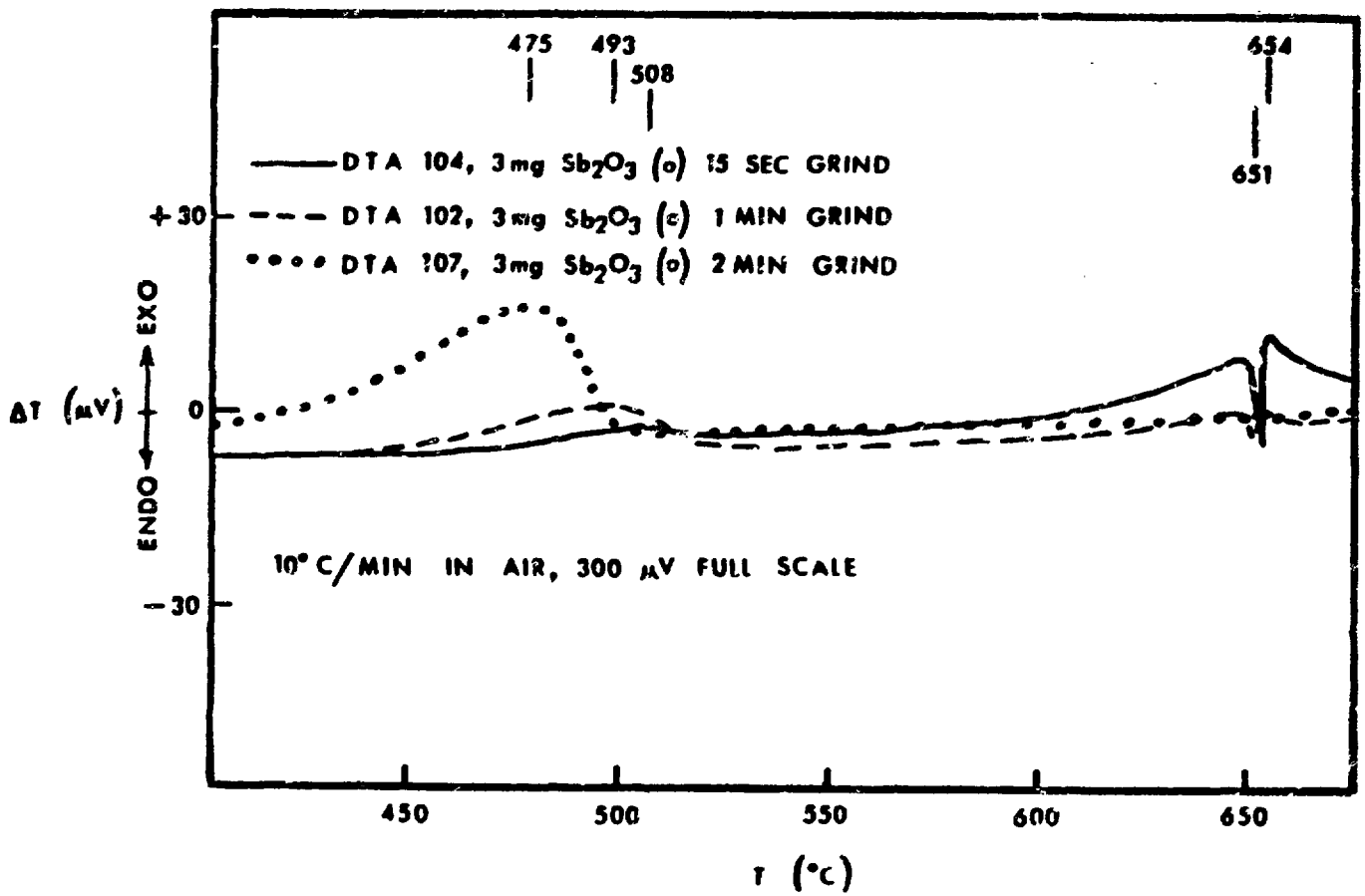

Figure 19. Effect of Grinding on Oxidation of Sb_2O_3(o).

ultimately, oxidation of very large crystals of $Sb_2O_3(o)$. Such grinding was, however, not reproducible from one lot of $Sb_2O_3(o)$ to another. For example, DTA 74 and 73 data from a different lot (#558649) of $Sb_2O_3(o)$ ground for eight and 16 minutes, respectively, were quite different from those for another lot as found in DTA 72 and 75. These results confirm the difficulty in reproducing particle size distribution in powders by simple grinding.

Because the effects of grinding $Sb_2O_3(o)$ occurred as would be predicted, additional studies of the oxidation of pure dimorphic Sb_2O_3 by DTA was terminated.

For $Sb_2O_3(o)$ thermally analyzed under argon, no exothermic peaks were observed in the oxidation region as shown in Figure 20. A slight endothermic trend which was attributed to sublimation of $Sb_2O_3(o)$ was found through the typical oxidation region.

To determine the effect of Sb_2O_4 on the oxidation of $Sb_2O_3(o)$, a mixture was prepared and analyzed by DTA. In Figure 21, the DTA are compared, where it is seen that addition of Sb_2O_4 actually shifts the oxidation peak to higher temperatures. Thus, the addition of Sb_2O_4 to $Sb_2O_3(o)$ appears to act as a diluent for the exothermic oxidation of $Sb_2O_3(o)$. For $Sb_2O_3(c)$, an addition of Sb_2O_4 did shift the oxidation peak to lower temperatures. To

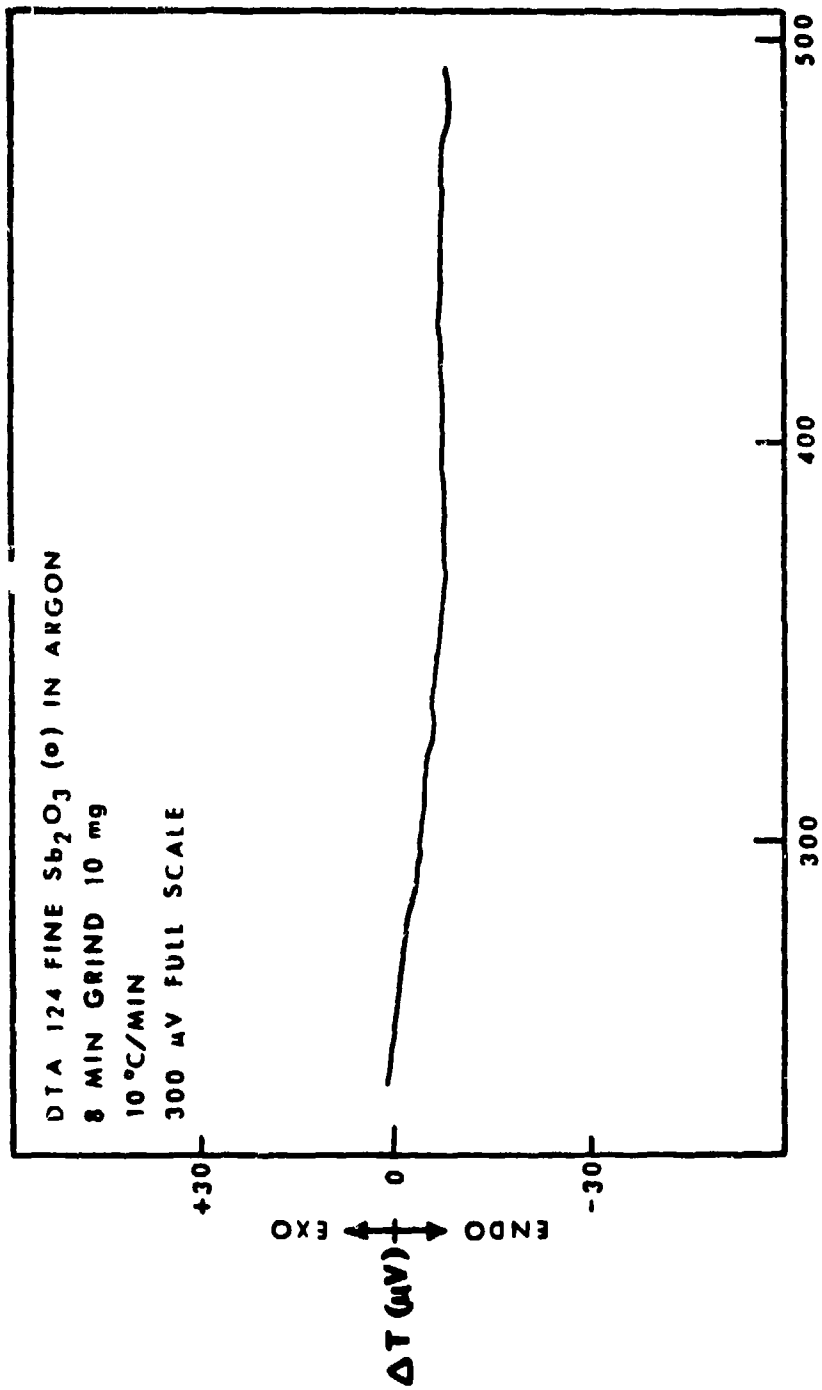

Figure 20. DTA of Sb_2O_3(o) Under Argon.

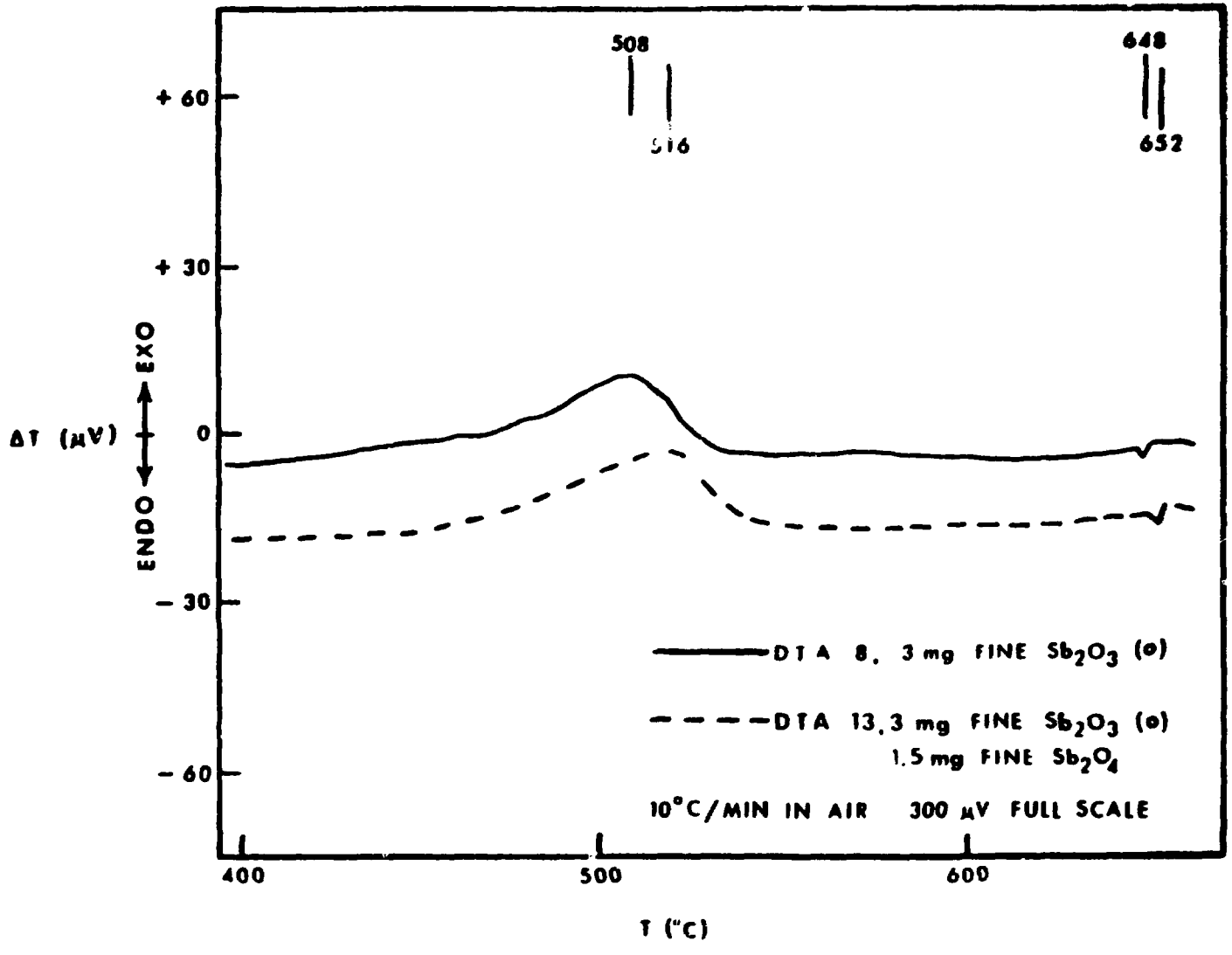

Figure 21. Effect of Sb_2O_4 Addition on Oxidation of Sb_2O_3(o).

compare Sb_2O_4 with another diluent, Al_2O_3 was added to Sb_2O_3(c) which did not significantly shift the oxidation peak. The area of the oxidation peak was, however, reduced, as shown in Figure 22.

In a similar fashion, DTA of a mixture of Sb_2O_3(o) and Sb_2O_3(c) was obtained and compared with DTA for Sb_2O_3(o) and Sb_2O_3(c). A composite of the DTA is presented in Figure 23. It is seen that oxidation of the mixture occurs at slightly below that of Sb_2O_3(o) and significantly lower than Sb_2O_3(c). The DTA for the mixed sample has two peaks which appears to be quite similar to very finely ground Sb_2O_3(o) and may imply that some structure changes occur during the mechanical grinding treatment.

The results for mixed Sb_2O_3 suggest that Sb_2O_3(o) or Sb_2O_4 surface does influence the oxidation of Sb_2O_3(c) as Trofimov, et al.(72) suggest. However, Sb_2O_3(o) oxidation does not appear to be influenced by the presence of Sb_2O_4; in fact, Sb_2O_4 acts only as a diluent, which may result from the fact that Sb_2O_3(o) is orthorhombic itself. The size of the unground Sb_2O_3(c) employed in mixed isothermal oxidation studies may be the influential factor in differences observed here and in those studies on the effect of mixing Sb_2O_3(o) and Sb_2O_3(c) on the rate of oxidation.

Additional DTA studies of mixed Sb_2O_3 samples were not pursued once it was established that there does appear to

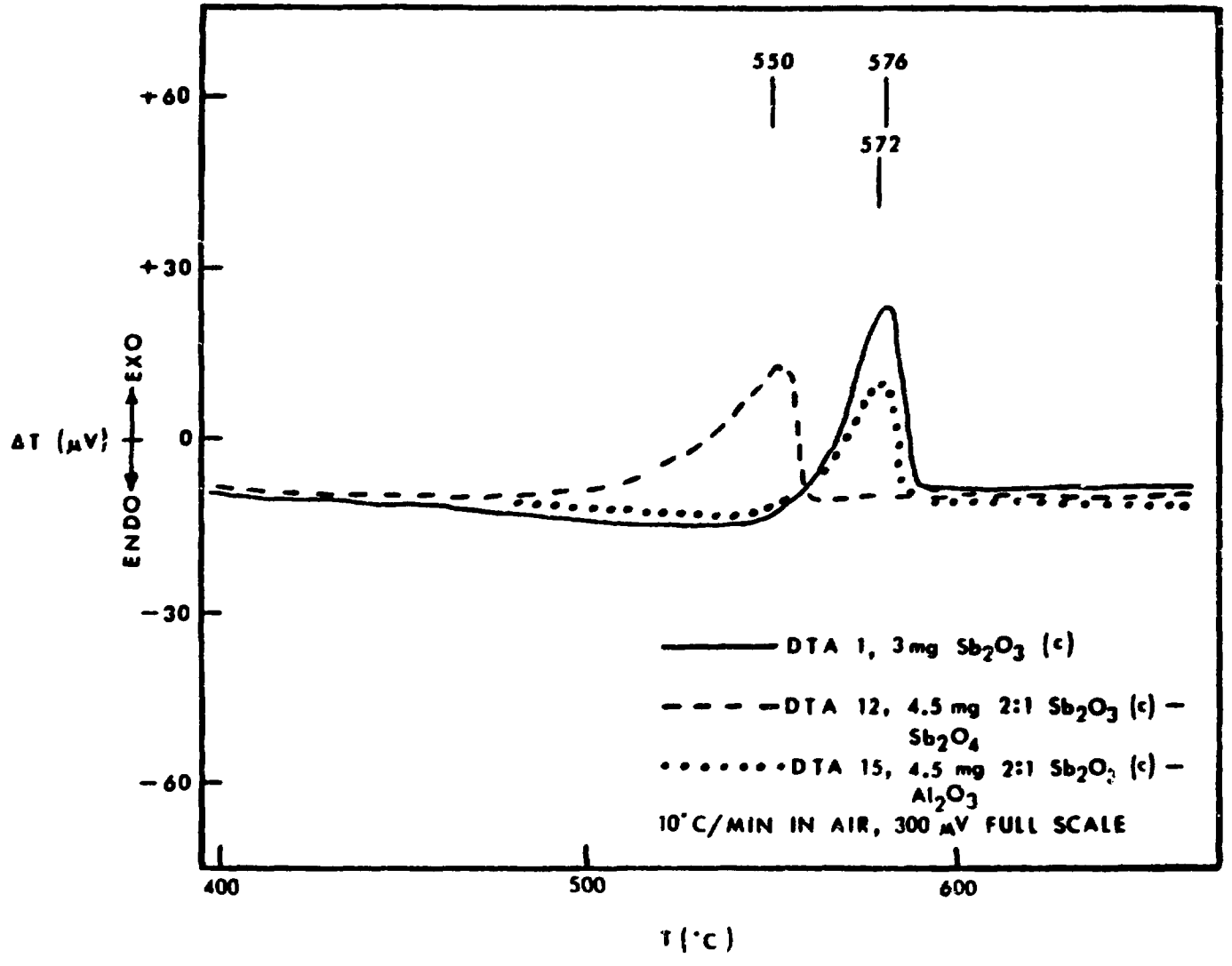

Figure 22. Effect of Sb_2O_4 and Al_2O_3 Additions on Oxidation of Sb_2O_3(c).

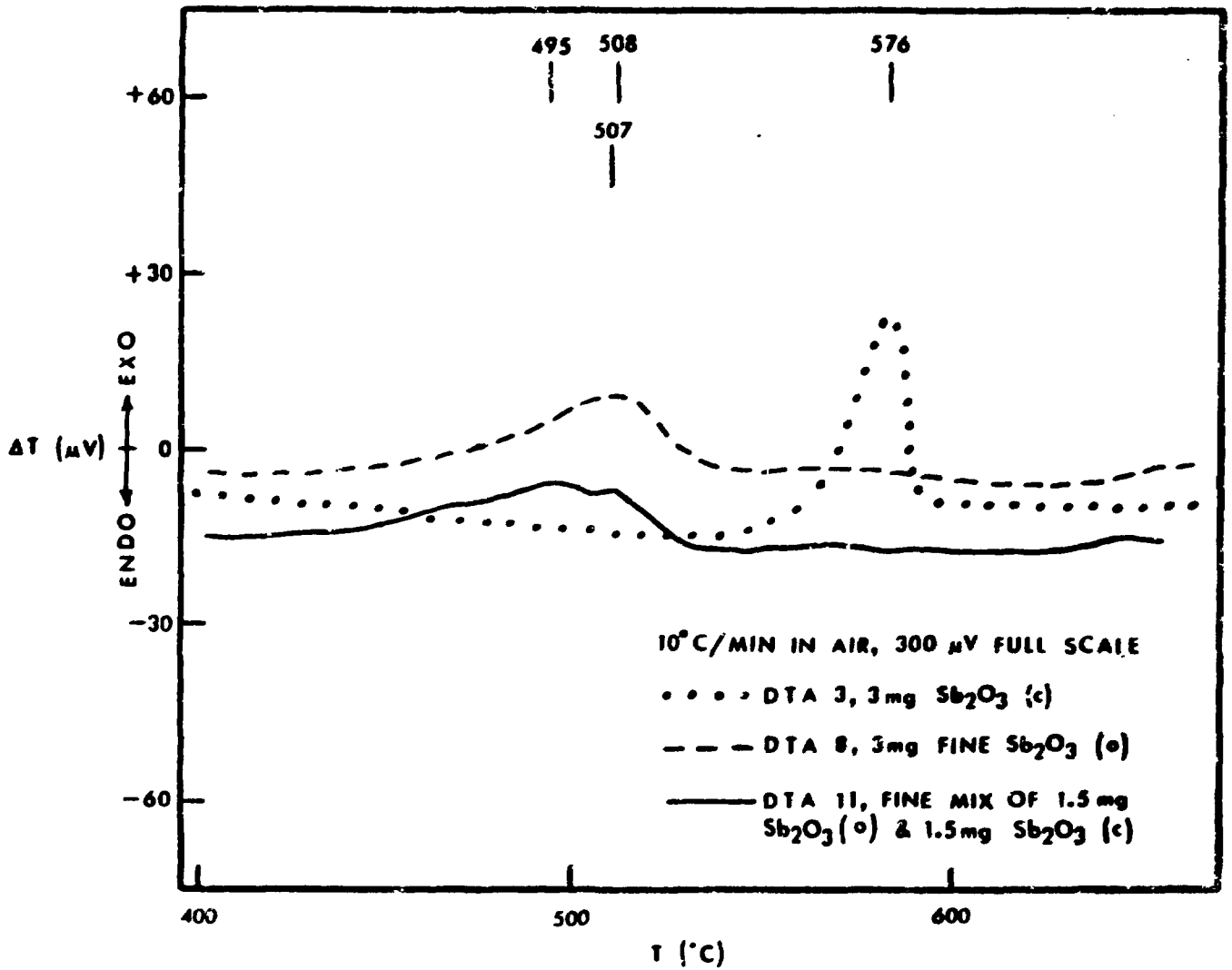

Figure 23. DTA of Sb_2O_3(c), Sb_2O_3(o) and Mixed Dimorphic Sb_2O_3.

be an effect of an orthorhombic surface on the oxidation of Sb_2O_3(c).

To determine if the presence of Sb_2O_3 alters the oxidation of MoS_2, DTA of MoS_2, MoS_2-Sb_2O_3 and Sb_2O_3 compacts were obtained. The DTA of powdered MoS_2 is presented in Figure 24. The onset of oxidation for MoS_2 is in agreement with data of Harmer and Pantano[8] and Peace[75]. DTA of compacts of MoS_2-Sb_2O_3 and Sb_2O_3 are given in Figure 25. As seen, the presence of Sb_2O_3 does not significantly influence the temperature of MoS_2 oxidation. These data suggest that there is not a role for antimony oxide in the oxidative protection of MoS_2. Concurrent wear studies presented later provided evidence that there is no significant anti-oxidant role for Sb_2O_3 in MoS_2 compacts, and this phase of the study was concluded.

SUMMARY OF Sb_2O_3 OXIDATION STUDIES

Isothermal oxidation studies of the oxidation under 140 torr oxygen sublimation is rate controlling for oxidation of either Sb_2O_3(o) or Sb_2O_3(c). The oxidation of Sb_2O_3(c) appears to require higher reaction temperatures for rates equivalent to Sb_2O_3(o). Mixtures of Sb_2O_3(c) and Sb_2O_3(o) appeared to be intermediate between Sb_2O_3(c) and Sb_2O_3(o); however, larger sized Sb_2O_3(c) was used inadvertently in the mixtures than in Sb_2O_3 oxidations. Since reaction rates involving sublimation are highly dependent upon surface area, the isothermal data for mixed

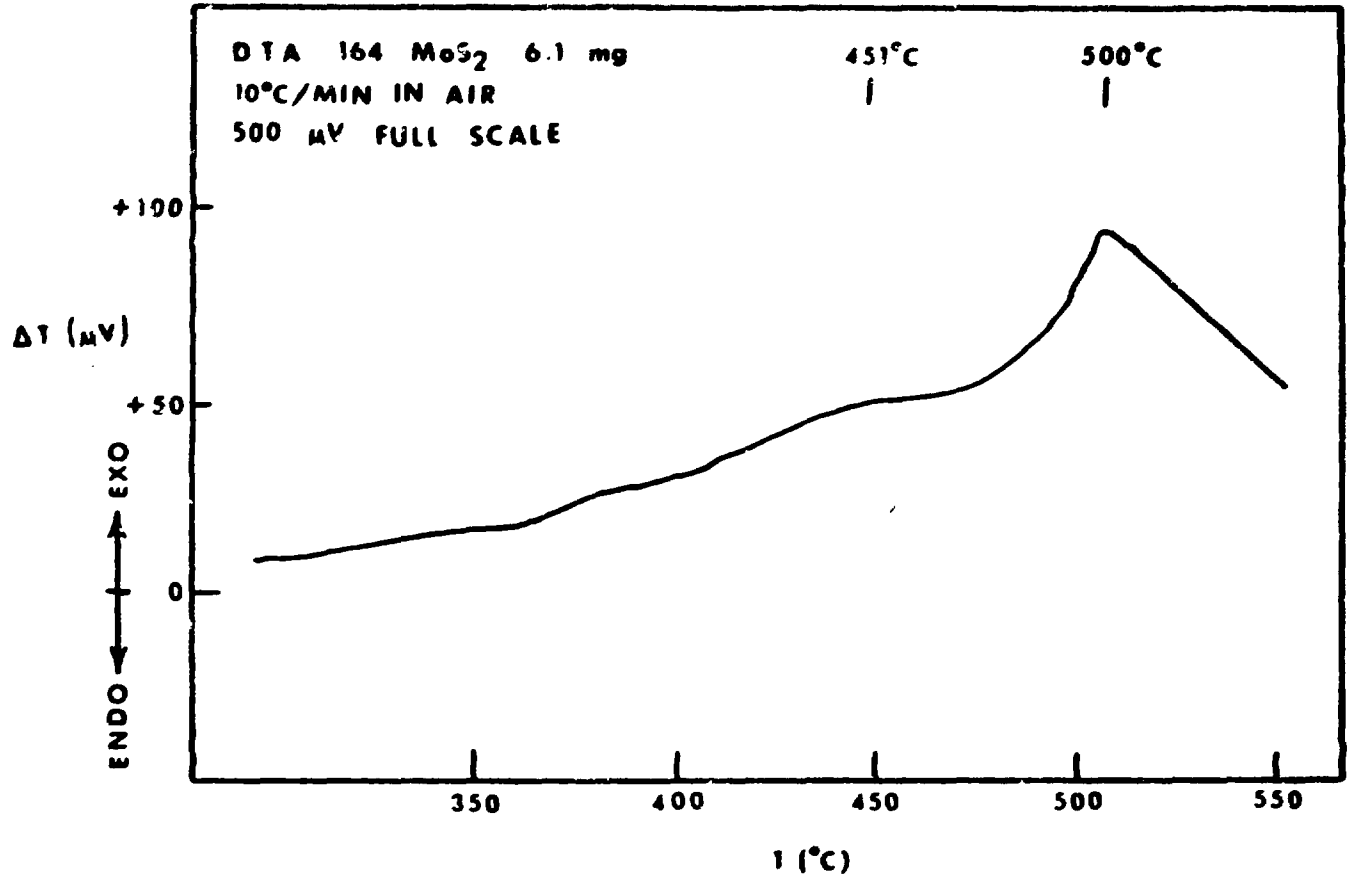

Figure 24. DTA of MoS_2.

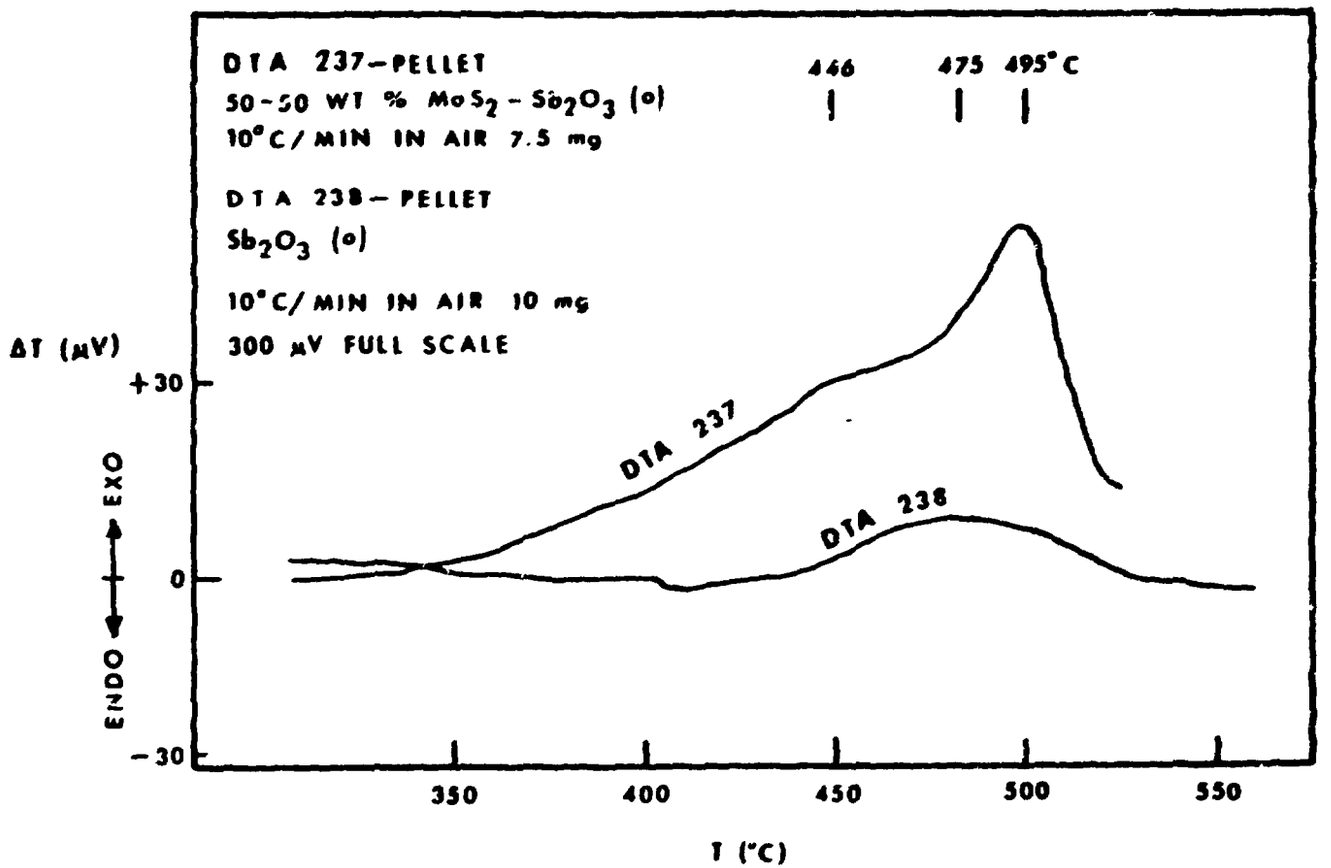

Figure 25. DTA of Compacts of MoS_2-Sb_2O_3 and Sb_2O_3.

Sb_2O_3 supports a mechanism of oxidation which includes sublimation but does not confirm the observations of Trofimov, et al.[72] The role of sublimation in oxidation of Sb_2O_3 is supported by calculations of free energies of oxidation for $Sb_2O_3(s)$ and the sublimed species, Sb_4O_6, which indicate a greater driving force for the oxidation of Sb_4O_6.

DTA results, however, indicate that mixtures of $Sb_2O_3(c)$ with $Sb_2O_3(o)$ or Sb_2O_4 do oxidize at lower temperatures supporting the observation of Trofimov and co-workers. DTA oxidation of $Sb_2O_3(o)$ or $Sb_2O_3(c)$ is in agreement with data of Golunski, et al.[56] Additionally, DTA of MoS_2 confirms that oxidation begins at about 300°C and is completed near 500°C. When a compact of MoS_2-Sb_2O_3 is analyzed, there is no significant difference in peak temperature for oxidation of MoS_2.

These data do not support a role for Sb_2O_3 in retarding oxidation of MoS_2 nor as sacrificially oxidizing instead of MoS_2 since Sb_2O_3 does not initially oxidize at temperatures comparable with the onset of oxidation of MoS_2.

CHAPTER V

PROPERTIES OF MoS_2-Sb_2O_3 SOLID LUBRICANT COMPACTS

Several properties of MoS_2-Sb_2O_3 compacts are critical to development of an understanding of that lubricating system. Areas of prime interest are how the compacts form, how they wear and what changes occur at the interface. The significance of each must be established to provide a basis for understanding of the beneficial mechanism of Sb_2O_3 additions to MoS_2.

COMPACTION

To establish if compaction of Sb_2O_3-MoS_2 plays an atypical role in its superior performance, previous efforts in the area were reviewed. In that review, it was found that Harmer and Pantano[8] compacted cylinders of MoS_2 with 25 and 45 wt% of Sb_2O_3 in a laboratory press to examine densification of solid lubricant compacts. Those data have been reduced and summarized in Table 9. The data were then employed to calculate the theoretical density fractions attained by compaction in Table 10. Those theoretical compact densities were plotted as a function of forming pressure in Figure 26. From Figure 26, several observations are apparent:

Table 9. DENSITY OF COMPACTS FOR DIFFERENT FORMULATIONS AND FORMING PRESSURES*

COMPOSITION				
Wt. %	Vol. %	FORMING PRESSURE (MPa)		
		PELLET DENSITY (g/cm^3)**		
		172	345	690
100% MoS_2	100	3.147	3.453 3.455	3.740
75% MoS_2 25% Sb_2O_3	77.26 22.74	3.319	3.636 3.605	3.940
55% MoS_2 45% Sb_2O_3	58.05 41.95	3.796	3.751 3.709	4.032

* Computed from Reference 8 data.

** Assuming densities of 4.80 g/cm^3 for MoS_2, 5.2 g/cm^3 for Sb_2O_3(c) and 5.67 g/cm^3 for Sb_2O_3(o) and that Sb_2O_3 used was a equimolar mixture of the Sb_2O_3 dimorphs.

Table 10. THEORETICAL COMPACT DENSITY FRACTION FOR DIFFERENT FORMULATIONS AND FORMING PRESSURES*

COMPOSITION		THEORETICAL DENSITY FRACTION		
		FORMING PRESSURE (MPa)		
wt. %	Vol. %	172	345	690
100% MoS_2	100.0	0.6556	0.7196	0.7792
75% MoS_2 25% Sb_2O_3	77.26 22.74	0.6693	0.7301	0.7946
55% MoS_2 45% Sb_2O_3	58.05 41.95	0.7464	0.7333	0.7928

* Computed from Reference 8 data.

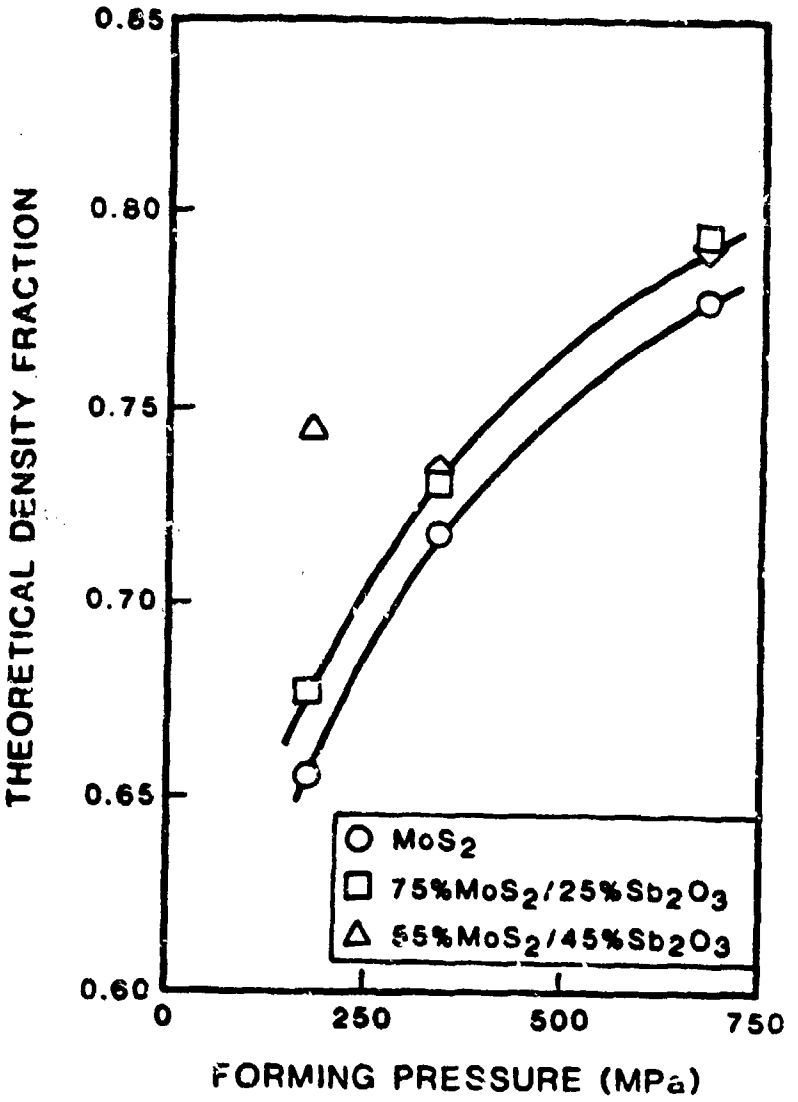

Figure 26. Theoretical Density Fraction as a Function of Forming Pressure from Harmer and Pantano.(8)

(i) Under the highest load for all compacts, only about 80% of theoretical density was obtained.

(ii) Both MoS_2 and MoS_2 containing 25 wt% Sb_2O_3 followed a similar pattern in that there was a gentle increase in fraction of theoretical density achieved as a function of increasing forming pressure.

(iii) For MoS_2 containing 45 wt% of Sb_2O_3, about 75% of theoretical density was achieved at the lowest pressure, or approximately 8% more than the compacts containing less Sb_2O_3. It also should be noted that the data for the intermediate pressure does not follow the expected trend. It is not known if there was a formulation, pressure, or other error or if the data presented are within a normal error distribution. Thus, it would be concluded that the addition of Sb_2O_3 aids in compaction and/or densification of solid compacts based upon their results. It is also seen that it might be possible to attain unusually high densification at lower pressures under optimum conditions if the low pressure, high Sb_2O_3 concentration data were valid.

To validate the previous compaction data of Harmer and Pantano[8], high purity Sb_2O_3(o) and MoO_3 (Alfa, Danvers, MA) were individually ground mechanically and sieved through a 30μm nickel screen. Oxides were weighed and thoroughly mixed with weighed technical grade MoS_2 (Bemol, Elmwood, CN) which is more adequately described in a later

section or wear of MoS_2-Sb_2O_3. These pellets were then compacted in a cylindrical die mounted in a laboratory press. Forming pressures were about 172 MPa (25,000 psi).

On removal from the die, compacts were measured and densities computed. Those data for each compact are presented in Table 11. The ratio of apparent density to theoretical density is a function of compact composition is given in Figure 27. It was found in these experiments that the addition of Sb_2O_3 or MoO_3 to MoS_2 does not improve compaction at relatively modest pressures at ambient. The trend for the MoS_2-Sb_2O_3 compacts is the opposite of that found by Harmer and Pantano. The opposite trends found are difficult to rationalize, although differences in oxide particle size may be significant. However, the largest difference is for pure MoS_2 where at similar forming pressure, Harmer and Pantano only achieved about 83% of the apparent density for MoS_2 obtained in this work. Although the difference in trends was obvious, efforts were not pursued to resolve the conflict since the experiments in this work indicate that large additions of Sb_2O_3 do not promote a typical densification of MoS_2 compacts at low pressures. Rather efforts were directed towards determining the influence of Sb_2O_3 and MoO_3 on compaction of MoS_2 at high temperatures.

Table 11. COMPACTION OF MoS_2 AND MoS WITH Sb_2O_3 OR MoO_3 AT AMBIENT

PELLET COMPOSITION	PELLET MASS	PELLET DIAMETER (cm)	PELLET HEIGHT (cm)	ρ DENSITY (g/cm^3)	ρ_T THEORETICAL DENSITY (g/cm^3)	$\frac{\rho}{\rho_T}$	MEAN $\frac{\rho}{\rho_T}$
MoS_2	0.5017	0.641	0.410	3.786	4.88	0.776	
	0.4768	0.641	0.390	3.788		0.776	0.777
	0.4758	0.641	0.388	3.800		0.779	±0.002
22.13 vol % MoO_3 77.87 vol % MoS_2	0.4865	0.641	0.431	3.498	4.84	0.723	
41.1 vol % MoO_3 58.9 vol % MoS_2	0.4823	0.641	0.457	3.265	4.80	0.680	
23.05 vol % Sb_2O_3 76.95 vol % MoS_2	0.4823	0.641	0.394	3.792	5.01	0.757	
42.33 vol % Sb_2O_3	0.4939	0.641	0.404	3.785	5.12	0.739	
57.67 vol % Sb_2O_3	0.7628	0.641	0.623	3.813		0.745	0.746
	0.7707	0.641	0.618	3.864		0.755	±0.008

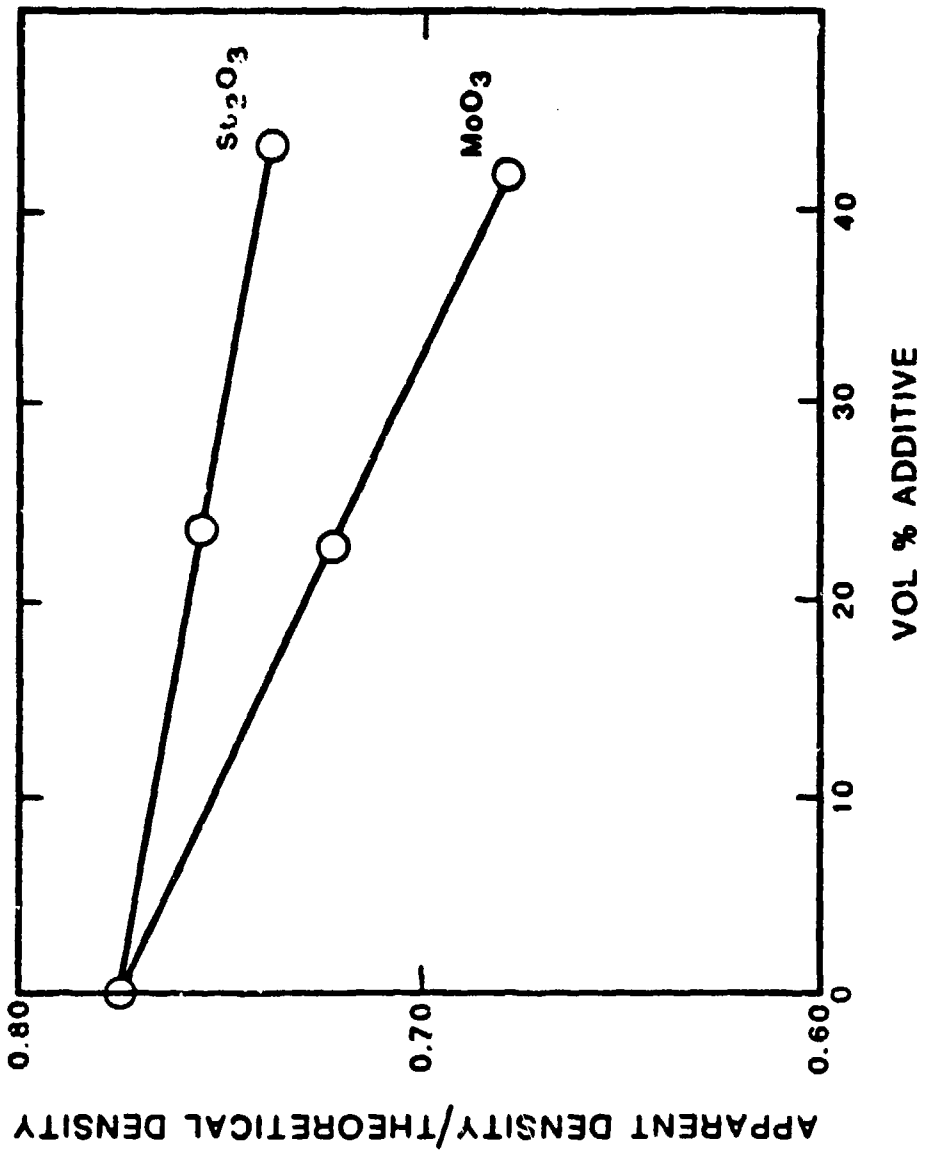

Figure 27. Density Ratio as Function of Volume Percent Additive.

To determine thermal expansion and softening properties of MoS_2 and MoS_2 plus additives at temperature, compressed cylinders were prepared in a 0.635 cm (0.25 in.) diameter die and pressed at 172.4 MPa. (25 ksi). The TMA employed a counterweighted loading system so it was possible to load all samples at one gram. The flat load rod was 2.48 mm in diameter and 4.83 mm^2 in contact area resulting in an extremely low pressure of 2.93 kPa (0.32 psi). The TMA increase in temperature was 2°C/min for all samples which were inerted under nitrogen.

For an Sb_2O_3 cylinder evaluated from room temperature to about 650°C under nitrogen, there appeared to be several regions of interest as the cylinder expanded in response to the increasing temperature. First, there is a region of modest expansion (15.5 μm/m/°C) from ambient to about 225°C after which the slope approached zero up to about 350°C. The rate of expansion then increased (43.1 μm/m/°C) in the approximate temperature range of 400°-510°C. Again, there was a region of reduced slope followed by a period of very rapid expansion near the $Sb_2O_3(c)$-$Sb_2O_3(o)$ transition. The expansion peaked at 610°C followed by rapid compression. These changes in the rate of thermal expansion for the polycrystalline compact are attributed to expansion of the crystal lattice, conversion of $Sb_2O_3(c)$ to $Sb_2O_3(o)$ followed by fusion of $Sb_2O_3(o)$.

For a MoS_2 cylinder, reduction in cylinder height was found from ambient to about 375°C. For the 7.57 mm length cylinder, the reduction in dimension was about 45 μm over that temperature interval. From 375°C to 769°C, the cylinder increased in length at a modestly accelerating rate (mean of ~ 40 μm/m/°C). Above 769°C, the cylinder again compressed until the end of the test at about 780°C.

The early compression of the MoS_2 cylinder is attributed to reorganization of the crystallites to a more stable structure. The pronounced effect in MoS_2 is thought to originate from the layered structure which would contribute to a strongly anisotropic structure initially formed in the die.

For a 50-50 weight percent sample of Sb_2O_3 and MoS_2, the expansion was virtually nil until about 300°C. To about 353°C, the structure expanded at a rate of about 45.8 μm/m/°C. Then expansion was very limited until 440°C, when rapid expansion took place which peaked at an estimated temperature region of 560°-570°C. The TMA results for the MoS_2 - Sb_2O_3 compact are given in Figure 28.

The expansion results for the Sb_2O_3 - MoS_2 cylinder are thought to be the result of balancing the expansion of Sb_2O_3 with the contraction of MoS_2 up to about 350°C followed by mutual expansion up to the point of fusion of Sb_2O_3.

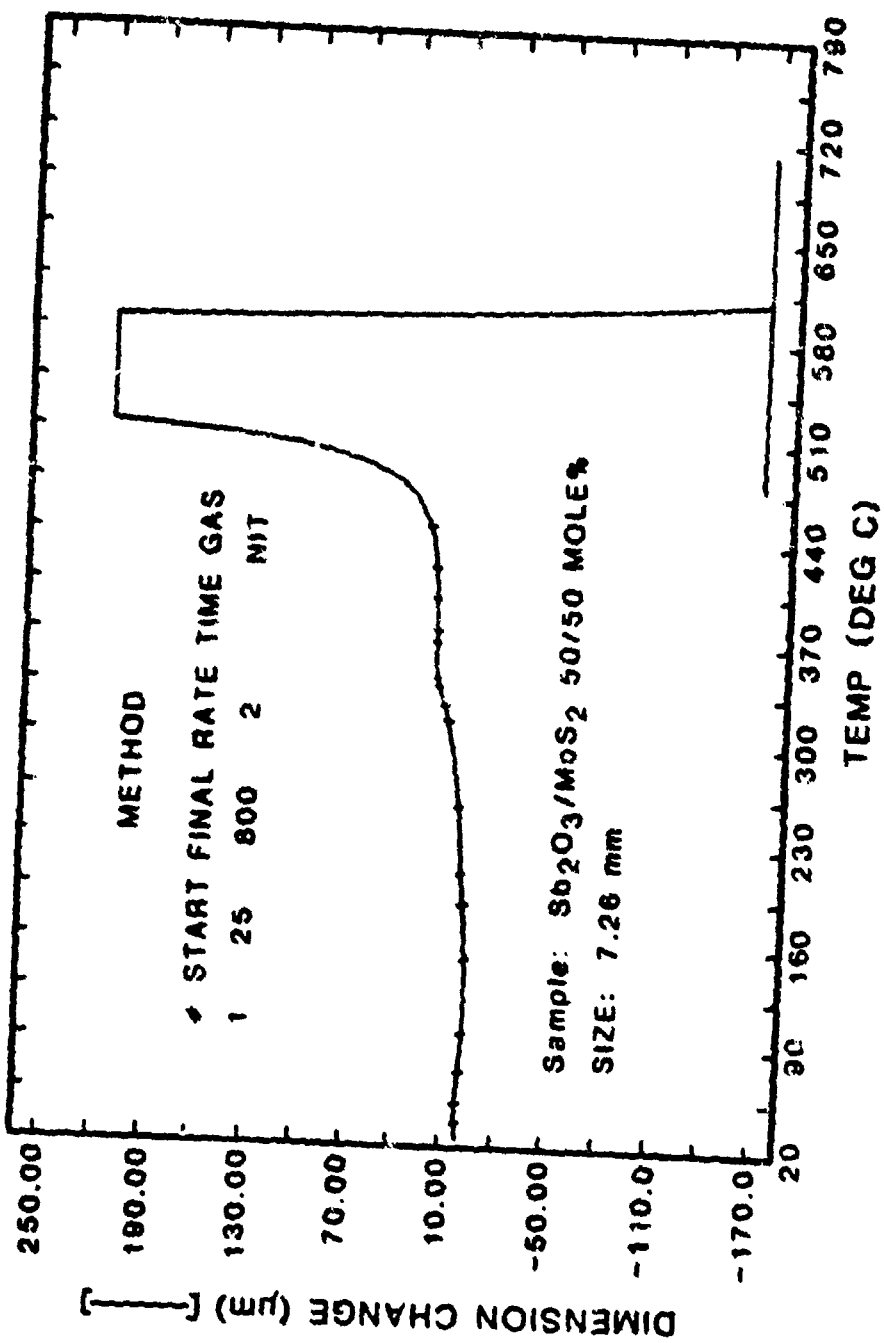

Figure 28. THA of MoS_2-Sb_2O_3 Compact.

A cylinder of 25 mole percent Sb_2O_3-25 mole percent MoO_3-50 mole percent MoS_2 was evaluated by TMA. The sample was initially heated under nitrogen to about 160°C when the TMA inadvertently held at that temperature until restarted. It was found that at about 275°C, the cylinder began to expand rapidly. After another 100°C temperature rise, the cylinder had expanded more than 5 μm longer than the original length of 8.49 mm, after which it was not instrumentally possible to record the rapid expansion. At about 725°C, the length of the cylinder had been sufficiently reduced so that the TMA was able to record the reduction in length. The expansion was attributed primarily to the presence of MoO_3 in the Sb_2O_3-MoS_2 compact. The Sb_2O_3-MoO_3-MoS_2 pellet began expanding significantly at a temperature about 175°C lower than the Sb_2O_3-MoS_2 pellet.

WEAR OF MoS_2-Sb_2O_3 COMPACTS

To study the effects of additions of Sb_2O_3 on the wear life of compacts, wear experiments were conducted at several temperatures under varying conditions. Compacts were formed and shaped for testing using the materials and procedures described below. Molybdenum sulfide was of technical grade from Bemol, Elmwood, CN; with composition and particle size specifications as given in Table 12.

Table 12. DESCRIPTION OF MoS_2 FOR COMPACTS

COMPOSITION	WEIGHT PERCENT	PARTICLE SIZE	WEIGHT PERCENT
MoS_2	98.2	On US Sieve No. 100 (>150 µM)	0
Acid Insoluble	0.35	Through 100 on 200 (<150 to >75 µM)	5
Iron	0.15	Through 200 or 325 (<75 µM to >45 µM)	10
Molybdenum Trioxide	0.01	Through 325 (<45 µM)	85
Water	0.00		
Oil	0.03		
Carbon	1.00		
Acid Number	0.01		

The molybdenum disulfide is representative of what is available commercially for solid lubricant applications and was used without modification.

The antimony oxides were prepared identically to those described previously for oxidation studies. Because of the size of Sb_2O_3(o) formed in the furnace, it was necessary to finely grind and sieve the product before compaction (<20 μm). Initially, it was thought that by simply sieving Sb_2O_3(c) through a 325 mesh screen (<44 μm) would be sufficient, however, it was found later that it was necessary to grind Sb_2O_3(c) also to obtain the least wear. The effects of Sb_2O_3(c) particle size on wear shall be discussed in a subsequent section. Materials were weighed to the nearest tenth of a milligram with a total cylinder weight of 300 mg. The compacts were prepared by thoroughly mixing the weighed components and pressing at 275.2 MPa (40 ksi) in a cylindrical die in a laboratory press. The compact mounted in the die was trimmed by lathe. The angle of cut was 21.8 degrees receding from the face. The substrates were 440C stainless steel disks with a surface hardness of 57-60 R_c.

Wear disks were prepared by initial light, wet sanding with 400 grit followed by 600 grit silicon carbide paper. Lapping was performed using a Lapmaster Model 12 machine employing 3 micrometer corundum powder. Disks were cleaned with Stoddard solvent and rinsed in water followed by

isopropyl alcohol prior to oven drying at approximately 60°F. A surface finish of 4-6 microinches was attained as measured by a Bendix Profilometer, Type 0B, Model 18. The profilometer was calibrated using a glass roughness standard.

Tripellet evaluation of solid lubricant compositions were performed initially using the Midwest Research Institute (MRI) pellet wear-life machine.(76) The machine as pictured in Figure 29 with the wear cone and mounting schematic shown in Figure 30, permits loading three lubricant compacts with a total load of 300 g. Sliding velocity is approximately 3.81 m/s (750 ft/min).

The frictional force generated during sliding was measured by use of a linear variable differential transformer (LVDT) mounted to measure deflection of a spring loaded retainer. The LVDT output was recorded by strip chart recorder. Run times were typically 20 minutes at room temperature, but test times were modified as necessary to achieve measurable cone diameters. Since cones were used, comparisons between tests must be based upon identical tests including time and sliding distance so that wear volume data may be useful. It is reasonable to assume that the wear equation such as the one proposed by Archard for adhesive wear and described previously,(14)

$$V = \frac{k\ Lx}{3p} \qquad (5.1)$$

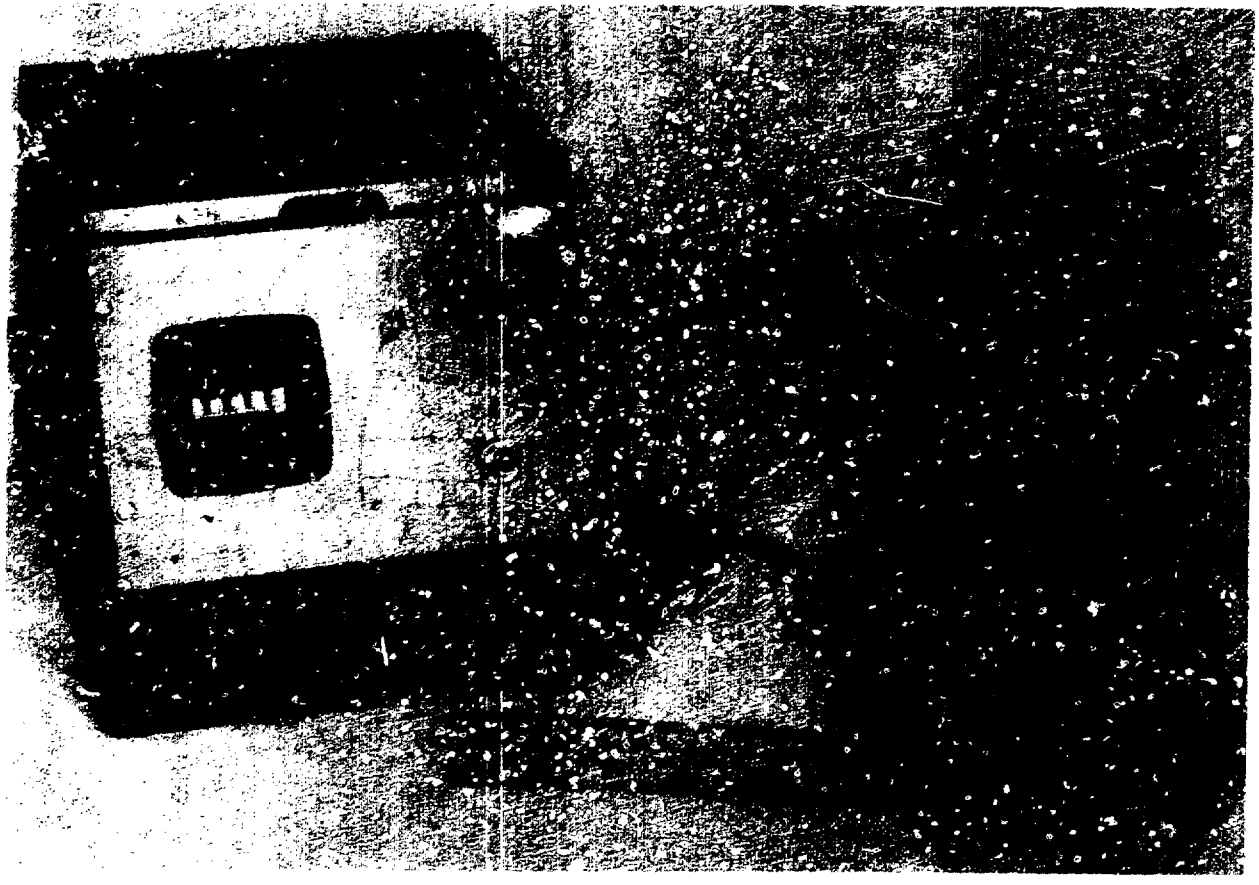

Figure 29. Triplellet Wear Test Machine.

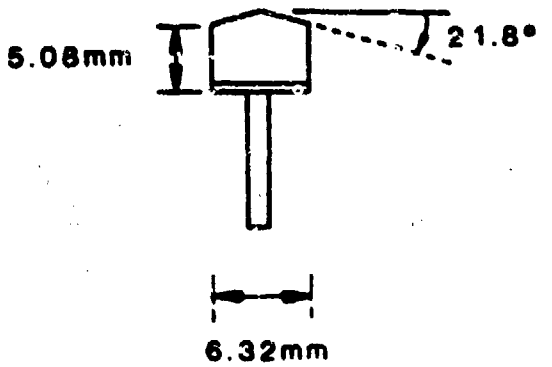

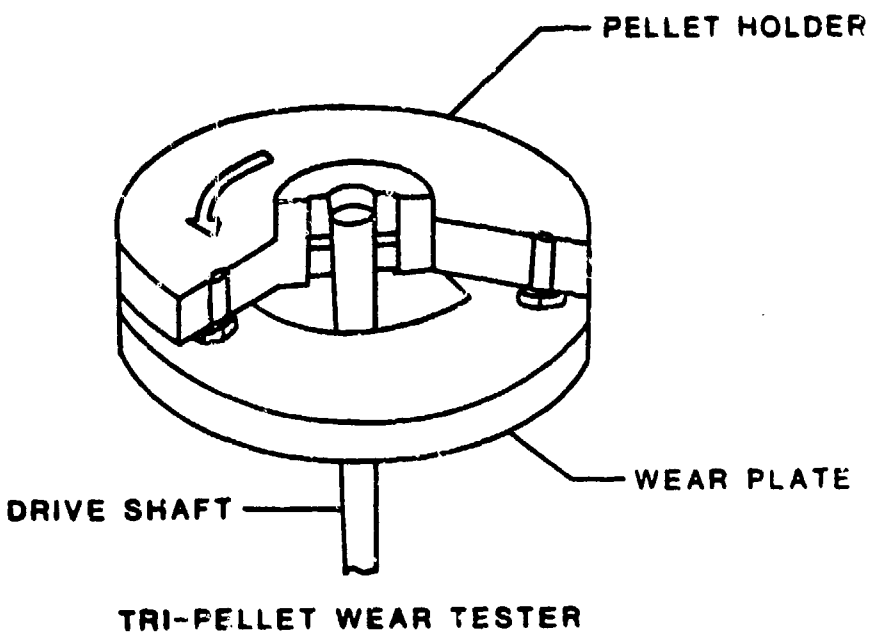

Figure 30. Wear Cone and Pellet Mount Configuration.

The wear volume, V may be calculated as follows:

$$V = \frac{\pi}{3} r^2 h = 1.047 r^2 h \qquad (5.2)$$

and for a 21.8° cone,

$$h = 0.39997\ r \qquad (5.3)$$

then substituting,

$$V = (1.047)(0.39997r)r^2$$
$$= 0.4188\ r^3$$

r = radius of worn cone base

h = worn cone height

After microscopic measurement of the cone diameter, wear volume was then calculated using the above relationship. The microscope was a Bausch and Lomb (25x). A stage micrometer was used for calibration.

Pellet loads were computed based upon the weight of the mount, holder and solid lubricant compact. Of course, as the pellet wears, the load is reduced insignificantly; however, the apparent contact stress decreases significantly during wear tests because the pellet contact area increases, so data may be used for comparative purposes only.

Some tripellet tests conducted at room temperature were performed with the test machine installed in a drybox manufactured by Vacuum/Atmosphere Co., Hawthorne, CA (Model HE-403 Dri-Train). Water removal was accomplished by use of a molecular sieve. The drybox atmosphere may be continuously circulated through the molecular sieve bed using a fan and duct system.

The concentration of atmospheric moisture was varied for wear of MoS_2-antimony oxide compacts. Trace moisture content was determined with a Shaw hygrometer manufactured in Bradford, England. The instrument permits the measurement of trace atmospheric moisture at the part per million level.

To obtain very high levels of moisture in the drybox, the atmosphere was saturated by bubbling air through water and passing through the drybox.

Only limited wear tests were conducted because a great amount of effort was required to prepare materials for each specimen and to evaluate the compacts.

TRIPELLET WEAR TESTS AT ROOM TEMPERATURE

Dry Air

Initial testing conducted in a drybox substantiated the dramatic effect of atmosphere upon MoS_2 wear properties, which has been reviewed previously.[77] In four hour tripellet tests on 440C steel substrates in very dry air (1-3 ppm H_2O), wear of MoS_2 was comparable with

MoS_2 containing 25 mole percent of Sb_2O_3 or Sb_2O_4 at about 0.2 to 0.3 mm^3 per compact with minor effects of the oxide additions found. Very low friction coefficients (≈0.05) were generated in most evaluations with the exception of MoS_2-Sb_2O_4 at 0.1-0.13. (Tests 2-9).

Wet Air

When the test environment was saturated with H_2O, it was necessary to shorten test times to one minute for MoS_2. The wear volume (3.9 mm^3) for MoS_2 in wet air was about an order of magnitude larger than tests that were 240 times longer in dry air (Tests 2 and 10). Data generated in the tests (Tests 11-16) indicates that MoS_2 with Sb_2O_3(o) or Sb_2O_3(c) wore less than compacts of MoS_2. A compact of MoS_2-Sb_2O_4 wore at a rate of about three times greater than compacts containing Sb_2O_3, but wore at a much slower rate than pure MoS_2 compacts. Friction coefficients for all compacts were uniformly high (0.1-0.33) and highly irregular in saturated air. Inspection of compacts by optical and scanning electron microscopy suggest that the oxides were providing a stable support structure in a soft matrix of MoS_2. Discrete antimony oxide particles could be found around which MoS_2 appeared to be flowing.

SINGLE PELLET WEAR TESTS

For the next series of wear tests, the single pellet MRI Mark-VB machine[76] was employed as shown in Figure

31. The tests (Tests 29-35) were conducted in air introduced through desiccant into the test chamber (≈50-80 ppm H_2O, except Test 35 because of a moisture leak) at room temperature for 20 minutes. With the Mark-VB apparatus, it was not possible to reduce H_2O levels to the level achieved with earlier tests in a dry box. The data are summarized in Table 13. The wear volumes were smaller than earlier tripellet tests conducted in either very dry or very wet atmospheres. The lowest wear exhibited was with MoS_2-Sb_2O_3(o). In fact, Sb_2O_3(o) was the only beneficial additive. Sb_2O_3(o) was also tribologically superior in earlier drybox tests but not to the extent seen in these tests. The larger wear volumes found for Sb_2O_3(c) were later attributed to the bipyrimidal crystal structure of Sb_2O_3(c), which, even though sieved through 325 mesh (< 44 μm), appeared to abrade wear surfaces. Lowest coefficients of friction were the lowest for MoS_2-Sb_2O_3(o) formulations. MoS_2-Sb_2O_4 compacts initially generated coefficients comparable with MoS_2-Sb_2O_3(o) but increased substantially during the test. Mechanical problems precluded the measurement of friction coefficients for MoS_2-Sb_2O_3(c) compacts. These data indicated a superiority for compacts containing Sb_2O_3(o).

WEAR EVALUATIONS AT 160°C

Five tests were run at 160°C for 10 minutes: two (Tests 37 and 38) in ambient air (50% RH), and three (Tests

Table 12. SINGLE PELLET WEAR VOLUMES

RT, Dry Air, 20 Minutes, 440C Wear Disks

TEST NUMBER	PELLET COMPOSITION (Mole Percentage)	WEAR VOLUME (mm^3)	COEFFICIENT OF FRICTION
29	MoS_2	0.17	0.1 - 0.13
30	MoS_2	0.16	0.11 - 0.13
31	75 MoS_2 - 25 Sb_2O_3(o)	0.05	0.06 - 0.07
32	75 MoS_2 - 25 Sb_2O_3(o)	0.07	0.05 - 0.06
35	75 MoS_2 - 25 Sb_2O_3(c)	2.46	---
36	75 MoS_2 - 25 Sb_2O_3(c)	0.71	---
33	75 MoS_2 - 25 Sb_2O_3	0.24	0.06 - 0.13
34	75 MoS_2 - 25 Sb_2O_4	0.22	0.05 - 0.17

Figure 31. MRI Mark-VB Single Pellet Wear Test Machine.

39-41) in dry argon (<80 ppm O_2). Those data are presented in Table 14. It was found that MoS_2 compacts with 25 mole percent Sb_2O_3(o) generated less wear volume than pure MoS_2 compacts under both conditions. These data suggest that the role of Sb_2O_3 in improvement of MoS_2 tribological properties does not involve oxygen or oxidation. Interpretation of friction data is difficult in that the values determined are closely grouped.

WEAR EVALUATIONS AT 232°C

A number of formulations were evaluated on the MRI Mark-VB single pellet machine at 232°C under a variety of atmospheric conditions (Test 42-57). Those data are summarized in Table 15. The tests indicated that wear volume from lowest to highest was in order of MoS_2-Sb_2O_3(o), MoS_2, MoS_2-Sb_2O_4 and MoS_2-Sb_3O_3(c). All friction coefficients were from 0.06 to 0.14 with MoS_2 compacts at the higher end of the range.

An important observation is that the wear volume of compacts containing Sb_2O_3(c) that was ground and sieved identically to Sb_2O_3(o) produced much lower wear volumes than compacts containing unground Sb_2O_3(c). Comparing wear data and scanning electron microscopy of pellets with both ground and unground Sb_2O_3(c) suggests that sieved unground Sb_2O_3(c) can abrade the wear surface much more easily than ground Sb_2O_3(c), because the unground particles tend to form masses of abrasive materials compared with ground

Table 14. SINGLE PELLET WEAR DATA AT 160°C

TEST NUMBER	COMPOSITION (Mole Percent)	WEAR VOLUME (mm^3) AIR 50% RH	WEAR VOLUME (mm^3) ARGON	COEFFICIENT OF FRICTION AIR 50% RH	COEFFICIENT OF FRICTION ARGON
37	MoS_2	0.13		0.09 - 0.11	
39	MoS_2		0.25		0.09 - 0.12
41	MoS_2		0.18		0.09 - 0.10
38	75 MoS_2 - 25 Sb_2O_3(o)	0.09		0.08 - 0.10	
40	75 MoS_2 - 25 Sb_2O_3(o)		0.06		0.05 - 0.07

Table 15. WEAR EVALUATIONS AT 232°C ON 440C WEAR DISKS

TEST #	COMPOSITION (Mole Percent)	WEAR VOLUME (mm^3)			FRICTION COEFFICIENT		
		DRY AIR	WET AIR	ARGON	DRY AIR	WET AIR	ARGON
46	MoS_2			0.35			0.11 - 0.12
47	MoS_2	0.16			0.12		
52	MoS_2		0.20			0.13 - 0.14	
42	75 MoS_2 - 25 Sb_2O_3(o)			0.05			0.08
50	75 MoS_2 - 25 Sb_2O_3(o)	0.02			0.06 - 0.07		
53	75 MoS_2 - 25 Sb_2O_3(o)	0.13				0.08 - 0.09	
57	75 MoS_2 - 25 Sb_2O_3(o)	0.13				0.07 - 0.09	
43	75 MoS_2 - 25 Sb_2O_3(c)			2.2			0.07 - 0.12
45	75 MoS_2 - 25 Sb_2O_3(c)			2.1			0.08 - 0.10
55	75 MoS_2 - 25 Sb_2O_3(c)		1.78			0.07 - 0.10	
56	75 MoS_2 - 25 Sb_2O_3(c)		0.39 (Ground)			0.06 - 0.07	
44	75 MoS_2 - 25 Sb_2O_4			0.23			0.07 - 0.10
49	75 MoS_2 - 25 Sb_2O_4	0.31			0.08 - 0.11		
54	75 MoS_2 - 25 Sb_2O_4		0.27			0.07 - 0.13	
69	75 MoS_2 - 25 Sb_2O_4		0.17 (Ground)				0.09 - 0.11

Sb_2O_3(c). These data invalidate earlier test data generated here at lower test temperature from pellets containing unground Sb_2O_3(c). Grinding Sb_2O_4 in a similar manner reduces compact wear volume. The grinding permits more intimate mixing with MoS_2 and reduces the probability that large abrasive particles will damage the substrate solid lubricant film.

Additionally, Lavik, Hubbell and McConnell[1] indicate that MoS_2 with additions of Sb_2O_3 are superior tribologically in both air and vacuum to MoS_2 compacts, strongly inferring that a role for oxidation of MoS_2 or Sb_2O_3 is non-existent. Limited wear studies of compacts presented in Table 15 in dry air and dry argon confirm that Sb_2O_3 addition to MoS_2 is beneficial for wear in both air and inert atmosphere at 232°C. Thus, a beneficial role involving oxidation for additions of Sb_2O_3 to MoS_2 cannot be supported.

SINGLE PELLET WEAR EVALUATIONS AT 316°C

All tests at 316°C were performed on the MRI Mark-VB machine. 440C steel wear disks were used for 10 minute tests 61 to 73; all other evaluations employed Type 302 stainless steel shim stock (0.05 mm thick) with test times of 1000 seconds.

The first series of evaluations at 316°C was to generate data for comparison with results from the tests at lower temperatures. This series of tests is summarized in

Table 16. At 316°C, the effects of atmosphere are apparent. Under argon, the wear is typically greater than for identical evaluations in air. These results confirm the effects of the atmosphere as reported in the literature,[77] where it is noted that MoS_2 wear in argon is high because MoO_3 does not form. MoO_3 is believed to bind MoS_2 crystals together for improved performance.

These results at 316°C indicate that antimony oxides improve the tribological performance of MoS_2. Results with Sb_2O_3(c) are believed to be the result of large, unground crystals of Sb_2O_3(c) which effectively abrade the interface. The significance of the shape and size of Sb_2O_3(c) was only established after these initial experiments at 316°C.

MoS_2 compacts containing Sb_2O_3(o) yielded not only lower wear volumes compared with pure MoS_2, but also lower coefficients of friction. Sb_2O_3(o) wear was marginally reduced in argon compared with air. Because previous tests showed that Sb_2O_3(o) additions were most beneficial, wear tests with Sb_2O_3(c) and Sb_2O_4 were not repeated.

Similar tests were performed on the stainless steel shim stock previously described, primarily to generate wear surfaces that could be easily mounted for examination by scanning and transmission electron microscopy. Those data are summarized in Table 17. The data indicated that 25

Table 16. INITIAL WEAR STUDIES AT 316°C

TEST #	COMPOSITION (Mole Percent)	WEAR VOLUME (mm^3) DRY AIR	WEAR VOLUME (mm^3) ARGON	FRICTION COEFFICIENT DRY AIR	FRICTION COEFFICIENT ARGON
62	MoS_2	0.36		0.14 - 0.15	
65	MoS_2		0.64		0.10 - 0.11
70	MoS_2	0.16		0.08 - 0.14	
61	75 MoS_2 - 25 Sb_2O_3(o)	0.19		0.07 - 0.09	
66	75 MoS_2 - 25 Sb_2O_3(o)		0.12		0.07 - 0.09
63	75 MoS_2 - 25 Sb_2O_3(o)	7.97		0.08 - 0.2	
68	75 MoS_2 - 25 Sb_2O_3(o)		5.6		0.05 - 0.14
64	75 MoS_2 - 25 Sb_2O_4	0.18		0.08 - 0.19	
67	75 MoS_2 - 25 Sb_2O_4		0.54		0.08 - 0.19

Table 17. INITIAL MoS_2 ANTIMONY OXIDE WEAR TESTS ON 0.05 mm SS SHIM STOCK IN DRY AIR (100 g LOAD) AT 316°C

TEST#	COMPOSITION (Mole Percent)	WEAR VOLUME (mm^3)	COEFFICIENT OF FRICTION (μ)
74	MoS_2	0.35	---
79	65 MoS_2 - 35 Sb_2O_3(o)	0.20	0.07
75	75 MoS_2 - 25 Sb_2O_3(o)	0.13	---
78	85 MoS_2 - 15 Sb_2O_3(o)	0.32	0.2 - 0.3
76	75 MoS_2 - 25 Sb_2O_3(c)	1.12	---
77	75 MoS_2 - 25 Sb_2O_4	0.25	0.21 - 0.36
81	75 MoS_2 - 12.5 Sb_2O_3(o) - 12.5 Sb_2O_3(c)	0.12	0.07 - 0.10

mole percent of Sb_2O_3(o) or a total of 25 mole percent of equimixed Sb_2O_3(o)-Sb_2O_3(c) are effective additives for MoS_2 under these conditions.

A simple evaluation of Sb_2O_3(o) concentration (Tests 75, 78, 79) is also given in Table 17 suggesting that the 25 mole percent concentration is better than 15 or 35 mole percent. However, as with many wear tests, the data are only single points, and substantial conclusions cannot be made; rather, trends were established to identify areas for additional effort.

EFFECT OF LOAD ON WEAR IN 316°C TESTS

Tests were also conducted to determine if variation of wear volume as a function of load for MoS_2-Sb_2O_3(o) compacts required any additional study. The results as given in Table 18 generated expected results, i.e., wear was reasonably proportional to load, and the effort was terminated.

EXAMINATION OF WEAR SURFACES BY ELECTRON MICROSCOPY

An attempt was made to examine wear tracks (Wear Tests 73-76) produced on the 0.05 mm stainless steel substrates using transmission electron microscopy (TEM). Using the standard preparative technique of embedding the sample in an organic resin, curing and cutting thin sections with a diamond edge, it was found that samples suitable for TEM could not be prepared. Evidently, the very soft wear track

Table 18. EFFECT OF LOAD ON WEAR VOLUME FOR TESTS AT 316°C FOR 1000 SECONDS

TEST #	COMPOSITION (Mole Percent)	LOAD (g)	WEAR VOLUME (mm^3)	COEFFICIENT OF FRICTION
82	75 MoS_2 - 25 Sb_2O_3(o)	50	0.05	.07 - .09
75	75 MoS_2 - 25 Sb_2O_3(o)	100	0.13	---
83	75 MoS_2 - 25 Sb_2O_3(o)	150	0.17	.06

materials varied so greatly in hardness from the steel foil that uniform cross-sections could not be removed as a whole.

When the foils were mounted in a standard metallurgical mount and polished, for scanning electron microscopic examination, the results were disappointing. Again, disturbance of the wear track and blending of that section into the mounting material appeared to limit the usefulness of the technique.

Wear compacts and tracks were also prepared for direct examination by scanning electron microscopy (SEM) in the following manner. Tracks and compacts were coated with a layer of silver to improve conductivity of the sample. Coating was done in a Ernest F. Fullum Vacuum Evaporator Model 12500, at a vacuum of 10^{-3} torr. The specimens were placed 10 cm from the tungsten basket which contained silver wire that was evaporated under vacuum at a current of less than 20 amperes.

The samples were examined in an Amrsy SEM Model 1600. Samples were positioned perpendicular to the electron beam at an accelerating voltage of 30 keV and a Z distance of 12 mm for accurate measurement capability. Since all conditions remained the same, the relative sizes of worn area could be estimated from photographs made at the same magnification.

Important SEM observations are that MoS_2 compacts worn at 316°C have a rough appearance compared with MoS_2 compacts containing Sb_2O_3 evaluated under the same conditions. For the MoS_2 sample, after wear at 316°C for 1000 seconds in dry air, the compact surface contained cracks and fissures as well as an abundance of wear debris (Wear Test 115). A comparative test of a wear compact (Test 116) containing Sb_2O_3 under the identical test conditions produced a much smoother surface. This is evident in SEM views of the two surfaces in Figures 32 and 33.

This observation is in agreement with that of Harmer and Pantano[8] who found that densification and sintering of worn compacts of MoS_2-Sb_2O_3 was obvious compared with MoS_2 wear compacts.

EUTECTIC FORMATION OF Sb_2O_3 WITH MoO_3

To determine if a eutectic of Sb_2O_3-MoO_3 is formed during sliding of MoS_2-Sb_2O_3 compacts, and to elucidate a possible beneficial role of such a eutectic in those compacts, a eutectic mixture was prepared and compared with materials formed on sliding of MoS_2-Sb_2O_3 compacts.

In the hypothesis advanced by Lavik, Hubbell and McConnell,[7] eutectics formed from bulk additives and oxides produced during sliding, e.g., Sb_2O_3 with MoO_3 from MoS_2, would improve the tribological process. The

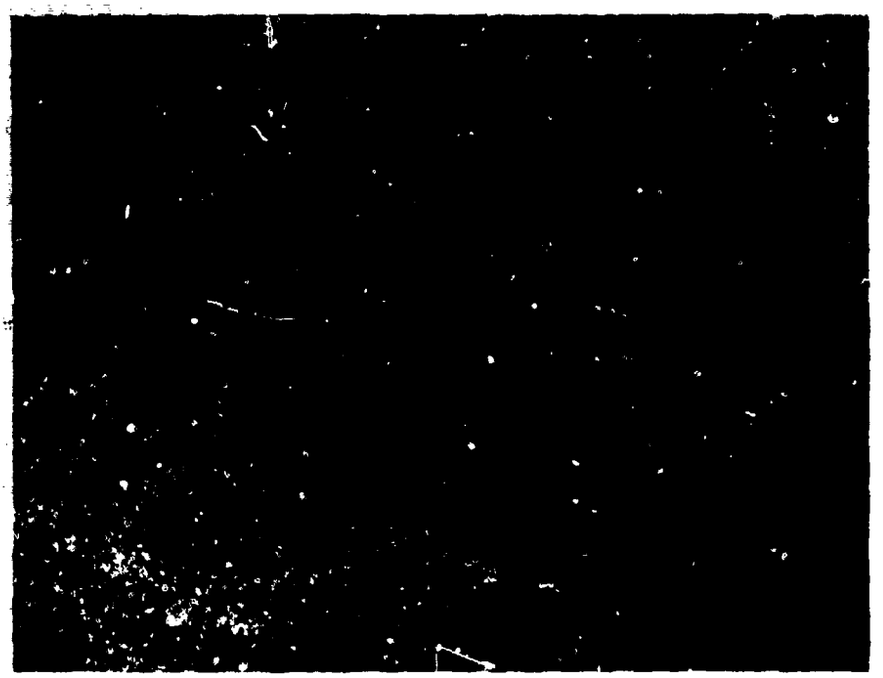

Figure 32. SEM Micrograph of MoS_2 Worn Surface Compact.

Figure 33. SEM Micrograph of MoS_2-Sb_2O_3 Worn Compact Surface.

mechanism of improvement was not investigated; however, those authors speculated that oxides bond to substrate surfaces which might improve attachment of the lubricant, i.e., act as "bonding" agents for MoS_2. The virtue of eutectic formation was speculated to be that oxide weldment and attachment would be possible or could occur at lower temperatures. At the time of that work, data had not been published on the eutectic formation between Sb_2O_3 and MoO_3. However, in 1975, Parmentier, et al.[64] did publish the results of an investigation of Sb_2O_3-MoO_3 eutectic formation. Those authors found that when mixtures of antimony oxide and molybdenum oxide were mixed and sealed under argon in glass ampules and heat-treated at 500°C for 24 hours, then eutectics were formed. While Sb_2O_3 melts at 656°C and MoO_3 melts at 795°C, three eutectic temperature minima were detected. The temperatures of the eutectic points are 518°, 536° and 596°C. The minima were determined by use of differential thermal analyses of the heat-treated materials. Diffraction patterns of Sb_2MoO_6 and $Sb_2(MoO_4)_3$ compositions were obtained using x-ray techniques.

Parmentier, et al. data indicate that indeed eutectic formation between Sb_2O_3 and MoO_3 is possible and that such materials in concentrations as required to produce the lowest melting combination is conceivable on the sliding interfaces of MoS_2-Sb_2O_3 compacts.

To investigate the possibility for a role of the Sb_2O_3-MoO_3 eutectic in the improvement of the tribological performance of MoS_2-Sb_2O_3 compacts, finely ground compositions of 25 mole percent Sb_2O_3-75 mole percent MoO_3, and 75 mole % Sb_2O_3-25 mole % MoO_3 were mixed and added to quartz tubes. The tubes were then evacuated (10^{-6} torr) three times and filled with 99.998% argon. On the fourth evacuation, the tubes were refilled to a pressure of 150 torr. The tubes were then separately inserted into a muffle furnace and allowed to stand for 24 hours at 500 ± 10°C. During the early phases of heat-treating, the tube containing the highest concentration of MoO_3 shattered. This experiment was not repeated. For the other composition, the tube was opened after air quenching. A sample of the material was examined using differential thermal analysis. 75 mole percent Sb_2O_3-25 mole percent MoO_3 mixture, in a differential thermogram was obtained using the Stone DTA. An endotherm was detected at 517°C for 10 mg sample heated at 10°C/min. under argon. When the DTA furnace was allowed to cool, an exotherm of about the same size and shape was observed as shown in Figure 34. Thus, the findings of Parmentier, et al. were confirmed in that a eutectic of Sb_2O_3-MoO_3 was produced and is detectable.

MoS_2-Sb_2O_3 compacts were then worn at ambient to generate surfaces suitable for x-ray diffraction and DTA

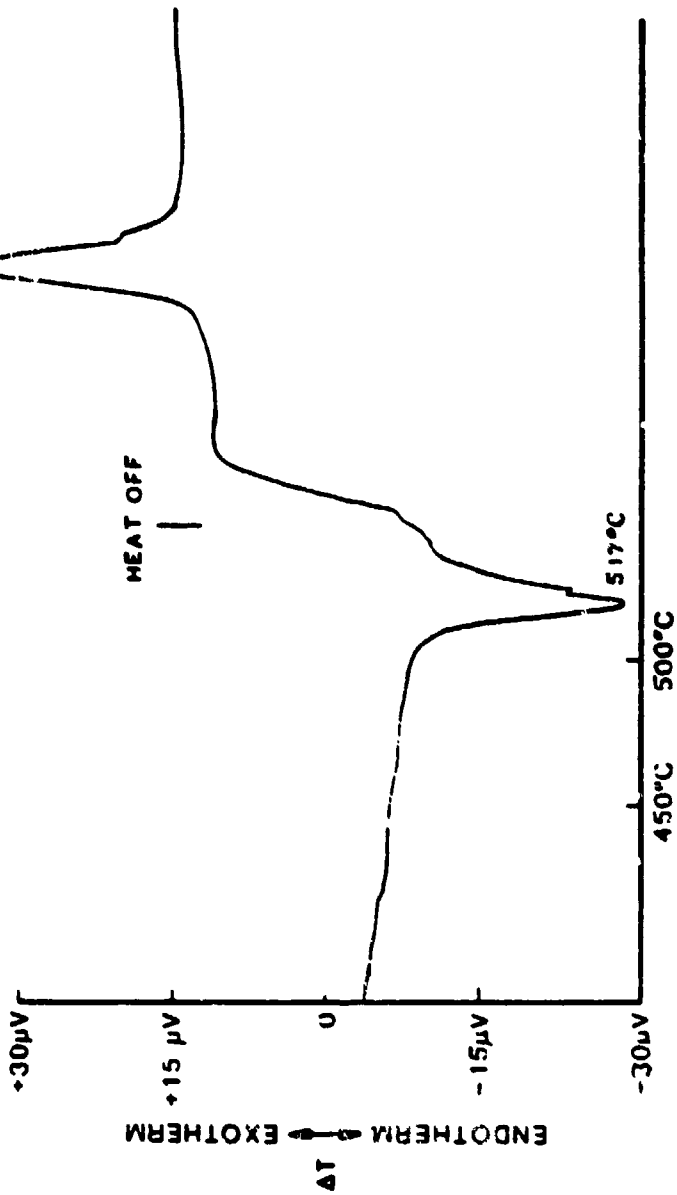

Figure 34. DTA of MoO_3-Sb_2O_3 Eutectic Composition

examination to determine if a eutectic is formed. Compacts of 25 mole percent Sb_2O_3(o) and 75 mole percent MoS_2 were prepared in cylinders rather than the standard conical shape and worn in the tri-pellet test three hours at 850 rpm.

Ten milligram samples of the worn surface areas of the compacts worn in air at room temperature on the tripellet machine were mechanically removed from the pellets and examined by DTA. Under argon, a sharp endotherm indicating the presence of a eutectic was not observed; rather, a small gentle endotherm was observed. The endotherm found is similar to that for small particle size Sb_2O_3(o) analyzed by DTA under argon. These data indicated that if a eutectic of Sb_2O_3-MoO_3 was formed at the pellet interface, then the concentration is so small as to be non-detectable using the DTA method.

Those areas and unknown areas of compacts were also analyzed using the technique of symmetric reflection wide angle x-ray diffraction (WAXD). Two instruments were employed, i.e., a Philips automatic powder diffractometer and Picker FACS-1 four-circle single crystal diffractometer. The Philips system used nickel filtered Cu Kα radiation at 35 kV and 22 ma. The worn compacts surface was scanned at either 1°/min. or 1/8°/min. The continuous scintillation detector output was recorded by a strip chart recorder. The Picker data was collected

digitally at 0.1° increments from selected areas (1 mm x 1 mm) of a sample. The Picker employed Cu Kα radiation at 30 kV and 20 mA a with an incident beam quartz crystal monochromator.

Operation of the Philips unit followed standard factory procedure. The Picker operation[78] and analysis[79] are described elsewhere.

X-ray diffraction data for non-worn and worn areas were compared. For each diffraction angle, the difference in counts was calculated and a spectrum of the differences plotted as given in Figure 35. Experimental x-ray data for values of 2θ, where θ is the angle of diffraction, were reduced using the Bragg relationship:[80]

$$n\lambda = 2d \sin\theta \qquad (5.4)$$

where

n = Order of diffraction

λ = Incident radiation wavelength

d = Distance between crystal lattice atomic planes

θ = Diffraction angle.

In the non-worn areas, the more prominent diffraction peaks listed in Table 19 were found to be stronger than in the worn area.

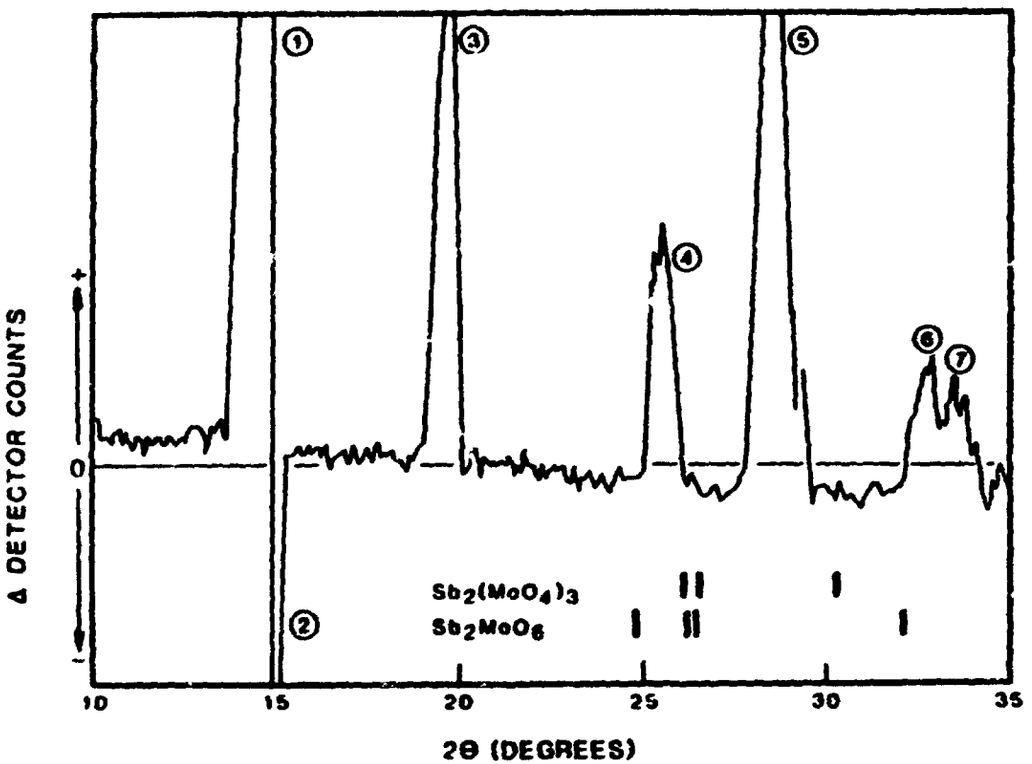

Figure 35. Differential X-ray Diffraction Pattern for Worn and Non-Worn compact Surface.

Table 19. X-RAY DIFFRACTIONS MORE PROMINENT IN THE NON-WORN AREAS

DIFFRACTION PEAK IN FIGURE 35	d(Å)	ASSIGNMENT
1	6.17	MoS_2
3	4.52	Sb_2O_3(o)
4	3.49	Sb_2O_3(o)
5	3.13	Sb_2O_3(o)
6	2.72	Sb_2O_3(o)
7	2.67	Sb_2O_3(o)

The spectra contained diffraction patterns coincident with those of MoS_2 and Sb_2O_3(o).[81]

The only diffraction peak found in worn areas at about 5.90Å and is attributed to broadening of the MoS_2 difraction.

MoS_2-Sb_2O_3 compacts were worn at 371°C using a small drill press to rotate on a temperature controlled hot surface. Again, DTA and x-ray analysis did not detect the presence of a eutectic of MoO_3-Sb_2O_3. However, a

significant change was the transformation of Sb_2O_3(c) to Sb_2O_3(o). This transformation which occurred under interface temperatures, provides direct evidence for contact temperatures of nearly 200°C in excess of test temperature since the transition temperature for Sb_2O_3 is 556°C. Evidence was also found for trace levels of Sb_2O_4 indicating some oxidation of Sb_2O_3 occurs under these conditions.

The lack of DTA and x-ray diffraction evidence indicates that eutectic compositions are not formed at the interface.

CHAPTER VI

DEVELOPMENT OF HYPOTHESIS FOR MoS_2-Sb_2O_3 SOLID LUBRICANT COMPACTS

Studies of Sb_2O_3 have shown that the rates of oxidation of both Sb_2O_3(o) and Sb_2O_3(c) to Sb_2O_4 are dependent upon surface area and the presence of an orthorhomic surface such as Sb_2O_3(o) or Sb_2O_4. It was found that the presence of MoS_2 or MoO_3 did not materially affect the rate of Sb_2O_3 oxidation in compacts.

It was also found that although a eutectic of Sb_2O_3/MoO_3 could be produced in the laboratory as other workers had done,[64] no evidence of eutectic formation on sliding interfaces produced at ambient or at 371.2°C (700°F) was detected.

Wear studies of MoS_2-Sb_2O_3 compacts from ambient to 315.6°C (600°F) confirmed studies of earlier investigators, e.g., high relative humidity or the absence of oxygen in the environment increases wear of both MoS_2 and MoS_2-Sb_2O_3 compacts in room temperature evaluations. Under the same conditions, MoS_2-Sb_2O_3 formulations were superior to MoS_2 only if particle size of the antimony oxide additions was small. For Sb_2O_3(c) additions, if the particle size were large, the relative

wear rate was high and was attributed to its larger bipyramid crystals abrasively ploughing and damaging the sliding interface. Under dry air conditions, with MoS_2-Sb_2O_3 pellet wear specimens containing small particle size Sb_2O_3(o), the wear track and compact surfaces produced in tests were routinely dense and coherent in appearance compared with other materials evaluated, including pure MoS_2 compacts. At higher temperatures, it was again found that wear compacts composed of Sb_2O_3 and MoS_2 were superior to test specimens of MoS_2 in that smoother frictional traces were produced, lower coefficients of friction were found, and wear volumes generated in identical tests were reduced. Also, MoS_2-Sb_2O_3 formulations were superior to MoS_2 whether evaluated in inert or oxygen-containing atmospheres. These experiments indicate that a role for Sb_2O_3 in MoS_2 in which Sb_2O_3 imparts superior tribological performance by acting in any way as an antioxidant or suppressing oxidation of MoS_2 cannot be supported.

Based upon this analysis, an alternative hypothesis is developed. The hypothesis is that Sb_2O_3 softens, i.e., plastically deforms under load and temperature conditions of this test so that it acts as a matrix to retain a preferred orientation of the primary solid lubricant crystallites, MoS_2, generated at asperity contact. Localized heating of the mixture permits softening of

the antimony oxide around and away from the sliding interface so that the lowest energy orientation of MoS_2 would be effectively "frozen in place" because asperity contact temperature rapidly recedes as sliding continues. This concept is supported by observations of others,[82] who state that "dense" wear tracks and/or test specimen surfaces are produced when the oxide is present. The concept is also supported by previous efforts[7] which found that the tribologically superior performance of MoS_2-Sb_2O_3 compacts compared wih MoS_2 specimens is independent of atmospheric oxygen content. Those authors alluded to an optimum formulation[7] which complements the hypothesis developed in that an optimum amount of additive is required to permit efficient construction of the best tribological surfaces; too much additive results in the matrix material acting as the solid lubricant, diminishing the tribolobical properties of the mixture because of reduced primary solid lubricant content.

The concept suggests that the additive, Sb_2O_3, should not be unique in its ability to improve MoS_2 performance. Also, bulk additions of stable materials properly selected should improve the performance of other solid lubricants. Again, data and observations of others support the hypothesis. For example, DiSapio[83] notes that the basis for improved tribological properties of MoS_2 in air versus in vacuum is that in air MoO_3 forms, which acts as a binder

for MoS_2. Similarly, in 1955, Peterson and Johnson[84] found that additions of CdO to graphite improved the tribological performance of graphite when tested up to temperatures of 537.8°C (1000°F).

A possible role of oxides in compacts can be seen in a study of the effectiveness of inorganic oxides as primary solid lubricants[85] in two standard four-ball machines.[86] The authors found that there was excellent correlation of the load-wear index as a function of the logarithm of Vickers hardness, equivalent to a correlation with Mohs hardness,[87] of those oxides. They concluded that the several oxides provided improved extreme pressure capability for a lubricant and suggested that the effect was a purely mechanical one, with better performance for the soft oxides. Softness of an oxide leads to tribological improvement because the oxide can then deform in a highly-loaded contact to prevent or reduce metal-to-metal contact, thereby lowering the contact loads at ball surfaces. These results indicate that the ability of an oxide to deform under tribological conditions is a critical factor in their beneficial performance.

This study suggests that hardness, shear strength and melting point or decomposition temperature are critical criteria in selecting additives in this concept. It also indicates that test conditions are equally important criteria, since tribological and material properties are

strongly dependent on temperature, load, etc. If one considers a correlation of hardness and melting point for oxides,[88,89] it would appear that there are limited choices for bulk additions once test conditions are known. The additive of choice will be one that is stable under the test conditions and softens effectively at asperity flash temperature.

Examination of these data also indicate that only those materials with very low hardness and relatively very high melt point are natural solid lubricants over a wide range of conditions. Consider, for example, that molybdenum disulfide has a Mohs hardness of 1.5 with a melting point of 1185°C, and that graphite has a Mohs hardness of 0.5 to 1.0 with a sublimation temperature of approximately 3650°-3700°.[28] The softness of these materials results from a layer lattice structure. These materials and a few other structural analogs are the only known natural solid lubricants over wide temperature ranges. Other solid lubricants not possessing such structure which permits the atypical low hardness-high temperature stability are evidently only useful in a narrow temperature range under specified test conditions. In that limited range, the solid is soft or perhaps even liquid permitting shear with only modest forces involved.

Test conditions are important in the evaluation of the solid as a lubricant. For example, in a pin on disk

experiment, flash temperatures may typically be 200°C over the experimental temperature. Often, those temperatures become extremely high, e.g., from 1000° to 1200°C for steel and ceramic pins slid over sapphire (90). Under those conditions it is easily visualized that the material deposited on a wear track may resolidify, and if the hardness and/or structure permit the residue to become abrasive, then the solid will be lowly ranked. If, however, the experiment is designed so that cooling cannot occur on the disk, e.g., the ends of two equal diameter shafts operating in counter-rotation, then the lubricant would be ranked higher because it would lubricate effectively at the higher overall temperature.

Peterson, et al.,[91] found that there is a correlation between coefficients of friction and melting points at a given test temperature, better for some classes of materials than others. For example, the friction coefficient of Na_2WO_4 at 704°C is 0.17. Friction coefficients of other tungstates and molybdates increased as the difference between melting point and test temperature increased. Peterson[92] also pointed out that these compounds, which lubricate fairly well at high temperature, were not effective at room temperature. He explained this difference by stating that both friction and heat are components of the total energy required to break bonds in shear. At low temperatures, more frictional

energy is required; as temperatures approach a solid's melting point, more heat is supplied and less frictional energy is required. Frictional energy is dissipated as heat, which is manifested by the asperity contact temperature rise or "flash temperatures".

ASPERITY CONTACT TEMPERATURES FOR MoS_2-Sb_2O_3 COMPACTS

The hypothesis developed herein for bulk additions to solid lubricants may be plausible if it is possible to demonstrate that the flash temperature is sufficient to soften or deform the bulk additive, resulting in densification of the compact and retention of an overall improved tribological orientation of the primary solid lubricant.

Flash temperatures may be calculated using the notation of Rabinowicz[93] and the methodology of Archard.[94] However, before a flash temperature calculation can be made, one must determine the size of an asperity contact. In the experiments of Quinn and Winer,[90] hot spots were approximately 50-100 μm in size, and the number observed at any one time found by successive shortening of photographic exposure time was 7 ± 3. It was also estimated that the ratio of total hot spot area to apparent contact area was 1:1000.

For the MoS_2-Sb_2O_3 tests, the worn pin diameter at test completion is on the order of one millimeter, and if one assumes that the dominant interfacial material is MoS_2,

then the hardness is 1.5 Mohs for MoS_2 which is approximately equivalent to 30 kg/mm^2 on the Vickers scale. Then

$$A_r \cong \frac{0.1\text{kg}}{30\ \text{kg/mm}^2}(\text{pin load}) \qquad (6.1)$$

$$= 0.00333\ \text{mm}^2$$

where A_r is the real contact area.

Since A_c is the apparent contact area = $\pi r^2 = \pi(0.5\text{mm})^2 = 0.7854\ \text{mm}^2$,

$\frac{A_r}{A_c} \cong 0.0042$ or $\cong$ 4:1000

which is of the correct magnitude compared to Quinn and Winer's data.

Consider two cases, probably the worst cases: Case A; the entire real area of contact is concentrated in one asperity, and Case B; the real area is split into three equal area contact zones that determine a plane. For Case A, the contact area equals A_r. The contact radius will be

$$r = \left(\frac{0.00333}{\pi}\right)^{1/2} = 0.0326\ \text{mm} = 3.26 \times 10^{-5}\text{m} \approx 35\ \mu\text{m} \qquad (6.2)$$

or, approximately 70 μm for asperity contact or hot spot diameter. The calculated diameter is within the same size range as those observed by Quinn and Winer, so it is reasonable to assume that only one asperity is in contact

at some times. For Case B, each contact will have an area of

$$\frac{0.00333 \text{ mm}^2}{3} = 0.00111 \text{ mm}^2 \qquad (6.3)$$

and the asperity contact or hot spot radius is,

$$r = \left(\frac{A}{\pi}\right)^{1/2} = \left(\frac{0.00111 \text{ mm}^2}{\pi}\right)^{1/2} = 0.0188 \text{ mm} = 1.88 \times 10^{-5} \text{ m} = 20 \text{ μm} \qquad (6.4)$$

or, approximately 40 μm for asperity contact or hot spot diameter. The calculated diameter is somewhat smaller than the diameter of asperity contacts observed by Quinn and Winer but very near their low value which indicates that the estimate is reasonable.

To calculate the flash temperature, θ_m, Rabinowicz[93] provides two equations derived from Archard.[94] At low speeds,

$$\theta_m = \frac{\mu L v}{4Jr(k_1 + k_2)} \qquad (6.5)$$

At high speeds,

$$\theta_m = \frac{\mu L v^{1/2}}{3.6\ J\ (\rho c r^3 k)^{1/2}} \qquad (6.6)$$

where

μ = friction coefficient

L = load (Newtons)

v = sliding velocity (meters/second)

J = mechanical equivalent of heat (J/cal)

k_1, k_2 = thermal conductivities of contacting materials

ρ = density

c = specific heat

In order to choose the appropriate equation, Rabinowicz[93] supplies an Archard-derived dimensionless parameter[94] to determine which equation to use. The parameter closely resembles the Peclet number:[95]

$$\lambda = \frac{vr\rho c}{2k} \qquad (6.7)$$

Rules of application are: if $\lambda < 0.1$, use Equation 6.5; if $\lambda > 5$, use Equation 6.6; if $0.1 < \lambda < 5$, use an intermediate value. In this case, λ is difficult to determine. Archard mentions that thin films on the substrate material (extended surface) will not influence the flash temperature calculation if its thickness is larger than, or much, much smaller than the asperity contact size. In this case, however, the thickness of the surface film is smaller than the asperity contact size, but of the same magnitude. Therefore, some allowance must be

made for both surface film and substrate thermal effects. Archard also defines λ as

$$\lambda = \frac{\tau_1}{\tau_2} \tag{6.8}$$

where τ_1 is the time it takes for heat generated on the surface of contact to reach a point underneath the contact area of depth r, and τ_2 is the time it takes for the asperity to travel through a distance r. If the surface film has thickness t, then the time it takes for surface heat to reach "r" meters beneath the surface becomes:

$$\tau_1' = \frac{t^2 \rho_3 c_3}{2k_3} + \frac{(r-t)^2 \rho c}{2k} \tag{6.9}$$

where subscript 3 refers to properties of the surface film. Therefore, if $\tau_2 = \frac{r}{v}$, then combining Equations 6.7, 6.8 and 6.9, one has

$$\lambda = \frac{\frac{t^2 \rho_3 c_3}{2k_3} + \frac{(r-t)^2 \rho c}{2k}}{\frac{r}{v}} = \frac{v}{2rkk_3} \left[k\rho_3 c_3 t^2 + k_3 \rho c (r-t)^2 \right] \tag{6.10}$$

In this case, $v = 0.62 \frac{m}{s}$ and $t = 10\ \mu m = 10^{-5} m$. Other values were obtained from The Chemical Engineer's Handbook,[95] The Handbook of Chemistry and Physics,[28] and a report by Harmer and Pantano.[8]

For stainless steel:

$k = 26$ J/m-s-°C

$c = 460$ J/kg-°C

$\rho = 7767$ kg/m^3

For MoS_2/Sb_2O_3:

$k = 0.0519$ J/m-s-°C (an approximation from related substances)

$c = 529.6$ J/kg-°C (calculation shown below)

$\rho = 3320$ kg/m^3

For MoS_2, $c = 19.7 + 0.00315\ T$ (T in K, c in cal/mol-K)

at = 600 K (= 327°C or 621°F)

$c = 19.7 + 0.00315\ (600) = 21.6$ cal/mol-K = 134.9 cal/kg-°C

For Sb_2O_3, $c = 19.1 + 0.0171\ (600) = 29.4$ cal/mol-K = 100.9 cal/kg-°C. Assuming equal contributions to specific heat based upon molar percentage:

$C_{compact} = (0.75 \times 134.9) + (0.25 \times 100.9) = 126.4$ cal/kg-°C x 4.19 J/cal = 529.6 J/kg-°C (6.11)

Flash temperature calculation: (No units given - all SI units used)

Case A -

$$\lambda = \frac{(0.62)}{2(3.26 \times 10^{-5})(26)(0.0519)}$$

$$\times[(26)(3320)(529.6)(10^{-5})^2 + (0.0519)(7767)(460)(3.26 \times 10^{-5} - 10^{-5})^2 \quad (6.12)$$

$$\lambda = 32.6 \quad (6.13)$$

Using Equation 6.6, with $\mu = 0.1$, $L = 0.98N$, $J = 1$ and all other values given

$$\theta_m = \frac{(0.1)(0.98)(0.62)^{1/2}}{(3.6)(1)[(3320)(529.6)(3.26 \times 10^{-5})^3(0.0519)]^{1/2}} \quad (6.14)$$

$$\theta_m = 381°C \quad (6.15)$$

Values for ρ, c and k are for the MoS_2-Sb_2O_3 compact, since it is the surface in contact.

Therefore, at 316°C operating temperature, contact temperature = 316°C + 381°C = 697°C

Case B -

$$\lambda = \frac{(0.62)}{2(1.88 \times 10^{-5})(26)(0.0519)}$$

$$\{(26)(3320)(529.6)10^{-5})^2$$

$$+ (0.0519)(7767)(460)(1.88 \times 10^5 - 10^5)^2 \qquad (6.16)$$

$$\lambda = 56.0 \qquad (6.17)$$

again, using Equation 6.6, as above, except L = 0.327N, r = 1.88×10^{-5}m

$$\theta_m = \frac{(0.1)(0.327N)(0.62)^{1/2}}{(3.6)(1)[(3320)(529.6)(1.88 \times 10^{-5})^3(0.0519)^{1/2}} \qquad (6.18)$$

$$\theta_m = 290°C \qquad (6.19)$$

Therefore, at 316°C operating temperature, contact temperature = 316°C + 290°C = 606°C.

These calculations indicate that the flash temperatures are high enough to cause localized softening of the Sb_2O_3, which has a melting point of 656°C. Softening implies lower shear strength, i.e., less resistance to flow, which enhances the effectiveness of the solid as a lubricant. Ernst and Merchant[96] developed a relationship, incorrectly reported by Peterson, et al.[91],

that the shear strength of a crystalline solid is an exponential function of its melting point.

Their equation is,

$$S = 0.142\ L\rho \ln\left(\frac{T_m}{T}\right) \qquad (6.20)$$

when S = Static shear strength of crystalline solid (kg/mm^2)

L = Latent heat of fusion (cal/g)

ρ = Density (g/cm^3)

T = Absolute test temperature (K)

T_m = Absolute fusion temperature (K)

Thus, temperature has a strong influence on the shear strength of an additive. This, along with the analysis of asperity contact temperature lends support to the additive hypothesis.

If the role of Sb_2O_3 is to soften at asperity contact temperatures, then other materials may perform in a similar fashion. Other materials would cause flash temperatures to be different because of their different material properties. Therefore, the optimum operating temperatures of solid lubricant compacts containing other materials will probably be different from that of MoS_2-Sb_2O_3 compacts.

The optimum operating temperature also changes if load or sliding velocity are changed. Once material selection

has been made, these are the only factors in the flash temperature calculations over which one has some control, as seen in Equation 6.6. If the load is changed, the flash temperature changes proportionately. If the sliding velocity is changed, the flash temperature changes parabolicially. Therefore, since load and speed influence the flash temperature of sliding pairs, these factors would also influence the optimum ambient temperature for a solid lubricant compact. Conversely, load and speed should be optimized for a given operating temperature of a particular sliding pair.

Based upon this analysis, one can predict the temperature range in which the additive will be most effective for a given set of conditions. Once materials are selected, the load and speed conditions must be specified in order to determine the flash temperature. The asperity contact temperature should be in a range that permits the additive to effectively deform. At temperatures too high, the additive will shear too easily, while at very low temperatures the additive cannot easily shear so that beneficial deformation does not occur.

CHAPTER VII

OTHER OXIDES AND SULFIDES AS BULK ADDITIONS TO MoS_2

WEAR STUDIES

Based upon the development of an hypothesis for bulk additions in MoS_2, several oxides and sulfides were selected as additives for MoS_2 to determine if tribological performance would be as predicted by the hypothesis.

Additives were selected primarily on the basis of earlier efforts by many investigators to find stable materials that would improve the performance of a variety of solid lubricants. Additives of this type, which typically have low values of Mohs hardness include As_2O_3, Bi_2O_3, Sb_2S_3, Sb_2S_4, PbO, CdO, and CuO. Other additives were selected because of their high hardness, i.e., TiO_2 and Al_2O_3, so that a comparison with softer materials could be made. Additionally, MoO_3 was selected since it might be an oxidation product of MoS_2 found at the interface.

All of these additives were ground, with the exception of PbO, on the mechanical amalgamator for a period of 16 minutes followed by sieving through a 30 μm nickel screen. PbO only sieved prior to compaction with MoS_2 since it oxidizes readily in the amalgamator, easily observed because of the color change.

Each of the sieved oxides or sulfides was weighed to the nearest tenth of a milligram and formulated based upon the volume equivalent to that of Sb_2O_3 additions to MoS_2. An exception was MoO_3 which was added on a molar basis for comparisons with possible eutectic compositions of Sb_2O_3 and the oxidation products of MoS_2.

With few exceptions, only a single compact of MoS_2 and each oxide or sulfide was prepared in a procedure identical to the one used for MoS_2-Sb_2O_3 compacts. Since these experiments were designed only to establish trends in wear volume and friction coefficient as functions of additive properties, repeat evaluations were not performed.

The compacts were shaped and then worn at 316°C on stainless steel shim stock as done with MoS_2-Sb_2O_3 compacts. The data generated as given in Appendix D are summarized in Table 20 along with the Mohs hardness[97] and temperature of melting, transition, sublimation or decomposition[28] for each additive.

As seen in Table 20, the variation in wear volumes was large, varying from 0.04 mm^3 to more than 0.4 mm^3. Coefficients of friction were as low as 0.06 and as high as 0.24 during wear tests. The lowest wear volumes were found for Sb_2S_4 and MoO_3 additions. These wear volumes were approximately one-half of the wear generated when Sb_2O_3 was the additive in MoS_2. These additives were beneficial if the Mohs hardness was less than or equal to 4.5. TiO_2 and

Table 20. PELLET WEAR IN DRY AIR AT 316°C

PELLET COMPOSITION	TEST NUMBER	MELTING POINT* (°C)	MOHS HARDNESS	WEAR VOLUME (mm^3)	μ_{k_i}	μ_{k_f}	$\bar{\mu}_k$
MoS_2		1185	1-1.5	0.157	0.07	0.08	0.08
MoS_2 + ADDITIVE							
Al_2O_3	146	2072	9	0.415	0.12	0.24	0.17
As_2O_3	145	312 (s)	1.5	0.070	0.11	0.16	0.14
Bi_2O_3	132	825	4.5	0.096	0.14	0.23	0.19
CdO	133	900 (d)	3	0.071	0.10	0.17	0.14
CuO	136	1326	3.5	0.072	0.06	0.16	0.11
MoO_3 **		795	2	0.044	0.11	0.17	0.14
PbO	130	886	2	0.061	0.12	0.20	0.16
TiO_2	135	1840	6	0.432	0.14	0.21	0.18
Sb_2O_3 **		656	2.75	0.093	0.09	0.14	0.12
Sb_2O_3**		550	2	0.088	0.11	0.17	0.13
Sb_2S_4	134	510	3	0.043	0.14	0.20	0.17

* s = sublimes; d = decomposes
** m = mean values

Al_2O_3 produced greater wear volume than did MoS_2 without additives. Those additions to MoS_2 produced wear volumes that were about two and one-half times greater than the wear volume for MoS_2, which may result from the inability of those oxides to deform under the tribological conditions of the test.

In Figure 36, wear volume is plotted as a function of Mohs hardness. The least square regression equation is as follows:

$$\text{Wear Volume } (mm^3) = 0.0563 \text{ (Mohs Hardness)} - 0.0664 \quad (7.1)$$

Correlation coefficient = r = 0.88

Therefore, about 78 percent of the variation in wear volume may be attributed to differences in hardness of the additive.

When the linear correlation coefficient is calculated for wear volume as a function of the absolute melting temperature of the additive, a result comparable with that of wear volume as a function of hardness. The linear regression equation is:

$$\text{Wear Volume } (mm^3) = 2.23 \times 10^{-4} \text{ (Melt. Temp., K)} - 0.0774 \quad (7.2)$$

r = 0.87

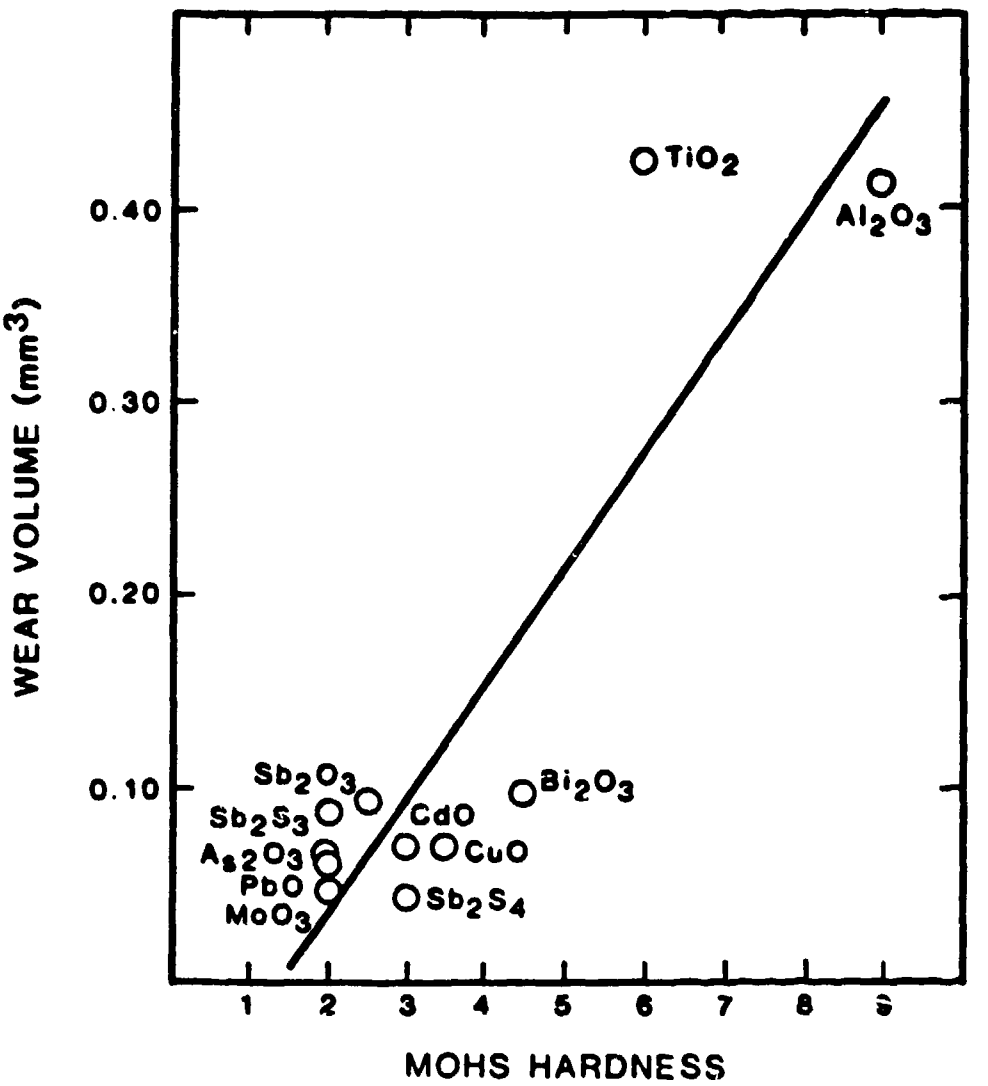

Figure 36. Wear Volume as a Function of Mohs Hardness.

Such a correlation is expected since Mohs hardness varies linearly, with some exceptions, with the melting temperature of materials.[88,89] For oxides, such a relationship is presented in Figure 37.

Correlation of initial coefficient of friction (30 sec), μ_{k_i}, or final coefficient of friction (15 min), μ_{k_f}, is with Mohs hardness or melting temperature is poorer. Linear regression suggests that correlation of basic additive properties is better with final coefficient of friction values ($r = 0.66$ for correlation with Mohs hardness, $r = 0.59$ for correlation with melting temperature) rather than with initial friction coefficient values ($r = 0.30$ and $r = 0.295$).

The data suggest that it is difficult to predict μ_{k_i} or μ_{k_f} by use of Mohs hardness or melting temperature. However, as seen in Figure 38, some trending of initial, mean and final friction coefficient as a function of Mohs hardness is apparent as reflected in higher correlation coefficients as frictional coefficients increase during the test.

Thus, it appears that the wear volume generated is related to the hardness and melting temperature of the additive, but the friction coefficient is not.

Mohs hardness reflects the shear strength of the additives. However, Mohs hardness is measured at ambient and wear volume was determined at 589 K with asperity

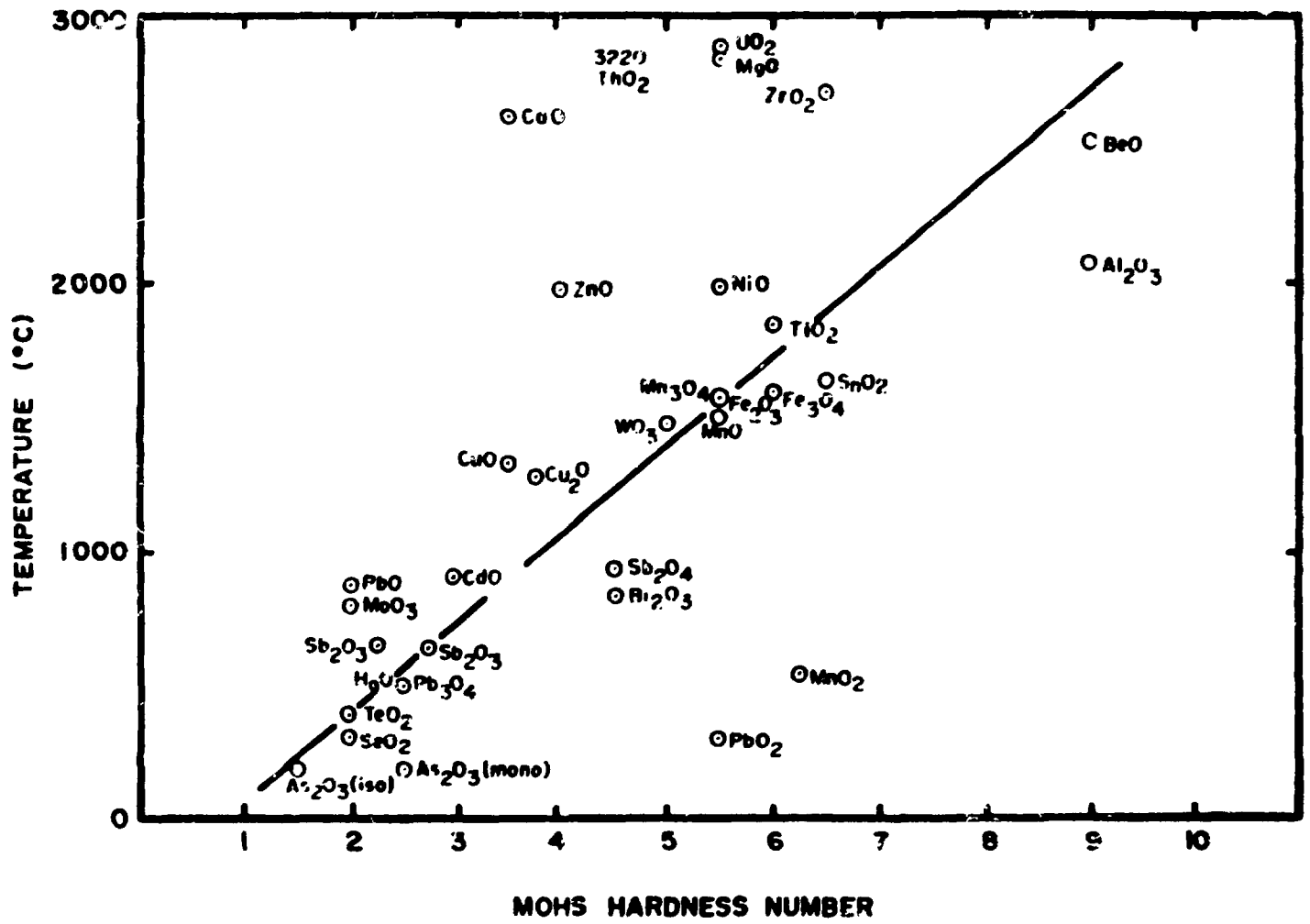

Figure 37. Melt Temperature of Oxides as Function of Mohs Hardness.

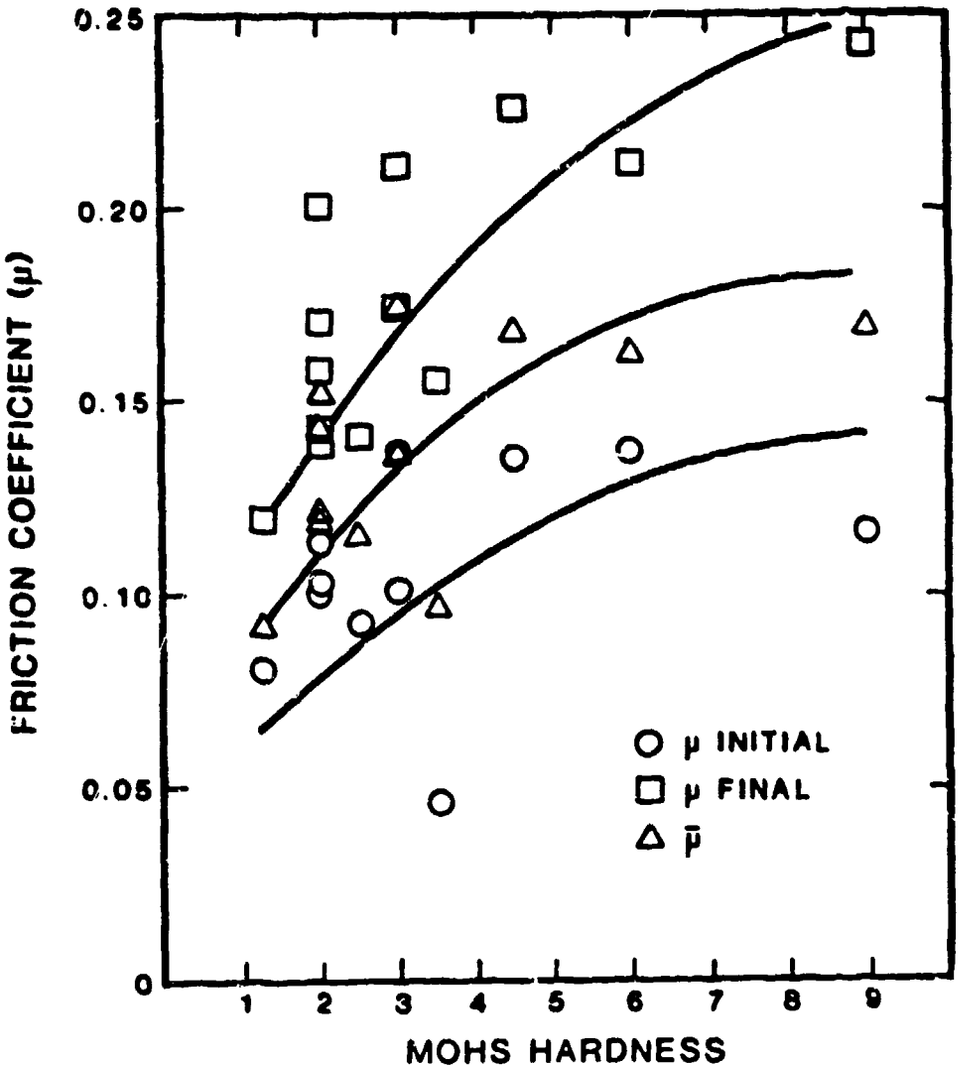

Figure 38. Friction Coefficient of MoS_2-Oxide Compacts as a Function of Mohs Hardness of Oxides.

contact temperatures even higher. Therefore, correlations of a) wear volume as a function of the difference between softening point and test temperatures, and b) wear volume as a function of additive shear strength at test temperature were calculated.

Handbook data for the required quantities and calculated values to be employed later are compiled in Table 21.

The relationship relating wear volume and friction coefficient to the difference of 0.7 absolute melting temperature and the test temperature was evaluated initially. 0.7 of the melting temperature is at the upper limit for transition from brittle to ductile behavior for materials similar to oxides and sulfides evaluated here.[98] That transition is, of course, related to deformation of the additive as hypothesized. The linear regression equation for wear volume is as follows:

$$\text{Wear Volume } (mm^3) = 3.18 \times 10^{-4}(0.7\ T_m - 589) + 0.0492 \qquad (7.3)$$

$$r = 0.87$$

The correlation coefficient suggests that wear volume is correlatable with the difference of $0.7\ T_m - 589$. Attempts to correlate friction coefficient with $0.7\ T_m - 589$ resulted in correlation coefficients of 0.20 (initial) and

Table 21. ADDITIVE DATA FOR EVALUATION OF SHEAR STRENGTH AT TEMPERATURE

ADDITIVE	HEAT OF FUSION (cal/g)	DENSITY (g/cm^3)	MELT TEMPERATURE T_m (K)	0.7 T_m-589	$\frac{T_m}{T}$	SHEAR STRENGTH MPa	SHEAR STRENGTH kg/mm^2 ($N/m^2 = 10^{-6}$)	WEAR VOL(mm^3)	σ_{b_1}	σ_{b_2}
Bi_2O_3	14.6	8.9	1098	179.6	1.86	11.49	112.68	0.096	0.134	0.226
Sb_2O_3	46.3	5.67	929	61.3	1.577	16.98	166.52	0.093	0.09	0.120
PbO	12.6	9.53	1159	272.3	1.968	11.54	113.17	0.061	0.113	0.200
MoO_3	17.3	4.69	1068	158.6	1.813	6.86	67.28	0.044	0.11	0.17
CuO	35.4	6.4	1599	530.3	2.715	32.14	315.20	0.072	0.046	0.155
CdO	*	8.15	1773		3.010	---				
TiO_2	219	4.26	2113	890.1	3.587	169.2	1659.30	0.423	0.137	0.211
Al_2O_3	256	3.965	2345	1052.5	3.981	199.1	1952.60	0.415	0.116	0.242
As_2O_3	22.2	4.15	585	-179.5	0.993	-0.092	-0.90(e)	0.07	0.1	0.157
Sb_2S_3	33.0	4.64	823	- 12.9	1.397	7.27	71.30	0.088	0.092	0.171
Sb_2S_4	*									

* NO DATA

0.59 (final), which suggest that friction coefficients are not strongly related to 0.7 T_m-589.

Computed negative values of 0.7 T_m-589 suggest that the softening temperature of the additive is exceeded in tests based upon that relationship. If those values are excluded from consideration, the linear regression equation relating wear volume to 0.7 T_m-589 is as follows:

$$\text{Wear Volume } (mm^3) = 3.928 \times 10^{-4}(0.7\ T_m - 589) - 0.0016 \qquad (7.4)$$

$$r = 0.91$$

Therefore, the correlation is improved when negative values of (0.7 T_m-589) are eliminated.

For an estimate of the shear strength of additives at test temperature, the theoretical relationship of Ernst and Merchant[96] as given in Equation (6.2) was employed. Values of the shear strength of the additives were not calculated for CdO and Sb_2S_4 since pertinent data were not available. The linear regression equation relating wear volume to shear strength as calculated is as follows:

$$\text{Wear Volume } (mm^3) = 0.0002\ (N/m^2 \times 10^{-6}) + 0.0524 \qquad (7.5)$$

$$r = 0.983$$

Wear volume data plotted as a function of shear strength is presented in Figure 39. Linear correlation coefficients for μ_{k_i} and μ_{k_f} as functions of calculated shear strength are 0.37 and 0.62, respectively, which are comparable with the correlation of μ with additive hardness and melting temperature. Thus, the wear volume is related very strongly to the calculated shear strength. Initial and final coefficients of friction are much more weakly related to shear strength. The high correlation coefficient between wear volume and calculated shear strength of the additive indicates that more than 97 percent of the variation in wear volume may be attributed to differences in calculated shear strength at test temperature.

The weakness of correlation of the friction coefficient shear strength indicates that the beneficial effect of an additive is not an interfacial phenomenon. Therefore, the effect must occur within the bulk of the solid lubricant, which supports the hypothesis of additive deforming to permit the solid lubricant to attain and retain a preferred orientation for improved tribological condition.

The weaker correlation of wear volume with additive hardness, melting temperature, or 0.7 T_m-589 might be expected since they are related to shear strength of the additives, but are, at best, poor predictors of shear strength at test temperature.

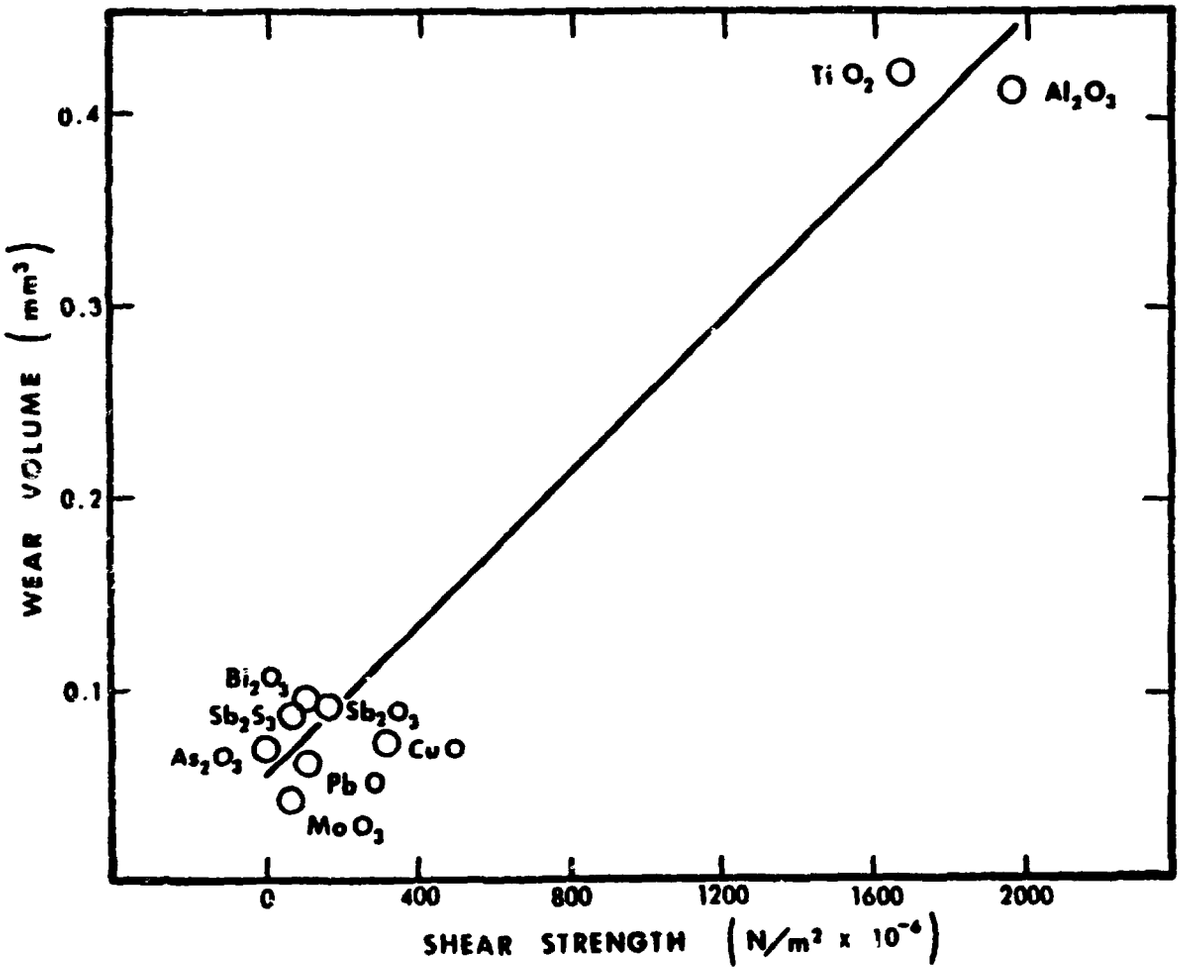

Figure 39. Wear Volume as Function of Additive Shear Strength.

Sb_2O_4 AS A BULK ADDITIVE

Wear of compacts of MoS_2 containing Sb_2O_4 were of special interest, since it may be possible for Sb_2O_3 to oxidize to Sb_2O_4 resulting in different tribological properties. Data are presented in Table 22 summarizing the results of the assessment. The wear of such compacts were higher than similar compacts containing Sb_2O_3(o) (Tests 84-86). These data indicate that oxidation of Sb_2O_3 to Sb_2O_4 at the compact interface would not be beneficial.

MoO_3 and MoO_3-Sb_2O_3 AS BULK ADDITIVES

MoO_3 as an additive and in combination with Sb_2O_3 was evaluated to examine whether any synergism or eutectic formation occurs between it and Sb_2O_3.

MoO_3 has some capability as a solid lubricant. It has been documented that molybdenum sliding against molybdenum in air under mild sliding conditions has rather high friction (μ=1) up to about 480°C, after which the friction remains low (μ=0.3) until about 790°C.[99] These temperatures correspond quite well with the onset of rapid molybdenum oxidation to MoO_3 and with melting point of MoO_3, respectively. As temperature is decreased below 480°C, friction is lower on MoO_3 than the bare metal, but higher than at temperatures from 480°-790°C. Under the conditions of the test, there is, apparently, about a 300°C temperature range below the melting point of MoO_3 in which it acts as a fair solid lubricant.

Table 22. EFFECT OF TEST TIME ON WEAR VOLUME OF MoS_2-Sb_2O_4 COMPACTS

(DRY AIR, 316°C; 100 g LOAD)

TEST NUMBER	ADDITIVE MOLE PERCENT	WEAR TIME TEST TIME (min.)			
		1.0	2.5	5.0	7.5
102	25 Sb_2O_4	0.077			
100	25 Sb_2O_4		0.099		
98	25 Sb_2O_4			0.108	
101	25 Sb_2O_4			0.150	
99	25 Sb_2O_4				0.167

Data generated in wear evaluations of MoO_3, Sb_2O_3, and MoO_3-Sb_2O_3 in MoS_2 compacts are summarized in Tables 23, 24, 25, 26 and 27.

Wear volumes and friction coefficients are plotted as functions of composition for MoO_3 in MoS_2, respectively, in Figure 40.

These data indicate, contrary to an assumption that MoO_3 could not be a beneficial additive because of its abrasive nature,[99,100] wear compacts containing MoO_3 produced only about half the wear volume of MoS_2-Sb_2O_3 compacts.

In Figure 41, the wear volumes of MoO_3 and Sb_2O_3 in MoS_2 are compared on a molar basis. It is seen that MoO_3 is superior in wear volume at each concentration.

Finally, Figure 42 shows that a MoS_2 compact containing equal parts of MoO_3 and Sb_2O_3 gives a wear volume between the wear volume of MoS_2-MoO_3 and MoS_2-Sb_2O_3 compacts. This observation, combined with the fact reported earlier that a eutectic of Sb_2O_3-MoO_3 could not be found, shows that there is no synergism between Sb_2O_3 and MoO_3. The results do show, however, that mixtures of MoS_2 with MoO_3 can be better solid lubricants than MoS_2-Sb_2O_3 under these test conditions.

When present with MoS_2, it is claimed that MoO_3 aids in forming a continuous film.[82] Peace[65] suggests that the oxide may act as a binder for MoS_2. Winer[17] suggests

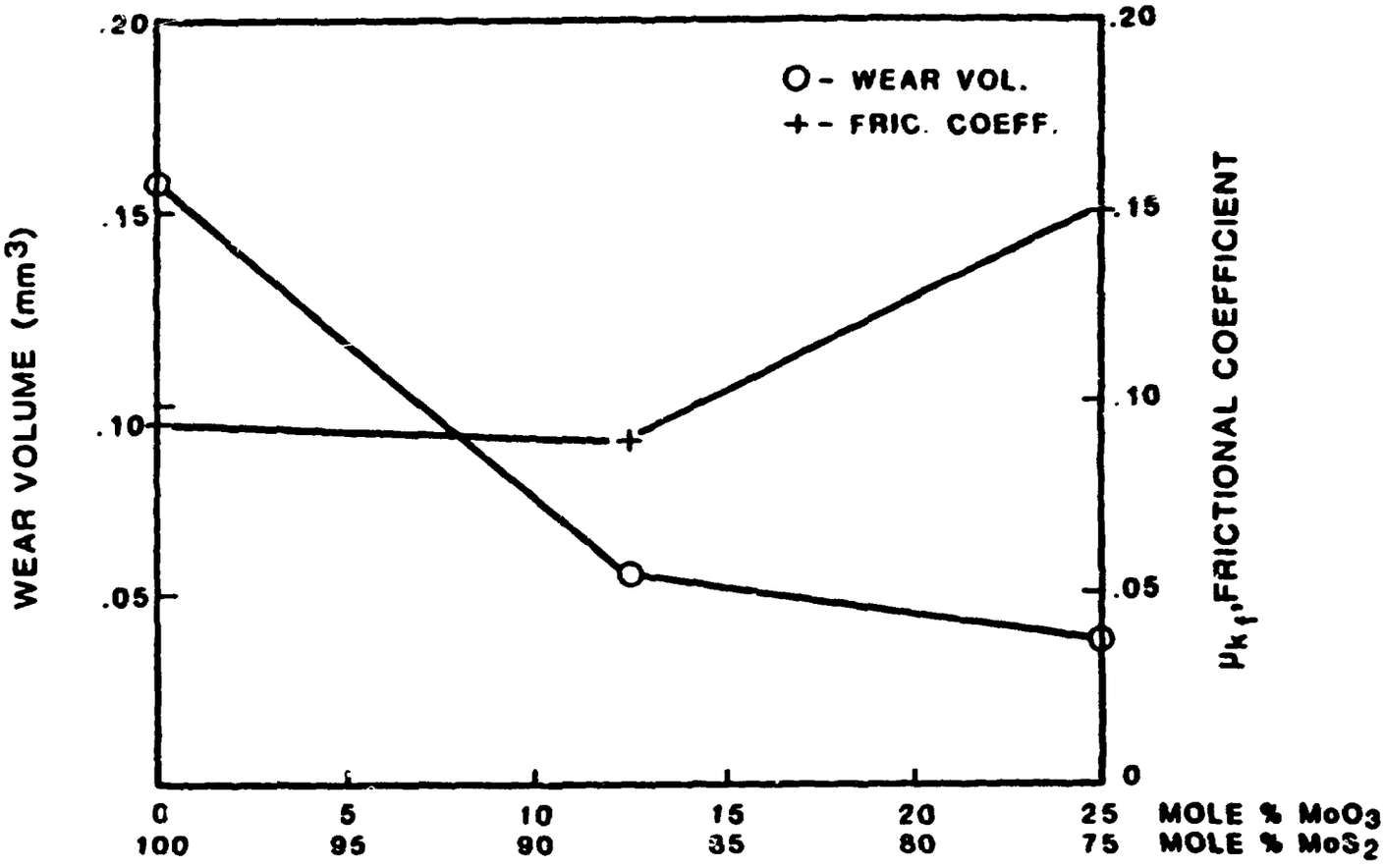

Figure 40. Wear Volume and Friction Coefficient for MoS_2-Sb_2O_3 Compacts.

Table 23. WEAR VOLUME OF MoS_2 AND MoS_2 WITH Sb_2O_3, OR MoS_2 WITH MoO_3 AND Sb_2O_3(DRY AIR, 316°C; 100 g LOAD)

TEST NUMBER	ADDITIVE MOLE PERCENT	WEAR VOLUME TEST TIME (min.)				
		1.0	2.5	5.0	7.5	16.7
88	---	0.047				
90	---		0.111			
89	---			0.120		
91	---			0.128	0.172	
92	---					
04	25 Sb_2O_3(o)	0.049				
85	25 Sb_2O_3(o)		0.060			
86	25 Sb_2O_3(o)					
0.073						
110	3.75 MoO_3					0.079
	3.75 Sb_2O_3(o)					
106	7.5 MoO_3					0.087
	7.5 Sb_2O_3(o)					
109	17.5 MoO_3					0.082
	17.5 Sb_2O_3(o)					
104	10 MoO_3					0.074
	5 Sb_2O_3(o)					
107	20 MoO_3					0.053
	5 Sb_2O_3(o)					

Table 24. WEAR VOLUME OF MoS_2 WITH Sb_2O_3, OR MoS_2 WITH MoO_3 AND Sb_2O_3 (DRY AIR, 316°C; 100 g LOAD)

TEST NUMBER	ADDITIVE MOLE PERCENT	WEAR VOLUME TEST TIME (min.)				
		1.0	2.5	5.0	7.5	16.7
88	---	0.047				
90	---		0.111			
89	---			0.120		
91	---			0.128		
92	---				0.172	
84	25 Sb_2O_3(o)	0.049				
85	25 Sb_2O_3		0.060			
86	25 Sb_2O_3(o)			0.073		
110	3.75 MoO_3 3.75 Sb_2O_3(o)					0.079
106	7.5 MoO_3 7.5 Sb_2O_3(o)					0.087
109	17.5 MoO_3 17.5 Sb_2O_3(c)					0.082
104	10 MoO_3 5 Sb_2O_3(o)					0.074
107	20 MoO_3 5 Sb_2O_3 (o)					0.053

Table 25. WEAR VOLUMES AND FRICTION COEFFICIENT FOR MoS_2, MoS_2 AND MoO_3, MoS_2 WITH MoO_3-Sb_2O_3 AND COMPOSITIONS (DRY AIR AT 589 k, 100 g LOAD, 16.7 mm)

TEST NUMBER	ADDITIVE MOLE PERCENT	WEAR VOLUME (mm^3)	TEST TIME (min.)						
			.5	1.0	2.5	5.0	7.5	10	15
			FRICTION COEFFICIENT						
114	---	0.181	.061	.061	.061	.061	.061	.072	.086
115	---	0.134	.075	.075	.075	.085	.095	.111	.118
113	12.5 Sb_2O_3	0.075	.079	.079	.080	.088	.096	.100	.113
116	25 Sb_2O_3	0.105	.109	.108	.108	.111	.111	.113	.115
123	25 Sb_2O_3	0.108	.078	.094	.103	.113	.121	.127	.136
124	25 Sb_2O_3	0.078	.100	.108	.123	.162	.165	.165	.192
112	12.5 MoO_3	0.057	.072	.076	.076	.079	.090	.097	.100
108	25 MoO_3	0.037	----	----	----	----	----	----	----
111	25 MoO_3	0.055	.100	.100	.100	.115	.119	.130	.140
117	25 MoO_3	0.045	.127	.127	.133	.145	.151	.163	.171
1[illegible]	25 MoO_3	0.031	----	----	----	----	----	----	----
12[illegible]	25 MoO_3	0.050	.106	.111	.123	.130	.142	.147	.158
103	12.5 Sb_2O_3 12.5 MoO_3	0.059	---	----	----	----	----	----	----
104	12.5 Sb_2O_3 12.5 MoO_3	0.074	----	----	----	----	----	----	----
118	12.5 Sb_2O_3 12.5 MoO_3	0.057	.078	.081	.094	.103	.112	.119	.129
122	12.5 Sb_2O_3 12.5 MoO_3	0.0811	.075	.081	.096	.107	.107	.117	.136
125	12.5 Sb_2O_3 12.5 MoO_3	0.079	.088	.095	.110	.129	.144	.154	.178
131	12.5 Sb_2O_4 12.5 MoO_3	0.036	.067	.071	.085	.109	.124	.142	.162
138	12.5 Sb_2O_4	0.077	.081	.084	.089	.106	.123	.137	.169

Table 26. EFFECT OF VARYING MoO_3-Sb_2O_3 ADDITIVE CONCENTRATION ON PELLET WEAR VOLUME (316°C, 1000 SEC., DRY AIR, 100 g LOAD)

MoO_3:Sb_2O_3	WEAR VOLUME (mm^3) and (TEST NO.) MoS_2 MOLE PERCENT					
Molar Ratio	65	75	85	87.5	92.5	100
1:4		.059 (103)				
1:1	.820 (109)	.057 (118)	.086 (106)		.079 (110)	
		.074 (104)				
		.081 (122)				
		.079 (125)				
2:1			.043 (105)			
4:1		.053 (107)				
1:0		.045 (117)	.0572 (112)			
		.037 (108)				
		.055 (111)				
		.031 (119)				
		.057 (121)				
0:1		.078 (124)	.075 (113)			
		.108 (123)				
		.105 (116)				
0:0						.181 (114)
						.134 (115)

Table 27. EFFECT OF VARYING MoO_3-Sb_2O_3 ADDITIVE CONCENTRATION ON COEFFICIENT OF FRICTION (316°C, DRY AIR, 100 g LOAD)

MoO_3:Sb_2O_3	COEFFICIENT OF FRICTION (μ) AND (TEST NO.) MoS_2 MOLE PERCENT					
	65	75	85	87.5	92.5	100
1:4		.13-.14				
1:1	---	.08-.13 .05-.07 .08-.14 .09-.18	---		---	
2:1						
4:1		---				
1:0		.13-.17 .11-.14 .11-.16		.07-.10		
0:1		.08-.14 .11-.19 .11-.12		.08-.11		
0:0						.06-.09 .08-.12

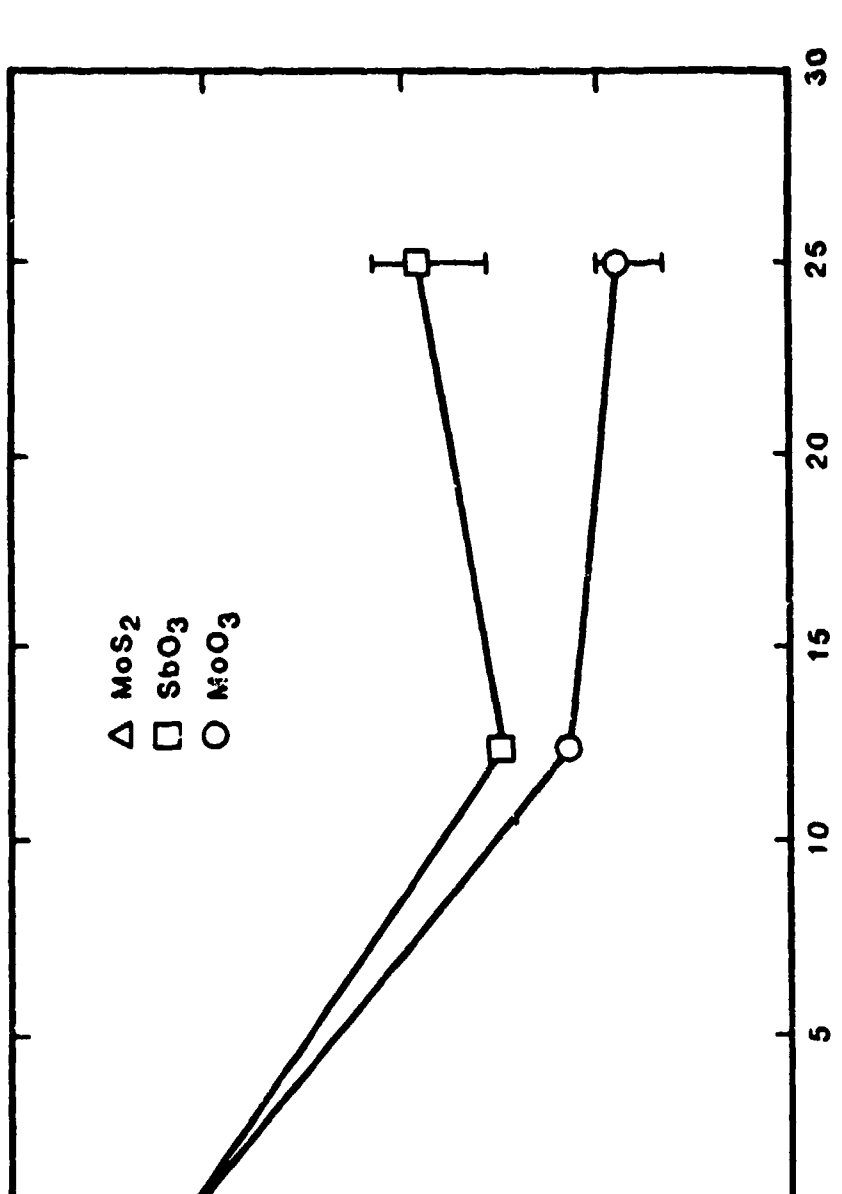

Figure 41. Wear Volume for MoO_3-MoS_2 and Sb_2O_3-MoS_2 Compacts.

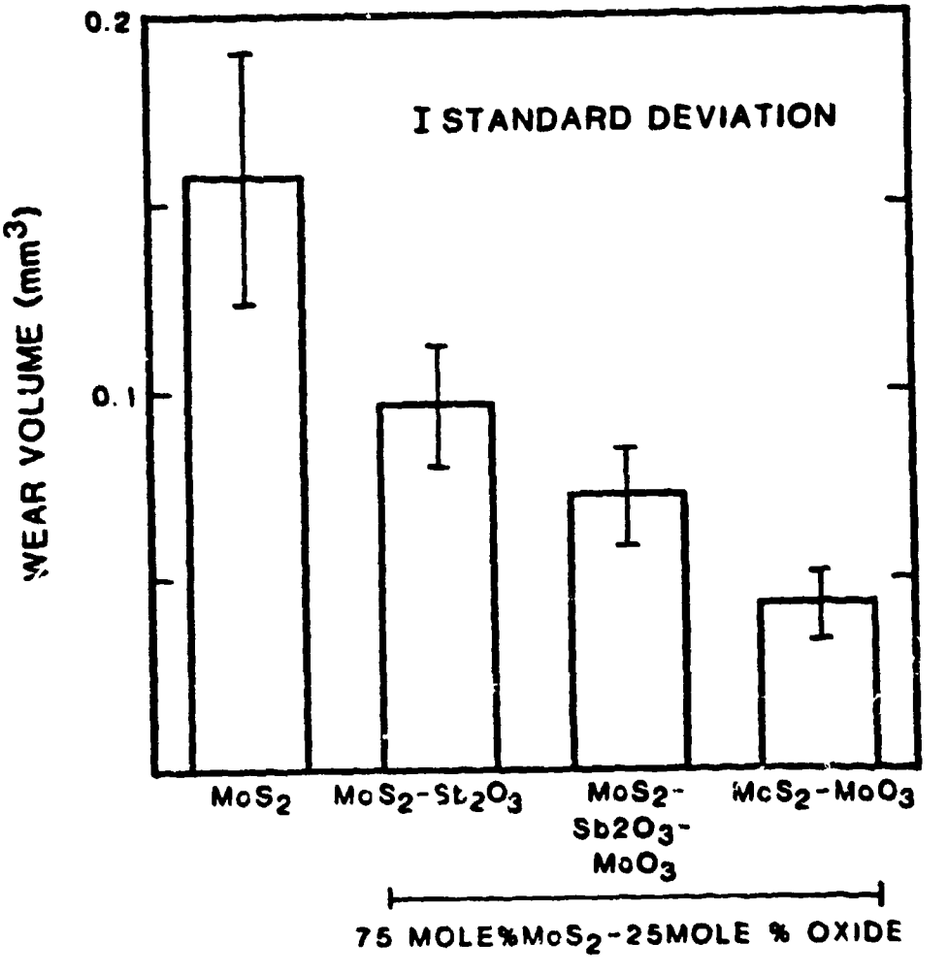

Figure 42. Wear Volume for MoS_2-MoO_3-Sb_2O_3 Compacts.

that the oxide formed on the outer layer of MoS_2 reduces the oxidation of the underlying layers of MoS_2. Thus, low values of friction are maintained in a MoS_2/MoO_3 mixture as long as a subfilm of MoS_2 remains. Fleischauer and Bauer's[101] results show that for long wear lifetimes, 30 to 40 percent of the interfacial layer for MoS_2 should be oxidized.

The MoS_2-MoO_3 formulation in this effort was not optimized tribologically; however, the concentration of MoO_3 in MoS_2 was, coincidentally, near the optimal concentration determined by Fleischauer and Bauer. This work and the observations of others support the hypothesis advanced that oxides, such as MoO_3 or Sb_2O_3, which can deform under environmental conditions encountered, aid in establishing a tribologically superior interface established by retaining the solid lubricant in referred orientation.

The tests with oxides other than Sb_2O_3, especially MoO_3, prove that Sb_2O_3 is not unique in its beneficial role in MoS_2 and that a eutectic of MoO_3-Sb_2O_3 that could be expected to form for compacts of MoO_3-Sb_2O_3 composition tested, do not play a significant tribological role.

CHAPTER VIII

GRAPHITE LUBRICANT COMPACT SYSTEM

In addition to MoS_2, graphite is often employed as a solid lubricant. In contrast to MoS_2 graphite requires chemisorption of oxygen at surface cracks, physical adsorption of water vapor, or some similar mechanism to reduce cleavage strength for good tribological performance.[102] If used in air, the performance of graphite rapidly decreases as a function of increasing temperature up to about 200°C because it desorbs such materials. At much higher temperatures, i.e., 425°C and above, performance again improves[84] possibly resulting from a more active role for oxygen.

ASPERITY CONTACT TEMPERATURE

To examine systems other than those using MoS_2 as the solid lubricant, an investigation of graphite containing antimony trioxide was conducted. Conditions in the graphite Sb_2O_3 system compared with MoS_2-Sb_2O_3 suggested that Sb_2O_3 might deform at the asperity contacts at different temperatures. A critical factor is the higher friction coefficient of graphite at the test temperature.

Other properties were also predicted to affect flash temperatures.

To estimate asperity contact flash temperatures, the procedure of Archard[94] was followed. First, the real area of contact is calculated.

$$A_r = \frac{L}{P} \tag{8.1}$$

where

A_r = area of real contact

L = load

P = hardness

Since the hardness of graphite is about 0.5 on the Mohs scale, this corresponds to about 63% less than MoS_2 hardness as shown by Tabor.[87] Thus,

$$P_{graphite} = 0.63\ P_{MoS_2} \text{ and since, } P_{MoS_2} = 30\ kg/mm^2 \tag{8.2}$$

$$P_{graphite} = 0.63\ (30\ kg/mm^2) = 19\ kg/mm^2 \tag{8.3}$$

and,

$$A_r = \frac{L}{P} = \frac{0.1\ kg}{19\ kg/mm^2} = 0.00526\ mm^2 \tag{8.4}$$

Two cases as stated in the analysis of the MoS_2-Sb_2O_3 compact will be considered.

Case A for single point contact:

$$A_r = \pi r^2 \qquad \text{or } r = \left(\frac{A_r}{\pi}\right)^{1/2} \tag{8.5}$$

$$r = \left(\frac{0.00526 \text{ mm}^2}{\pi}\right) = 0.0490 \text{ mm} = 4.09 \times 10^{-5} \text{m} \tag{8.6}$$

Case B for three point contact:

$$\frac{A_r}{3} = \frac{0.00526 \text{ mm}^2}{3} = 0.00175 \text{ mm}^2 \tag{8.7}$$

$$r = \left(\frac{0.00175 \text{ mm}^2}{\pi}\right)^{1/2} = 0.0236 \text{ mm} = 2.36 \times 10^{-5} \text{m} \tag{8.8}$$

The value of λ must be determined using Equation (6.7) to determine which flash temperature equation should be used for the final calculation. Once again $v = 0.62$ m/s and $t = \mu = 10^{-5}$

For stainless steel:

$k = 26$ J/m-s-°C

$c = 460$ J/kg - °C

$\rho = 7767$ kg/m^3

For graphite - Sb_2O_3:

$k = 0.13$ J/m-s-°C

$c = 1133$ J/kg-°C

$\rho = 2239$ kg/m^3

For graphite:

Density of solid graphite = 2169 kg/m^3

$c = 2.673 + 0.002617T - 116900/T^2$ (T in K, c in cal/mol K)

at 600 K, $c = 2.673 + 0.002617(600) - 116900/(600)^2$

$= 3.92$ cal/mol K = 327 cal/kg-°C

For Sb_2O_3:

$\rho = 5435$ kg/m^3

$c = 100.9$ cal/kg-°C

Assuming equal contribution according to the law of mixtures for specific heat and density according to pellet composition percentage:

Theoretical density = $\rho_T = (0.75 \times 2169) + (0.25 \times 5435) = 2986$ kg/m^3

For compacted particles, real density is estimated at about 75 percent of theoretical so

$\rho = 0.75 \times$ (theoretical density) $= 0.75 \times 2986 = 2239$ kg/m^3

$c = 0.75 \times 327 + 0.25 \times 100.9 = 270.5$ cal/kg°C = 1133 J/kg°C

Therefore:

Case A for single point contact:

$$\lambda = \frac{(0.62)}{2(4.09 \times 10^{-5})(26)(0.18)} [(26)(2239)(1133)(10^{-5})^2 + (0.18)(7767)(460)(<409 \times 10^{-5} - 10^{-5})^2]$$

$$= 11.7 \qquad (8.9)$$

Using Equation (6.6), with $\mu = 0.4$, $L = 0.98N$, $J = 1$, all other values given.

$$\theta_m = \frac{(0.4)(0.98)(0.62)^{1/2}}{(3.6)(1)[(2239)(1133)(4.09 \times 10^{-5})^3(0.18)]}$$

$$= 485°C \qquad (8.10)$$

Therefore, at 316°C test temperature, contact temperature = 316°C + 485°C = 801°C

Case B for three point contact:

$$\lambda = \frac{0.62}{2(2.36 \times 10^{-5})(26)(0.18)]} x$$

$$[(26)(2239)(1133)(10^{-5})^2 + (0.18)(7767)(460)x$$

$$((2.36X10^{-5}) - 10^{-5})^2)]$$

$$= 18 \qquad (3.11)$$

Using Equation (6.6), as above, except $L = 0.327N$

$$\theta_m = \frac{(0.4)(0.327)(0.62)^{1/2}}{(3.6)(10[(2239)(1133)(2.36 \times 10^{-5})^3(0.18)]^{1/2}}$$

$$\theta_m = 369°C \qquad (8.12)$$

therefore, at 316°C test temperature, contact temperature = 316°C + 369°C = 685°C.

Both of the above temperatures are much higher than the melting point of Sb_2O_3 (656°C). To get the same effect as that that occurs in the MoS_2-Sb_2O_3 system, all other parameters being equal, the ambient temperatures would need to be reduced as follows:

Case A for single point contact:

Contact temperature in MoS_2-Sb_2O_3 system = 697°C

Contact temperature in Graphite-Sb_2O_3 system = 801°C

Test temperature reduction necessary = 801°C - 697°C = 104°C

316°C - 104°C = 212°C for equivalent test temperature

Case B for three point contact:

Contact temperature in MoS_2-Sb_2O_3 system = 606°C

Contact temperature in Graphite-Sb_2O_3 system = 685°C

Test temperature reduction necessary = 685°C - 606°C = 79°C

316°C - 79°C = 237°C for equivalent test temperature

Therefore, in the standard test, if one reduces test temperatures to about 210°C-230°C (410°-446°F), then asperity contact temperature in the graphite-Sb_2O_3 system

would approximate those in the MoS_2-Sb_2O_3 system evaluated at 316°C (600°F).

WEAR STUDIES

To determine if the relative sliding wear of the graphite-Sb_2O_3 system compared with graphite would be improved by lowering the test temperature appropriately, pellets of graphite (U.S. Army Specification, 2-64A, Graphite Powder, Dixon Jersey City, NJ) and graphite-Sb_2O_3 were prepared in the standard configuration and evaluated at 232°C (450°F) and 361°C (600°F). It was predicted as shown earlier that at the higher temperature the matrix of Sb_2O_3 would be expected to deform severely because of localized melting, while at lower temperature the Sb_2O_3 matrix would only soften to accommodate a preferred reorientation of graphite.

The raw and reduced data are summarized in Table 28. The significance of the tests is that at the higher temperature, the wear rate of the graphite-Sb_2O_3 pellet was much greater than that of graphite due most probably to excessive softening or melting of Sb_2O_3. At the lower temperature of 232°C, the graphite-Sb_2O_3 pellet wore less than a graphite pellet at the same temperature. Here Sb_2O_3 softening rather than melting is expected by the flash temperature calculations.

The friction coefficient data are significant. For graphite, the friction coefficient as a function of time

Table 28. GRAPHITE AND GRAPHITE/Sb_2O_3(c) WEAR DATA

TEST NUMBER	TEST TEMP., °C (°F)	PELLET COMPOSITION	WEAR VOLUME (mm^3)	k_1	k_2	$\bar{k}$
141	21.1	Graphite	0.082	0.107	0.138	0.123
143	(70)	Graphite/Sb_2O_3(c)	0.1125	0.165	0.196	0.178
129	232.2	Graphite	0.0375	0.160	0.271	0.215
128	(450)	Graphite/Sb_2O_3(c)	0.0342	0.126	0.240	0.183
140	273.9	Graphite	0.0606	0.161	0.198	0.180
142	(525)	Graphite/Sb_2O_3(c)	0.1246	0.094	0.202	0.148
127	315.6	Graphite	0.0427	0.227	0.343	0.285
126	(600)	Graphite/Sb_2O_3	0.0898	0.101	0.247	0.174
		RATIOS OF NORMALIZED DATA				
	21.1	Graphite	1.92	0.47	0.40	0.432
	(70)	Graphite-Sb_2O_3(c)	2.63	0.73	0.57	0.62
	232.2	Graphite	0.878	0.705	0.790	0.754
	(450)	Graphite-Sb_2O_3(c)	0.801	0.555	0.700	0.642
	273.9	Graphite	1.419	0.709	0.577	0.632
	(525)	Graphite-Sb_2O_3(c)	2.918	0.414	0.589	0.519
	315.6	Graphite	1.00	1.000	1.000	1.000
	(600)	Graphite-Sb_2O_3(c)	2.10	0.145	0.720	0.611
		GRAPHITE-Sb_2O_3(c)/GRAPHITE RATIO OF NORAMLIZED DATA				
	21.1 (70)		1.370	1.553	1.425	1.435
	232.2 (450)		0.912	0.787	0.886	0.851
	273.9 (525)		2.056	0.585	1.02	0.82
	315.6		2.10	0.445	0.720	0.610

was relatively constant, while pellets containing Sb_2O_3 produced friction coefficients that increased almost linearly from the initial to final value. At the higher temperature, the initial value, μ_{k_i}, was lower than the corresponding value at 232°C while a reversal was observed in final values. These data may be rationalized if Sb_2O_3 is severely deforming or melting at the higher temperatures which would contribute to an initial low friction coefficient and deposit material onto the relatively cooler wear track, which would result in a gradual increase in friction coefficient. At lower temperatures, the effect of asperity contact flash temperature on coefficient of friction is minimized. Graphite and graphite-Sb_2O_3 compacts were also evaluated at room temperature (Tests 141 and 143, respectively) and at 274°C (Tests 140 and 142, respectively). Results at 274°C were intermediate between those at 232°C and 310°C, with relative wear of the graphite-Sb_2O_3 compacts higher than at 232°C. Frictional coefficient ratios were uniformly higher at lower temperatures as shown in Figure 43.

In summary, as predicted by flash temperature calculation, for 274°-316°C test temperatures, additions of Sb_2O_3(c) to graphite are not beneficial. At those temperatures, Sb_2O_3(c) may fuse rather than deform at asperity contact and, thus, the compact wears at a higher rate than graphite alone. When ratios of data for tests

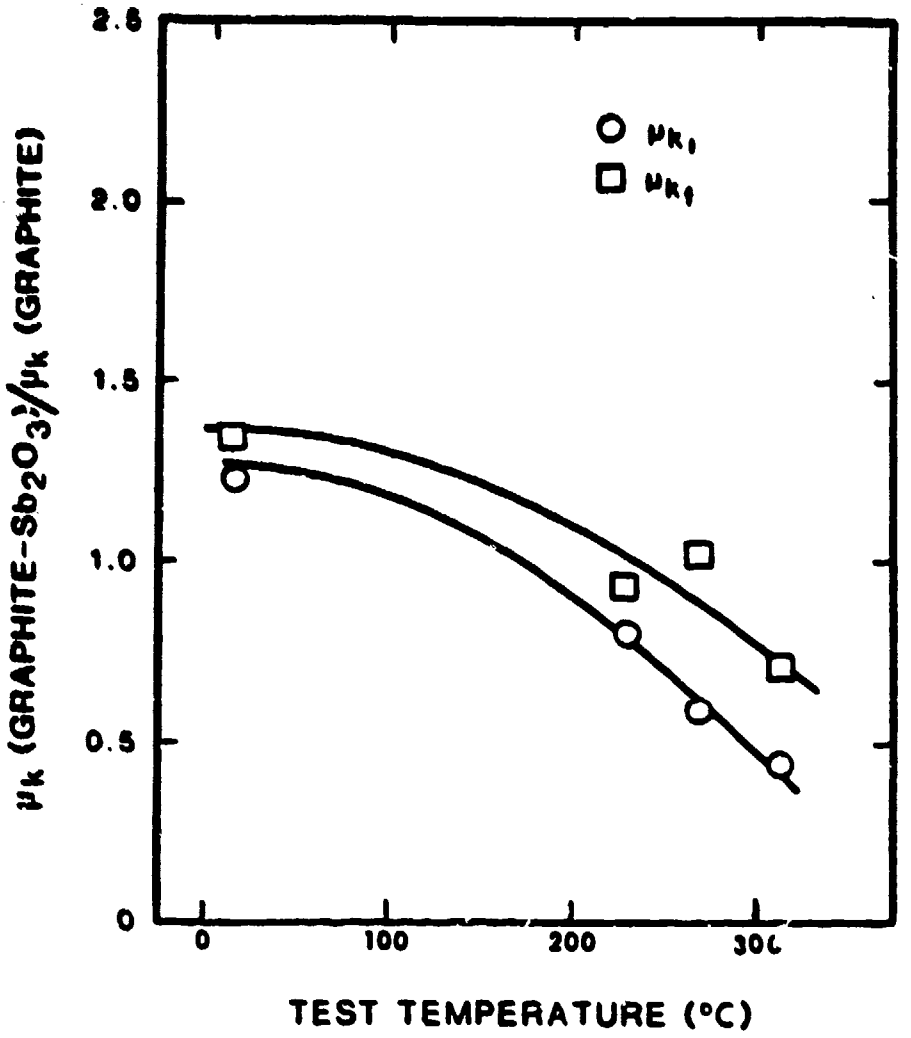

Figure 43. Ratio of Graphite-Sb_2O_3 to Graphite Friction Coefficients as Function of Test Temperature.

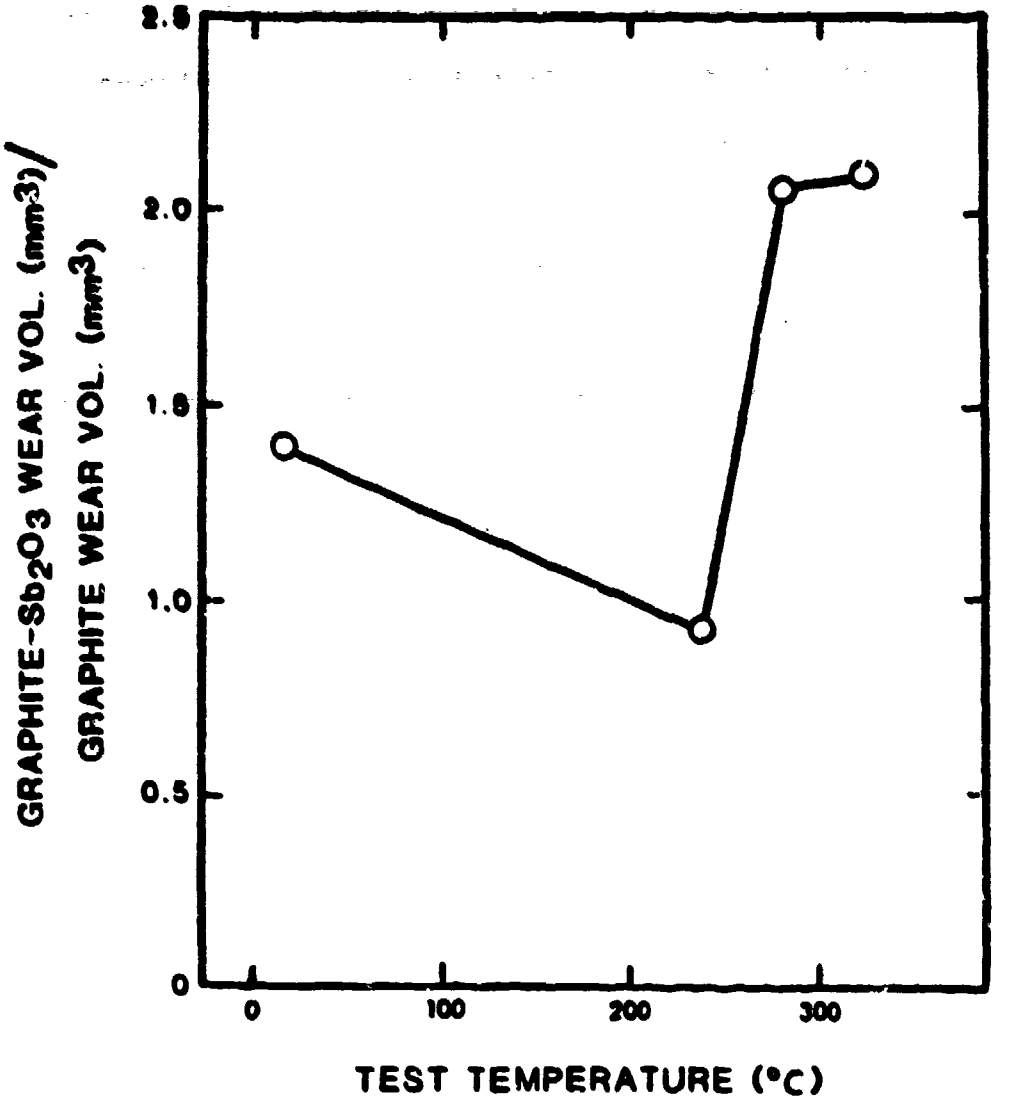

Figure 44. Ratios of Graphite-Sb_2O_3 to Graphite Compact Wear Volumes as a Function of Test Temperature.

over the range 21°-316°C are examined as given in Figure 44, it is found that at a test temperature of 232°C, the relative wear volume is less for a compact containing Sb_2O_3(o). At ambient, the effect of Sb_2O_3 additions to graphite does not appear to be beneficial, which may be due to an inability of the additive to sufficiently deform under those conditions. These data support a concept of bulk additives plastically deforming for improved tribological surfaces under selected conditions. If the asperity contact temperatures are too high, the additive may deform excessively and the addition becomes tribologically detrimental. Of course, other factors such as load and sliding velocity are also crictical factors with temperature in determining the range of conditions over which the additive may be beneficially compounded with a solid lubricant.

The data also indicate that at temperatures in these tests where Sb_2O_2(o) might be expected to be beyond its beneficial addition range, i.e., 274° and 316°C, the initial coefficient of friction, μ_{k_i}, is low followed by a gradual increase to a much higher value, μ_{k_f}, by the end of the test. It is hypothesized that the additive may act as a fluid or sublime at a very high rate during initial asperity contact; as wear progresses, graphite-Sb_2O_3 is deposited on the cooler wear track which results in the increasing coefficient of friction. A much more minor

upward trend in the coefficient of friction for graphite observed under the same conditions.

Because of the number of wear tests completed, the findings of the graphite-Sb_2O_3 study are not conclusive, however, support is provided for the additive deformation concept.

CHAPTER IX

DISCUSSION

The role of bulk additions to solid lubricants may be one of simply permitting the formation of an improved tribological surface by deformation of the additive at or near asperity contact which results in densification or sintering of the surface. Since tribological surfaces are complex, it is difficult to provide direct evidence of such a role; however, qualitative improvement of compacts which contain beneficial additions are easily observed either by optical or scanning electron microscopy. This effort shows that the several alternative hypotheses proposed to date cannot be supported, and that the hypothesis advanced is consistent with observations in this effort and with those of others[8,10] in studies of the MoS_2-Sb_2O_3 system.

Harmer and Pantano[8] conclude that a role of Sb_2O_3 might be to retard oxidation of MoS_2. However, oxidation studies of Sb_2O_3 here support those of others who have concluded that sublimation of $Sb_2O_3(c)$ occurs simultaneously with oxidation which rationalizes the thermal behavior of MoS_2-Sb_2O_3 compacts without hypothesizing that Sb_2O_3 in some way retards MoS_2

oxidation. Data do indicate that the oxidation rates of finely ground Sb_2O_3(c) or Sb_2O_3(c), or mixtures are related to equilibrium sublimation pressure in a pseudo-isobaric reaction.

DTA data also indicate that the oxidation rate is dependent upon Sb_2O_3 surface area, which is as expected for an oxidation rate dependent on sublimation of Sb_4O_6.

Such a reaction is supported by calculation of free energies which indicate a greater driving force for oxidation of Sb_4O_6 than Sb_2O_3(s).

Development of a more adequate understanding of the oxidation of Sb_2O_3 indicates that Harmer and Pantano's conclusions regarding a proposed protective role for Sb_2O_3 in retarding oxidation of MoS_2 cannot be supported.

In DTA studies more directly related to lubricant compacts, when Sb_2O_3 was mixed with MoS_2, no significant influence on oxidation of MoS_2 by Sb_2O_3 was found, suggesting that the role proposed for Sb_2O_3 to oxidize sacrificially, preventing oxidation of MoS_2, cannot be supported. When MoS_2 was oxidized in DTA, it was found that the oxidative exotherm started at about 345°C (DTA 181), while the oxidation endotherm began at about 415°-420°C (DTA 175). Thus, MoS_2 begins to oxidize before Sb_2O_3 and, therefore, cannot be protected sacrificially by Sb_2O_3 for loose mixtures of powders as evaluated in DTA. However, Sb_2O_3 may promote densification of the

tribological surface. Dense packing of Sb_2O_3 around MoS_2 could retard the diffusion of oxygen into subsurface MoS_2 sites and would certainly be beneficial.

One might propose that addition of Sb_2O_3 to MoS_2 allows the compact t· reach closer to theoreticl density at relatively low loads. Compaction of MoS_2-Sb_2O_3 (<30 μM) and MoS_2-MoO_3 (<30 μM) formulations at modest pressures (=172 MPa) indicate that additives do not aid in achieving theoretical density. In fact, a smaller fraction of theoretical density was achieved for MoS_2 with additives than for MoS_2 alone. The data are in contrast to Harmer and Pantano's[8] results in which there was modest improvement in compaction on a theoretical basis when Sb_2O_3 was added to MoS_2. Data from this work show that the fraction of theoretical density achieved linearly decreased with increasing additive concentrations. The differences are not inconsistent if the Sb_2O_3 used by Harmer and Pantano contained large masses with voids which collapsed under high loading, or if their MoS_2 was particularly difficult to densify.

The data generated in this effort suggest that densification of MoS_2 is not aided by bulk additions and a relatively low pressure. If, indeed, surface densification of MoS_2 films containing selected oxides and sulfides does occur during contact, as proposed then tribological conditions must generate asperity contact temperatures

sufficient to deform the additive, allowing effective densification of the surface layer.

It has been suggested that a eutectic of Sb_2O_3-MoO_3 forms at tribological interfaces.[7] A eutectic compositon of these oxides was prepared in the laboratory, and the eutectic endotherm was detected by DTA under argon. Interfacial materials removed from the sliding interface of compacts and debris gathered in the area of sliding contact generated at room temperature and at 370°C during wear tests were analyzed by DTA and x-ray diffraction techniques. No evidence of Sb_2O_3-MoO_3 eutectic formation was found. After sliding at room temperature, compacts showed a slight broadening of the most intense MoS_2 reflection, and Sb_2O_3 peaks were lower in intensity, This may be due to MoS_2 coverage of much of the interface after sliding. After wear at 370°C, x-ray spectra indicated that the dimorph Sb_2O_3(c), as added, changed to Sb_2O_3(o), and suggested trace oxidation of Sb_2O_3 to Sb_2O_4. Therefore, the concept that improved tribological properties are the result of eutectic formation cannot be supported by these analyses. Additionally, previous wear data[7] in air and vacuum and data of this work for 232°C wear tests indicate that MoS_2 containing Sb_2O_3 is tribologically superior to MoS_2 alone whether evaluated in air, vacuum or inert atmosphere. These data do not support of a role in which

oxidation of either Sb_2O_3 or MoS_2 is required for the additive effects of Sb_2O_3 additions to be beneficial.

In other wear studies, it was found that additions of MoO_3 are superior to Sb_2O_3 additions to MoS_2 compacts when worn at 316°C in air. These data prove that the benficial role of Sb_2O_3 as an additive to MoS_2 is not unique. Additionally, mixtures of MoO_3-Sb_2O_3 as MoS_2 additions are linearly intermediate in tribological benefit. Therefore, there does not appear to be beneficial synergism of MoO_3-Sb_2O_3 additions. Such synergism should be expected if formation of an MoO_3-Sb_2O_3 eutectic performs a significant tribological role in MoS_2-Sb_2O_3 solid lubricant compacts.

When other oxides and sulfides are added to MoS_2 on a volumetric basis equivalent to 25 mole percent Sb_2O_3 addition, many of the compacts were found to be tribologically superior to pure MoS_2. Additives that resulted in improved tribological performance appeared to have smoother compact surfaces when examined by both optical and scanning electron microscopy. This improvement in tribological condition could not be quantified but was easily observed. For the additions investigated, there is an excellent correlation of wear volume with additive shear strength. These data also support a concept that Sb_2O_3 is not unique in its ability to improve the tribological performance of MoS_2.

For the oxides and sulfides used in this study as compact additions, a transition from brittle to tough behavior should occur at 0.5 to 0.7 of the absolute melting temperatures[98] of those materials. Comparison of computed transition temperatures for the additions to MoS_2 suggests that such a temperature region of ductility is achievable for the beneficial additives. Based upon calculations for the MoS_2-Sb_2O_3 lubricant compact system, deformation of Sb_2O_3 at asperity contact is certainly possible, since temperatures in the region and above 0.5 to 0.7 of Sb_2O_3 melting temperature are achieved.

An evaluation of the wear of graphite-Sb_2O_3 compacts in which additions of Sb_2O_3 marginally improve graphite performance at temperatures lower than MoS_2-Sb_2O_3. The properties of graphite and MoS_2 affect asperity contact temperatures resulting in higher asperity contact temperatures for the graphite-Sb_2O_3 system compared with MoS_2-Sb_2O_3. Therefore, the beneficial tribological effect is found at a lower test temperature for graphite-Sb_2O_3. These data support a hypothesis that MoS_2 is not a unique solid lubricant in its role in MoS_2-Sb_2O_3 formulations.

Thus, it appears that the beneficial mechanism of Sb_2O_3 addition to MoS_2 is not unique, neither for additive or solid lubricant. It does appear that the shear strength of the additive is critical in performance of compacts under tribological conditions, which supports the concept

of the bulk additive accommodating a preferred tribological position for the solid lubricant resulting in overall improved performance.

Excellent correlation of additive shear strength with wear volume and poorer correlation with friction coefficient supports the hypothesis in that critical beneficial deformation for solid lubricant accommodation occurs in the bulk of the compact and not at the interface.

CHAPTER X

CONCLUSIONS

Three main hypotheses have been proposed to date to rationalize the beneficial effects of Sb_2O_3 additions to MoS_2. They are:

(i) Sb_2O_3 oxidized sacrificially, rather than MoS_2.

(ii) Sb_2O_3 retards the oxidation of MoS_2 by some ill-defined protective mechanism.

(iii) A eutectic of Sb_2O_3-MoO_3 forms, aiding transfer film formation.

These hypotheses cannot be supported based upon the following observations:

(i) Initial oxidation of MoS_2 occurs at lower temperatures than for Sb_2O_3.

(ii) Sublimation of Sb_4O_6 appears to be a critical step in the oxidation mechanism of Sb_2O_3, which aids in rationalizing observations of others regarding the effects of Sb_2O_3 on MoS_2 oxidation.

(iii) Bulk additions of Sb_2O_3 to MoS_2 are beneficial whether such compacts are evaluated in vacuum, inert atmosphere or air.

(iv) DTA or x-ray diffraction evidence of Sb_2O_3-MoO_3 eutectic formation or wear surfaces could not be found, although such a eutectic could be prepared and detected in the laboratory.

(v) Mixtures of MoO_3 and Sb_2O_3 as bulk additives to MoS_2 did not act synergistically to provide tribological benefits greater than either of the additives individually.

Alternatively, it is proposed that the beneficial effect of Sb_2O_3 additions to MoS_2 is the result of deformation of Sb_2O_3 at asperity contact temperatures to permit and retain a tribologically preferred orientation of the solid lubricant. This hypothesis is supported by the following observations:

(i) Bulk, rather than trace quantities of the additive are required.

(ii) SEM micrographs show that MoS_2-Sb_2O_3 compact wear surfaces appear to be much smoother and more dense compared with MoS_2 compact wear surfaces.

(iii) MoO_3 as an additive for MoS_2 is superior to Sb_2O_3 with regard to wear volume and is equivalent in comparison of friction coefficient.

(iv) Other stable oxides and sulfides are also beneficial as additives to MoS_2 compacts when evaluated up to 316°C in air; thus, Sb_2O_3 is not a unique additive.

(v) Limited wear studies of graphite-Sb_2O_3 compacts suggest that the beneficial effects of additives are not unique to MoS_2.

(vi) The low wear volumes of oxide and sulfide additions to MoS_2 appear to be related strongly to additive shear strength at test temperature. Correlation of wear volume with basic properties of the additive such as Mohs hardness or melting temperature is not as good. The weaker correlation is probably due to the limited utility of using such properties as predictors of shear strength.

(vii) Basic properties of the additives could not be used to predict coefficients of friction of compacts containing additives. The poor correlation of frictional coefficient with basic additive properties such as shear strength, Mohs hardness and melt temperature

compared to excellent to good correlation of those properties with wear volume indicates that the additions are not beneficial at the interface rather in the bulk.

This conclusion supports the hypothesis that the additives deform to permit and retain a tribologically preferred orientation for the solid lubricant.

These observations suggest that a beneficial additive must be thermally and chemically stable at such temperatures, yet shear to permit deformation at asperity contact temperatures. Thus, although many additives may be beneficial, selection of the solid lubricant, bulk additive and tribological conditions must be considered to define an optimum compact system.

REFERENCES

1. M. N. Gardos and B. D. McConnell, "Development of a High-Load, High-Temperature Self-Lubricating Composite - Part III: Additive Selection," ASLE-ASME Lubrication Conference, October 5-7, 1981, New Orleans, LA.

2. J. W. R. Taylor, ed., Jane's All the World's Aircraft, Jane's Publ. Co., New York, NY, 1984, p. 893.

3. G. P. Murphy, Jr., U.S. Patent 3,314,885, April 18, 1967 (CA 67: 1265t).

4. M. Campbell and V. Hopkins, "Development of Polyimide Bonded Solid Lubricants," Lub. Eng., 23, 7 (1967).

5. R. D. Hubbell and B. D. McConnell, "Wear Behavior of Polybenzimidazole Bonded Solid-Film Lubricants," J. Lub. Tech., 92, Series F, 2 (1970).

6. B. D. McConnell, "Solid Lubricating Films - Friction-Wear Improvement with Poly(benzothiazole) Binders," Ind. Eng. Chem. Prod. Res. Develop., 9, 4 (1970).

7. M. T. Lavik, R. D. Hubbell and B. D. McConnell, "Oxide Interaction - A Concept for Improved Performance with Molybdenum Disulfide," Lub. Eng., 31, 20-27 (1975).

8. R. S. Harmer and C. G. Pantano, "Synergistic Mechanisms of Solid Lubricants," AFML-TR-77-227, December 1978.

9. M. I. Nosov, "The Lubricating Properties of Molybdenum Disulfide with Antimony Oxides and Sulfides," Khim. Tech. Topliv Masel, 7, 43-44 (1978).

10. E. Yamamoto, K. Wada, T. Fukuzuka, K. Shimogori, K. Fujiwara and K. Tanji, "Lubricating Films to Prevent Galling of Stainless Steel Threaded Parts," Lub. Eng., 40, 588-597 (1984).

11. F. J. Clauss, Solid Lubricants and Self-Lubricating Solids, Academic Press, New York, NY, 1972, pp. 1-4.

12. F. P. Bowden and D. Tabor, The Friction and Lubrication of Solids, Part II, Oxford Univ. Press, 1964.

13. E. Rabinowicz, Friction Wear of Materials, Wiley, New York, NY, 1965, pp. 114-117.

14. J. F. Archard, "Contact and Rubbing of Flat Surfaces," J. Appl. Phys., 24, 981-988 (1953).

15. A. Cameron, The Principles of Lubrication, John Wiley and Sons, New York, NY (1966).

16. W. E. Campbell, "Solid Lubricants," in Boundary Lubrication, An Appraisal of World Literature, F. F. Ling, E. E. Klaus, and R. S. Fein, Pub. by ASME, New York, NY, 1969.

17. W. O. Winer, "Molybdenum Disulfide as a Lubricant: A Review of the Fundamental Knowledge," Wear, 10, 422-452 (1967).

18. P. M. Magie, "A Review of the Potentials of the New Heavy Metal Derivative Solid Lubricants," Lub. Eng., 22, 262-269 (1966).

19. W. E. Jamison, "Structure and Bonding Effects on the Lubricating Properties of Crystalline Solids," ASLE Trans., 15, 296-305 (1972).

20. W. E. Jamison, Final Report on Solid Lubricant Research to Hughes Aircraft, Contract F33615-78-C-5196, October 1980.

21. A. Madhukar, "Structural Classification of Layered Dichalcogenides of Group IVB, VB and VIB Transition Metals," Solid State Comm., 16, 383-388 (1975).

22. W. E. Jamison and S. L. Cosgrove, "Frictional Characteristics of Transition Metal Disulfides and Diselenides," ASLE Trans., 10, 19-27 (1967).

23. D. J. Boes, "Unique Solid Lubricating Materials for High Temperature Applications," ASLE Trans., 10, 19-27 (1967).

24. D. J. Boes and B Chamberlain, "Chemical Interactions Involved in the Formation of Oxidation-Resistant Solid Lubricant Composites," ASLE Trans., 11, 131-139 (1968).

25. R. D. Dayton, "Experimental Investigation of Ag-Hg-WTFE-$MoSe_2$ Solid Lubricated Ball Bearings for High Speed, High Temperature, and High Load Applications," AFAPL-TR-71-100, January 1972.

26. D. H. Killeffer and A. Ling, Molybdenum Compounds: Chemistry and Technology, Interscience, New York, NY, 1952.

27. C. A. Hampel, Uncommon Metals, Reinhold Publ. Co., 283 (1961).

28. R. C. Weast, ed., Handbook of Chemistry and Physics, 61st ed., Chemical Rubber Co., Cleveland, OH, 1981.

29. M. M. Spivak, A. S. Pashinkin, R. A. Isakova and K. S. Amoseva, "Thermodynamic Analysis of the Mo-S-O System," Zhin. Prik. Khin, 51, 549-553 (1978).

30. R. G. Dickinson and L. Pauling, J. Am. Chem. Soc., 45, 1466 (1923).

31. C. R. Cardoen, "The Kinetics of Molybdenum Disulfide Oxidation," Doctoral Disseratation, Univ. of Utah, 1969.

32. N. B. Pilling and R. G. Bedworth, J. Inst. Metals, 29, 532 (1922).

33. A. N. Zelikman and L. B. Belaevskaya, "Concerning the Melting Temperature of Molybdenite," J. Inorg. Chem (USSR), 10, 2245-2256 (1956).

34. D. H. Buckley, "Examination of Molybdenum Disulfide with LEED and Auger Emission Spectroscopy," NASA TN D-7010, December 1970.

35. W. E. Swartz and D. M. Hercules, "X-Ray Photoelectron Spectroscopy of Molybdenum Compounds," Anal. Chem., 43, 1774 (1971).

36. L. B. Atkinson and P. Swift, "A Study of the Tribo-Chemical Oxidation of Molybdenum Disulfide Using X-Ray Photo-Electron Spectroscopy," Wear, 29, 129-133 (1974).

37. F. Lepage, P. Baillif and J. Bardolle, "Study of Electron Spectrometry (ESCA) of the Oxidation States of Molybdenum," C. R Hebd. Seances Acad. Sci., Series C, 280, 1089-1092 (1975).

38. F. Lepage, P. Baillif and J. Bardolle, "Study of Various Degrees of Oxidation of Molybdenum and Tungsten by Electron Spectroscopy (ESCA)," Vide, Series: 30A, 2nd Colloq. Int. Phys. Chim. Surfaces, 101-103 (1975).

39. S. O. Grim and Luis J. Matienzo, "X-Ray Photoelectron Spectroscopy of Inorganic and Organometallic Compounds of Molybdenum," Inorg. Chem., 14, 1014-1018 (1975).

40. J. M. Wilson, "Energy Loss Spectroscopy of Sulfide Films on Mo(100)," Surf. Sci., 57, 499-508, (1976).

41. T. T. Lin and D. Lichtman, "AES Studies of Chemical Shift and Beam Effect on Molybdenum Oxides," J. Vac. Sci. Tech., 15, 1689-1694 (1978).

42. Y. Toga, A. Isogai, and K. Nakajima, "LEED-AES Study of Sulfide Single Crystals," Surf. Sci., 86, 591-600 (1979).

43. C. Y. Wang, Antimony: Its Geology, Metallurgy, Industrial Uses and Economics, C. Griffen and Co., London, 1952.

44. D. J. Stewart, O. Knop, C. Ayasse and F. W. D. Woodhams, "Pyrochlores VII. The Oxides of Antimony: An X-Ray and Mossbauer Study," Can. J. Chem., 50, 690-700, (1972).

45. H. Remy, Treatise on Inorganic Chemistry, Vol. I, Elsevier, New York, NY, 1956.

46. E. J. Roberts and F. Fenwick, "The Antimony-Antimony Trioxide Electrode and Its Uses as a Measure of Acidity," J. Am. Chem. Soc., 50, 2125-2147 (1988).

47. W. B. White, F. Dachille and R. Ray, "High-Pressure Polymorphism of As_2O_3 and Sb_2O_3," Z. Krist., 125, 450-458 (1967).

48. P. Gopalakrishnan and H. Manohar, "Kinetics and Mechanism of the Transformation in Antimony Trioxide from Orthorhombic Valentinite to Cubic Senarmontite," J. Solid State Chem., 15, 61-67 (1975).

49. W. B. Hincke, "The Vapor Pressure of Antimony Trioxide," J. Amer. Chem. Soc., 3869-3877 (1930).

50. E. Jungermann and K. Plieth, "Dampfdrucke und Kondensations-geschwindig-keiten der polymorph Arsen-und Antimontrioxide," Z. Phys. Chem. Neue Folge, 53, 215-228 (1967).

51. C. G. Maier, U.S. Bur. Mines Rep. Investigations, Nr. 3262, December 1934, pp. 22-28.

52. C. A. Cody, L. DiCarlo and R. K. Darlington, "Vibrational and Thermal Study of Antimony Oxides," Inorg. Chem., 18, 1572-1576 (1979).

53. Y. K. Agrawal, A. L. Shashimohan and A. B. Biswas, "Studies on Antimony Oxides: Part 1, Thermal Analysis of Sb_2O_3 in Air, Nitrogen and Argon," J. Thermal Anal., 7, 635-641 (1975).

54. P. Gopalakrishnan and H. Manohar, "Topotoxy in the Oxidation of Valentinite, Sb_2O_3, to Cervantite, Sb_2O_4," Pramana, 3, 277-285 (1974).

55. P. Gopalakrishnan and H. Manohar, "Topotactic Oxidation of Valentininte Sb_2O_3, to Cervantite, Sb_2O_4: Kinetics and Mechanisms," Journal of Solid State Chemistry, 16, 301-306 (1976).

56. S. E. Golunski, T. G. Nevell and M. I. Pope, "Thermal Stability and Phase Transitions of the Oxides of Antimony," Thermochimica Acta, 51, 153-168 (1981).

57. D. Rogers and A. C. Skapski, "The Crystal Structure of β-Sb_2O_4 : A New Polymorph," Proc. Chem. Soc., 400 (1964).

58. T. Birchall, J. A. Conner and I. H. Hiller, "High-Energy Photoelectron Spectroscopy of Some Antimony Compounds," J. Chem. Soc., Dalton Trans., 20, 2003-2006 (1975).

59. F. Garbassi, "XPS and AES Study of Antimony Oxides," Surf. and Interface Anal., 2, 165-169 (1980).

60. C. D. Wagner, "Chemical Shifts of Auger Lines, and the Auger Parameter," Faraday Discuss., 60, 291-300 (1975).

61. V. Hopkins and M. Campbell, "Friction and Wear-Life of Selected Solid Lubricant Films at -100°F, R.T., and 400°F," Lub. Eng., 430-435 (1969).

62. A. E. Standage and W. N. Turner, "A High-Temperature Polyimide Reinforced with Silica Fiber," J. Materials Sci., 2, 103-111 (1967).

63. R. L. Fusaro, "Polyimides-Tribological Properties and Their Use as Lubricants," in K. L. Mittal, ed. Polyimides: Synthesis, Characterization and Applications, Vol. II, Plenum Press, New York, NY, 1982, p. 1066.

64. M. Parmentier, A. Courtoir and C. Gleitzer, Bull. Soc. Chem. Fr., 1-2 (Pt 1) 75-77 (1974).

65. J. B. Peace, "Solid Lubricants" in E. R. Braithwaite, ed., Lubrication and Lubricants, Elsevier, Amsterdam, 1967, p. 95.

66. J. B. Peace, "Solid Lubricants" in E. R. Braithwaite, ed. Lubrication and Lubricants, Elsevier, Amsterdam, 1967, p. 72.

67. J. W. Lyons, The Chemistry and Uses of Fire Retardants, Wiley-Interscience, New York, NY, 1970, pp. 209-218.

68. D. A. Church and F. W. Moore, "Molybdenum-Based Flame Retardants are Now in the Plastics Ball Game," Plast. Eng., 31, 36 (1975).

69. D. Edelson, V. J. Kuck, R. M. Lum, E. Scalco, W. H. Starnes and S. Kaufman, Jr., "Anomalous Behavior of Molybdenum Oxide as a Fire Retardant for Polyvinyl Chloride," Comb. and Flame, 38, 271 (1980).

70. O. Borger and J. Krogh-Moe, "The Infrared Spectra of Some Modifications of Arsenic Trioxide and Antimony Trioxide, Acta Chem. Scand., 11, p. 265-267.

71. J. R. Ferraro, J. S. Ziomek and G. Mack, Spectrochem. Acta, 17, 802 (1961).

72. V. G. Trofimov, A. I. Sheinkman and G. V. Kleshchev, "Oriented Crystallization of Cervantite on Heating Sb_2O_3," Izvestiga VSZ, Fizika, 3, 135-137 (1973).

73. I. Langmuir, Physik, Z., 14, 1273 (1913).

74. P. J. Durrant and B. Durrant, Introduction to Advanced Inorganic Chemistry, Wiley, NY, 1970, p, 773.

75. J. B. Peace, "Solid Lubricants" in E. R. Braithwaite, ed. Lubrication and Lubricants, Elsevier, Amsterdam, 1967, p. 76.

76. M. E. Campbell, "Solid Lubricants, A Survey," NASA SP-5059(01) National Aero Space Adm., Washington, DC, 1972.

77. J. B. Peace, "Solid Lubricants" in E. R. Braithwaite, ed. in Lubrications and Lubricants, Elsevier, Amsterdam, 1967, p. 91.

78. P. G. Lenhert, J. F. O'Brien, W. W. Adams, "A User's Guide to the Picker Diffractometer for Polymer Morphology Studies," AFWAL-TR-86-4024, Air Force Materials Laboratory, Wright-Patterson Air Force Base, OH, July 1985.

79. D. P. Anderson, "X-ray Analysis Software: Operation and Theory Involved in Program DIFF," AFWAL-TR-85-4079, Air Force Materials Laboratory, Wright-Patterson Air Force Base, OH, June 1985.

80. W. L. Bragg, "The Crystalline State," MacMillan, New York, 1933.

81. "Alphabetical and Grouped Numerical Index of X-ray Diffraction Data," American Society of Testing Materials, Special Technical Publication, No. 48E (1955).

82. G. Salomon, A. W. J. DeGee, and J. H. Zaat, "Mechano-Chemical Factors in MoS_2 Film Lubrication," in Mechanisms of Solid Friction, P. J. Bryant, M. Lavik and G. Salomon (Eds.), Elsevier, Amsterdam, 1964, p. 87.

83. A. DiSapio, "Bonded Coatings Lubricate Metal Parts," Product Engineering, 31, 48-53 (1960).

84. M. B. Peterson and R. L. Johnson, "Friction Studies of Graphite and Mixtures of Graphite with Several Metallic Oxides and Salts at Temperatures to 1000°F," NACA TN3657, Dec 1955.

85. J. M. Palacios, A. Rincon and L. Arizmendi, "Extreme Pressure Lubricating Properties of Inorganic Oxides," Wear, 60, 393-399 (1980).

86. American Standard for Testing Material Test Method D2783-82, "Measurement of Extreme Pressure Properties of Lubricating Fluids (Four-Ball Method)," Vol. 05.02, Petroleum Products and Lubricants, ASTM Philadelphia, PA, 1983.

87. D. Tabor, "Mohs's Hardness Scale - A Physical Interpretation," Phys. Soc. Proceed. (London), B-67, 249-257 (1954).

88. E. Rabinowicz, Friction, Wear and Lubrication: Tribology I, MIT Press, Cambridge, MA, 1981, p. 1.12.

89. M. B. Peterson, S. B. Calabrese and B. Stupp, "Lubrication with Naturally Occurring Double Oxide Films," DARPA Report, AD 124248 (1982).

90. T. F. J. Quinn and W. O. Winer, "The Thermal Aspects of Oxidational Wear," Wear, 102, 67-80 (1985).

91. M. B. Peterson, S. F. Murray and J. J. Florek, "Consideration of Lubricants for Temperatures Above 1000°F," ASLE Transactions, 2, pp. 225-234 (1960).

92. M. B. Peterson, "High Temperature Lubrication," Proceedings of Lubrication and Wear, D. Muster and B. Sternlicht, eds., McCutchan Publishing Co., Berkely, CA, 1965.

93. E. Rabinowicz, Friction Wear of Materials, Wiley, New York, NY, 1965, pp. 87-89.

94. J. F. Archard, "The Temperature of Rubbing Surfaces," Wear, 2, 438-455 (1958/59).

95. R. H. Perry and C. H. Chilton, eds., Chemical Engineers Handbook, 5th Ed., McGraw-Hill, New York, NY, 1973.

96. H. Ernst and N. E. Merchant, "Surface Friction of Clean Metals - A Basic Factor in the Metal Cutting Process," Proceedings of the Special Summer Conference on Friction and Surface Finish, Mass. Inst. of Tech., Cambridge, MA, pp. 76-101, 1940.

97. C. Palache, H. Berman and C. Fronkl, "The System of Mineralogy of James Dwight Dana and Edward Salisbury Dana, Yale University 1837-1892," 7th ed., Wiley, New York, NY, 1955.

98. G. E. Dieter, Mechanical Metallurgy, McGraw-Hill, New York, NY, 1976, p. 496.

99. M. B. Peterson, J. J. Florek and R. E. Lee, "Sliding Characteristics of Metals at High Temperatures," ASLE Transactions, 3, 101-109 (1960).

100. E. R. Braithwaite, Solid Lubricants and Surfaces, McMillan, New York, NY, 1964, p. 159.

101. P. Fleischauer and R. Bauer, "The Influence of Surface Chemistry on MoS_2 Transfer Film Formation," ASLE Preprint No. 86-AM-5G-2, Amer. Soc. of Lub. Eng. Annual Meeting, Toronto, Ont., May 1986.

102. J. B. Peace, "Solid Lubricants" in E. R. Braithwaite, ed., Lubrication and Lubricants, Elsevier, Amsterdam, 1967, p. 90.

APPENDIX A

PROCEDURE FOR ISOTHERMAL OXIDATION OF Sb_2O_3

1. The initial rig conditions are as follows:
   a) All valves closed. Record atmospheric pressure and temperature.
   b) Furnace lowered.
   c) P_2O_5 tube installed in O_2 supply line.
2. Weigh Sb_2O_3 and record weight (0.1 milligram).
3. Using stopcock fitting, mount Sb_2O_3 sample in rig.
4. Bring Hg level to that of the gas buret valve by opening system vent and Hg bulb manipulation. Close buret valve bring system to atmospheric pressure.
5. Slowly open vacuum valve and evacuate system to ~1 torr. Close vacuum valve, and by opening O_2 valve bring system to atmospheric pressure.
6. Repeat Step 5 two additional times.
7. Fill a gas buret wih O_2* to atmospheric pressure using the O_2 valve. Loosen gas valve.
8. Use vacuum valve to reduce system pressure to 140 torr, typically, or other pressure desired.

* 99.99 percent O_2, research grade, Matheson, East Rutherford, NJ introduced through P_2O_5 drying tube.

9. Bring furnace into test position and start heating. When test zone temperature has reached equilibrium at the desired temperature, again bring O_2 pressure to 140 torr then drop sample into reaction zone. Start clock and record sample temperature.

10. As oxidation proceeds, O_2 pressure in the system is reduced. Periodically, using the gas buret valve, gently bring the system O_2 pressure back to 140 torr. Record the volume of O_2 remaining in the buret at atmospheric pressure by Hg bulb manipulation. Record O_2 vol/time data until calculated volume of O_2 is consumed or for a period of up to two (2) hours. After 0.5 hour, if no more than 8 cm^3 of O_2 has been consumed, take reading volumetric at five or ten minute intervals.

11. At test termination, turn off and lower furnace.

12. When reaction tube is cool, bring system to atmospheric pressure with air. Remove and label sample. Use a new tube for the next determination.

APPENDIX B

ISOTHERMAL Sb_2O_3 OXIDATION DATA

	TIME (SEC)	OXYGEN CONSUMPTION MG O_2 @ STP/g Sb_2O_3	/TIME ($SEC^{1/2}$)
Run #52	1441	4.39	38.0
Sb_2O_3(c)	1660	6.58	40.74
	2023	10.09	45.0
521°C	2175	12.23	46.64
	2225	12.67	47.20
	2378	15.30	48.8
	2501	17.49	50.01
	2754	20.56	52.5
	2869	22.76	53.60
	3072	26.70	55.41
	3110	27.14	55.81
	3297	28.02	57.4
	3447	31.96	58.7
	3520	32.40	59.3
	3686	34.11	60.7
	4000	37.62	63.3
Run #55	515	3.456	22.7
Sb_2O_3(c)	631	5.529	25.1
	779	8.985	27.9
542°C	869	11.749	29.5
	940	14.514	30.7
	993	15.896	31.5
	1056	18.660	32.5
	1100	21.424	33.2
	1147	23.498	33.9
	1189	25.571	34.5
	1225	28.336	35.0
	1273	30.409	35.7
	1325	33.174	36.4
	1402	37.200	37.4
	1475	40.085	38.4
	1539	42.158	39.2
	1628	44.923	40.4
	1698	46.996	41.2
	1815	48.378	42.6
	1928	49.760	43.9
	2218	51.834	47.1

	TIME (SEC)	OXYGEN CONSUMPTION mg O_2 @ STP/g Sb_2O_3	√TIME ($SEC^{1/2}$)
RUN #57	555	2.469	
Sb_2O_3(c)	641	6.172	
	698	9.875	
542°C	745	13.578	
COATED TUBE	812	19.750	
	879	24.069	
	935	26.538	
	1022	29.007	
RUN #58	456	6.347	21.6
Sb_2O_3(c)	527	9.520	23.0
	641	14.28	25.3
559°C	731	22.214	27.0
	800	26.974	28.3
	862	31.734	29.4
	941	36.494	30.7
	1036	42.841	32.2
	1138	46.015	33.7
	1260	49.187	35.5
RUN #59	341	6.098	18.5
Sb_2O_3	461	11.518	21.5
	527	15.583	23.0
579°C	587	21.004	24.2
	648	27.778	25.5
	687	30.489	26.2
	743	35.910	27.3
	802	41.329	28.3
	916	49.461	30.3
	1031	53.526	32.1
RUN #60	1364	5.395	36.9
Sb_2O_3(o)	1802	8.631	42.5
	2240	11.328	47.3
453°C	2442	12.408	49.4
	3260	16.184	57.1
	4600	18.341	67.8

	TIME (SEC)	OXYGEN CONSUMPTION mg O_2 @ STP/g Sb_2O_3	/TIME $SEC^{1/2}$
RUN #61	467	6.886	21.6
Sb_2O_3(o)	627	10.329	25.0
	780	14.92	27.9
506°C	913	18.364	30.2
	1053	21.233	32.4
	1180	24.102	34.4
	1301	26.715	36.1
	1421	29.267	37.7
	1518	31.562	39.0
	1661	34.432	40.8
	2155	39.597	46.4
	2800	43.61	52.9
RUN #62	691	4.721	26.3
Sb_2O_3(o)	836	7.419	28.9
	941	9.441	30.7
492°C	1124	12.814	33.5
	1304	15.848	36.1
	1568	20.232	39.6
	1827	24.953	42.7
	2151	29.336	46.4
	2551	34.392	50.5
	2690	36.417	51.9
	3780	41.475	61.5
	4672	43.161	68.4
	6000	44.510	77.5
RUN #63	308	9.587	
Sb_2O_3(o)	387	12.143	
	478	17.256	
521°C	517	28.534	
	710	26.204	
	830	31.317	
	1060	38.347	
	1489	43.780	
	3129	46.656	

	TIME (SEC)	OXYGEN CONSUMPTION mg O_2 @ STP/g Sb_2O_3	$\sqrt{TIME}$ ($SEC^{1/2}$)
RUN #64	274	6.586	16.6
Sb_2O_3(o)	373	11.298	19.3
	438	14.245	20.9
521°C	524	18.667	22.9
	600	22.597	24.5
	735	28.000	27.1
	847	31.685	29.1
	1006	37.334	31.7
	1156	40.772	34.0
	1643	44.702	40.6
	2375	46.422	48.7
RUN #68	1495	6.405	38.7
50%	2125	10.551	46.1
Sb_2O_3(o)	3145	15.449	56.1
50%	4467	21.854	66.8
Sb_2O_3(c)	6168	30.144	78.5
492°C			
RUN #69	708	6.714	26.6
50%	1130	13.092	33.6
Sb_2O_3(o)	1594	20.141	39.9
	1878	24.841	43.3
50%	2390	32.555	48.9
Sb_2O_3(c)	3111	37.597	55.8
	6200	41.626	78.7
520°C			
RUN #83	2315	16.545	48.1
50%	3196	21.715	56.5
Sb_2O_3(o)	3815	25.335	61.8
	4640	28.437	68.1
50% Sb_2O_3(c)			
504°C			
RUN #84	887	11.75	29.8
50%	1036	14.20	32.2
Sb_2O_3(o)	1242	17.14	35.2
	1475	20.56	38.4
50%	1690	23.99	41.1
Sb_2O_3(c)	1967	27.91	44.4
	2430	31.82	49.3
530°C	3100	34.76	55.7

APPENDIX C

DIFFERENTIAL THERMAL ANALYSIS SUMMARY
HEATING RATE, 10°C/MIN.

DTA RUN #	SAMPLE	COMPOSITION (wt. basis)	TEMP. (°C) EXO PEAK	TEMP. (°C)* ENDO PEAK	REMARKS
1	Sb_2O_3(c)		576		No peaks
3	Sb_2O_3(c)		576		Gentle Endotherm
8	Sb_2O_3(o)		508		
11	Sb_2O_3(c)/Sb_2O_3(o)	1:1	495, 407		
12	Sb_2O_3(c)/Sb_2O_4	2:1	550		
13	Sb_2O_3(o) /Sb_2O_4	2:1	516	652	
14	Sb_2O_4				No peaks
15	Sb_2O_3(c)/Al_2O_3	2:1	572		
34	MoO_3		--	--	
72	FINE Sb_2O_3(o) Ground 8 Min.		514	653 (s)	
75	FINE Sb_2O_3(o) Ground 16 Min.		508	656 (s)	
73	FINE Sb_2O_3(o) Ground 8 Min.		473	Diff.	Sb_2O_3(o) #72
74	FINE Sb_2O_3(o) Ground 16 Min.		352, 464	Diff.	Sb_2O_3(o) #72
82	Sb_2O_4/Sb_2O_3(c) 8 Min	3:1	485		
83	Sb_2O_4/Sb_2O_3(c) Ground 8 Min.	1:1	530		
84	Sb_2O_4/Sb_2O_3(c) Ground 8 Min.	3:1	487		

APPENDIX C (CONT'D)

DIFFERENTIAL THERMAL ANANLYSIS SUMMARY

DTA RUN #	SAMPLE	COMPOSITION (wt. basis)	TEMP. (°C)* EXO PEAK	TEMP. (°C) ENDO PEAK	REMARKS
85	Sb_2O_3(c) - Sb_2O_3(o)	57:43	481(m) Onset at 380 with shoulder 429		Each ground 8 Min., Mixed
102	Sb_2O_3(o), 1 Min Grind		493	651	
104	Sb_2O_3(o), 15 Sec Grind		508	654	
107	Sb_2O_3(o), 2 Min Grind		475	--	
124	FINE Sb_2O_3(o) Grind 8 Min		--	--	In argon, gentle Endotherm
131	Sb_2O_3(c)		584		
164	MoS_2		451, 500(m)		
169	Sb_2O_3 Ground 16 Min.		558		
175	Sb_2O_3 (Alfa)		456, 487(m), 548		
181	MoS_2		465, 521(m)		
182	75 Mole % Sb_2O_3 (Alfa) 25 Mole % MoS_2		479(m), 509, 566		
183	25 Mole % Sb_2O_3(Alfa) 75 Mole % MoS_2		440, 496(m), 547		
237	50-50 wt% MoS-Sb_2O_3(o) Pellet (Sb_2O_3(o) Grind 8 Min)		446, 495(m)		
238	Sb_2O_3(o) Pellet (Sb_2O_3(o) Ground 8 Min)		475		

* = small, l = large, m = major

** ALFA Sb_2O_3 Contains Both Dimorphs

APPENDIX D

WEAR DATA

TEST #	PELLET COMPOSITION	LOAD (g)	TEMPERATURE °C	ATMOSPHERE	TEST TIME	COEF. OF FRICTION 30 SEC	COEF. OF FRICTION 15 MIN	WEAR VOLUME (mm^3)
2	MoS_2	100	22	DRY AIR	4 HRS	.051	.060	0.375
3	MoS_2+Sen	100	22	DRY AIR	4 HRS	.038	.051	0.204
4	MoS_2+Cer	100	22	DRY AIR	4 HRS	.038	.070	0.222
5	MoS_2+Val(Crushed)	100	22	DRY AIR	4 HRS	.042	.059	0.281
6	MoS_2+Val(Crushed)	100	22	DRY AIR	4 HRS	.032	.060	0.263
7	MoS_2	100	22	DRY AIR	4 HRS	.056	.055	0.325
8	MoS_2	100	22	DRY AIR	4 HRS	.059	.060	0.316
9	MoS_2+Val(Crushed)	100	22	DRY AIR	4 HRS	.040	.045	0.250
10	MoS_2	100	22	WET AIR	20 MIN	.090	.115	ALL
11	MoS_2+Sen	100	22	WET AIR	5 MIN	.155	--	0.286
12	MoS_2+Cer	100	22	WET AIR	5 MIN	.245	--	0.76
13	MoS_2	100	22	WET AIR	5 MIN	.190	--	ALL
14	MoS_2	100	22	WET AIR	1 MIN	.241	--	3.86
15	MoS_2+Val(Crushed)	100	22	WET AIR	5 MIN	.180	--	0.196
16	MoS_2+Cer	100	22	WET AIR	5 MIN	.205	--	0.92
17	MoS_2	100	160	DRY AIR	1 MIN	.016	--	0.059
18	MoS_2	100	160	WET AIR	5 MIN	.177	--	0.151
19	MoS_2+Val(Crushed)	100	160	DRY AIR	20 MIN	.091	--	0.090
21	MoS_2+Cer	100	160	DRY AIR	20 MIN	.120	.250	0.121
22	MoS_2+Sen	100	160	DRY AIR	20 MIN	.150	.172	0.170
23	MoS_2+Val	100	160	WET AIR	20 MIN	.060	.218	0.094
24	MoS_2+Val	100	160	WET AIR	20 MIN	.125	.175	0.072
25	MoS_2+Sen	100	160	WET AIR	20 MIN	.106	.151	2.12
26	MoS_2+Sen	100	160	WET AIR	20 MIN	.085	.152	1.42
29	MoS_2	100	22	DRY AIR	20 MIN	.100	.133	0.1691
30	MoS_2	100	22	DRY AIR	20 MIN	.110	.113	0.1611
31	MoS_2+Val	100	22	DRY AIR	20 MIN	.066	.067	0.052
32	MoS_2+Val	100	22	DRY AIR	20 MIN	.055	.057	0.070
33	MoS_2+Cer	100	22	DRY AIR	20 MIN	.062	.115	0.236
34	MoS_2+Cer	100	22	DRY AIR	20 MIN	.050	.269	0.224
35	MoS_2+Sen	100	22	WET AIR	20 MIN			2.461
36	$MoS_2Sb_2O_3$(c)	100	22	WET AIR	20 MIN	10 MIN		0.707
37	MoS_2	100	212	50% Rel. Hum.	10 MIN	.093	.107	0.126
38	MoS_2+Val	100	212	50% Rel. Hum.	10 MIN	.098	.080	0.091
39	MoS_2	100	212	DRY ARGON	10 MIN	.120	.093	0.251
40	MoS_2+Val	100	212	DRY ARGON	10 MIN	.073	.050	0.056
41	MoS_2	100	212	DRY ARGON	10 MIN	.087	.095	0.175
42	MoS_2+Val	100	212	DRY ARGON	10 MIN	.082	.075	0.054

TEST #	PELLET COMPOSITION	LOAD (g)	TEMPERATURE °C	ATMOSPHERE	TEST TIME	COEF. OF FRICTION 30 SEC	10 MIN	15 MIN	WEAR VOLUME (mm^3)
43	MoS_2+Sen	100	232	DRY ARGON	10 MIN	.072	.080	--	2.206
44	MoS_2+Cer	100	232	DRY ARGON	10 MIN	.079	.100	--	2.232
45	MoS_2+Sen	100	232	DRY ARGON	10 MIN	.083	.083	--	2.082
46	MoS_2	100	232	DRY ARGON	10 MIN	.111	.117	--	0.352
47	MoS_2	100	232	DRY AIR	10 MIN	.123	.123	--	0.167
48	MoS_2+Sen	100	232	DRY AIR	350 SEC	.069	--	--	2.638
49	MoS_2+Cer	100	232	DRY AIR	10 MIN	.080	.110	--	0.307
50	MoS_2+Val	100	232	DRY AIR	10 MIN	.063	.063	--	0.024
51	MoS_2	100	232	WET AIR	10 MIN	.110	.140	--	0.039
52	MoS_2	100	232	WET AIR	10 MIN	.130	.133	--	0.200
53	MoS_2+Val	100	232	WET AIR	10 MIN	.088	.075	--	0.126
54	MoS_2+Cer	100	232	WET AIR	10 MIN	--	.133	--	0.265
55	MoS_2+Sen	100	232	WET AIR	10 MIN	.022	.080	--	1.780
56	MoS_2+Sen	100	232	WET AIR	10 MIN	.067	.063	--	0.393
57	MoS_2+Val	100	232	WET AIR	10 MIN	.087	.073	--	0.131
58	MoS_2	100	232	DRY AIR	10 MIN	.018	.130	--	0.212
59	MoS_2	100	232	DRY ARGON	10 MIN	.104	.107	--	0.169
60	MoS_2	100	232	WET AIR	10 MIN	.090	.087	--	0.369
61	MoS_2+Val	100	316	DRY AIR	10 MIN	.065	.090	--	0.193
62	MoS_2	100	316	DRY AIR	10 MIN	.143	.150	--	0.364
63	MoS_2+Sen	100	316	DRY AIR	10 MIN	.085	.204	--	7.972
64	MoS_2+Cer	100	316	DRY AIR	10 MIN	.077	.188	--	0.181
65	MoS_2	100	316	DRY ARGON	10 MIN	.108	.100	--	0.641
66	MoS_2+Val	100	316	DRY ARGON	10 MIN	.065	.085	--	0.125
67	MoS_2+Cer	100	316	DRY ARGON	10 MIN	.075	.187	--	0.536
68	MoS_2+Sen	100	316	DRY ARGON	10 MIN	.052	.137	--	5.652
69	MoS_2+Cer(Crushed)	100	232	WET AIR	10 MIN	.109	.114	--	0.166
70	MoS_2	100	316	DRY AIR	15 MIN	.079	.142	.153	0.158

TEST #	PELLET COMPOSITION	LOAD (g)	TEMPERATURE °C	ATMOSPHERE	TEST TIME	30 SEC	10 Min	15 MIN	WEAR VOLUME (mm^3)
71	MoS_2+Val	100	316	DRY AIR	18.3 MIN	.062	.100	.110	0.108
72	MoS_2+Sen	100	316	DRY AIR	22.8 MIN	.043	.082	.116	2.843
74	MoS_2	100	316	DRY AIR	1000 SEC	--	--	--	0.352
75	MoS_2/Val	100	316	DRY AIR	1000 SEC	--	--	--	0.126
76	MoS_2/Sen	100	316	DRY AIR	1000 SEC	--	--	--	1.121
77	MoS_2+Cer	100	316	DRY AIR	1000 SEC	.208	.267	.364	0.251
78	85 MoS_2/15 Val	100	316	DRY AIR	1000 SEC	.213	.259	.299	0.318
79	65 MoS_2/35 Val	100	316	DRY AIR	1000 SEC	.073	.064	.068	0.203
80	MoS_2/Sen/Val	100	316	DRY AIR	10 MIN	.047	.029	--	0.344
81	MoS_2/Sen/Val	100	316	DRY AIR	1000 SEC	.069	.069	.094	0.116
82	MoS_2/Val	50	316	DRY AIR	1000 SEC	.077	--	--	0.047
83	MoS_2/Val	150	316	DRY AIR	1000 SEC	.056		.056	0.166
84	MoS_2+Val	100	316	DRY AIR	60 SEC				0.048
85	MoS_2+Val	100	316	DRY AIR	150 SEC				0.060
86	MoS_2+Val	100	316	DRY AIR	300 SEC				0.073
87	MoS_2	100	316	VACUUM	60 SEC				0.056
88	MoS_2	100	316	DRY AIR	60 SEC				0.047
89	MoS_2	100	316	DRY AIR	300 SEC				0.120
90	MoS_2	100	316	DRY AIR	150 SEC				0.111
91	MoS_2	100	316	DRY AIR	300 SEC				0.128
92	MoS_2	100	316	DRY AIR	450 SEC				0.172
93	MoS_2+Sen	100	316	DRY AIR	450 SEC				0.263
94	MoS_2+Sen	100	316	DRY AIR	150 SEC				0.440
95	MoS_2+Sen	100	316	DRY AIR	300 SEC				0.183
96	MoS_2+Sen	100	316	DRY AIR	60 SEC				0.110
97	MoS_2+Val(Heated Treated	100	316	DRY AIR	300 SEC				0.140

98	MoS_2+Cer	100	316	DRY AIR	300 SEC			0.108
99	MoS_2+Cer	100	316	DRY AIR	450 SEC			0.167
100	MoS_2+Cer	100	316	DRY AIR	150 SEC			0.099
101	MoS_2+Cer	100	316	DRY AIR	300 SEC			0.150
102	MoS_2+Cer	100	316	DRY AIR	60 SEC			0.077
103	MoS_2+$Sb_2O_3MoO_3$	100	316	DRY AIR	1000 SEC	--	.139	0.059
104	MoS_2+$Sb_2O_3MoO_3$	100	316	DRY AIR	1000 SEC	.052	.069	0.074
105	MoS_2+Sb_2O_3(o)+MoO_3	100	316	DRY AIR	1000 SEC	.083	.150	0.043
106	MoS_2+Sb_2O_3(o)+MoO_3	100	316	DRY AIR	1000 SEC			0.087
107	MoS_2+Sb_2O_3(o)+MoO_3	100	316	DRY AIR	1000 SEC			0.053
108	MoS_2+MoO_3	100	316	DRY AIR	1000 SEC			0.037
109	MoS_2+Sb_2O_3(o)+MoO_3	100	316	DRY AIR	1000 SEC			0.082
110	MoS_2+Sb_2O_3(o)+MoO_3	100	316	DRY AIR	1000 SEC			0.079
111	MoS_2+MoO_3	100	316	DRY AIR	1000 SEC	.100	.140	0.055
112	MoS_2+MoO_3	100	316	DRY AIR	1000 SEC	.072	.100	0.057
113	MoS_2+Sb_2O_3(o)	100	316	DRY AIR	1000 SEC	.079	.113	0.075
114	MoS_2	100	316	DRY AIR	1000 SEC	.061	.086	0.181
115	MoS_2	100	316	DRY AIR	1000 SEC	.075	.118	0.134
116	MoS_2+Sb_2O_3(o)	100	316	DRY AIR	1000 SEC	.109	.115	0.105
117	MoS_2+MoO_3	100	316	DRY AIR	1000 SEC	.127	.171	0.045
118	MoS_2+Sb_2O_3(o)+MoO_3	100	316	DRY AIR	1000 SEC	.078	.129	0.057
119	MoS_2+MoO_3	100	316	DRY AIR	1000 SEC	.014	.069	0.031
120	MoS_2	100	316	DRY AIR	1000 SEC	.105	.154	
121	MoS_2+MoO_3	100	316	DRY AIR	1000 SEC	.106	.158	0.050
122	MoS_2+Sb_2O_3+MoO_3	100	316	DRY AIR	1000 SEC	.075	.136	0.081

TEST #	PELLET COMPOSITION	LOAD (g)	TEMPERATURE (°C)	ATMOSPHERE	TEST TIME	COEF. OF FRICTION 30 SEC	COEF. OF FRICTION 15 MIN	WEAR VOLUME (mm^3)
123	$MoS_2+Sb_2O_3$(o)	100	316	DRY AIR	1000 SEC	.078	.138	0.108
124	$MoS_2+Sb_2O_3$(o)	100	316	DRY AIR	"	.100	.192	0.078
125	$MoS_2+MoO_3+Sb_2O_3$(o)	100	316	DRY AIR	"	.088	.178	0.079
126	Graphite+Sb_2O_3(o)	100	316	DRY AIR	"	.106	.228	0.090
127	Graphite	100	316	DRY AIR	"	.269	.304	0.043
128	Graphite+Sb_2O_3(o)	100	232	DRY AIR	"	.127	.235	0.034
129	Graphite	100	232	DRY AIR	"	.169	.269	0.038
130	MoS_2+PbO	100	316	DRY AIR	"	.113	.200	0.061
131	$MoS_2+MoO_3+Sb_2O_4$	100	316	DRY AIR	"	.067	.162	0.036
132	$MoS_2+Bi_2O_3$	100	316	DRY AIR	"	.134	.226	0.096
133	MoS_2+CdO	100	316	DRY AIR	"	.100	.173	0.071
134	$MoS_2+Sb_2S_4$	100	316	DRY AIR	"	.135	.202	0.043
135	MoS_2+TiO_2	100	316	DRY AIR	"	.137	.211	0.423
136	MoS_2+CuO	100	316	DRY AIR	"	.046	.155	0.072
137	$MoS_2+Sb_2S_3$	100	316	DRY AIR	"	.089	.154	0.109
138	$MoS_2+MoO_3+Sb_2O_3$(o)	100	316	DRY AIR	"	.081	.169	0.077
139	$MoS_2+Sb_2S_3$	100	316	DRY AIR	"	.095	.188	0.067
140	Graphite	100	274	DRY AIR	"	.138	.195	0.061
141	Graphite	100	22	DRY AIR	"	.113	.133	0.082
142	Graphite+Sb_2O_3(o)	100	274	DRY AIR	"	.059	.196	0.125
143	Graphite+Sb_2O_3(o)	100	22	DRY AIR	"	.165	.196	0.113
144	$As_2O_3+MoS_2$	100	22	DRY AIR	"	.147	.209	0.224
145	$As_2O_3+MoS_2$	100	316	DRY AIR	"	.100	.157	0.070
146	$Al_2O_3+MoS_2$	100	316	DRY AIR	"	.116	.242	0.415

☆U.S.Government Printing Office: 1987 – 748-061/60944